



THIS REPORT WAS INADVERTENTLY DISSEMINATED IN THE PUBLIC DOMAIN/ONLINE SINCE 09/2015 WITHOUT A DISCLAIMER. DISCLAIMER HAS BEEN ADDED – “THIS INFORMATION IS DISTRIBUTED SOLELY FOR THE PURPOSE OF PEER REVIEW UNDER APPLICABLE INFORMATION QUALITY GUIDELINES. IT HAS NOT BEEN FORMALLY DISSEMINATED BY BSEE. IT DOES NOT REPRESENT AND SHOULD NOT BE CONSTRUED TO REPRESENT ANY AGENCY DETERMINATION

OR POLICY

FINAL REPORT:

WELL STIMULATION EFFECTS ON ANNULAR SEAL
OF PRODUCTION CASING IN OCS OIL AND GAS
OPERATIONS

Prepared for: BSEE
Contract Number: E14PC00037

9/28/2015
Prepared By: Paul Sonnier
Position: Research and
Development Manager,
Lab Manager

CONTENTS

1 Acronyms and Abbreviations.....	8
2 Introduction	10
2.1 Objective	10
2.2 Conclusions and Recommendations.....	10
2.2.1 Literature Review	10
2.2.2 Failure modes.....	11
2.2.3 Small Scale Physical Modeling.....	12
2.2.4 Large scale modeling	13
2.2.5 Finite Element Analysis	13
2.2.6 Design and Performance Topics Considered for Regulation.....	15
2.2.7 Recommendations	15
2.3 Background and Report Structure.....	15
3 Literature Review	17
3.1 Objective	17
3.2 Background	17
3.3 Summary of Selected Literature.....	18
3.3.1 Regulatory Information	18
3.3.2 Annular Pressure Build Up	18
3.3.3 Industry Trends	19
3.3.4 Well Architecture	20
3.3.5 Completion Data	20
3.3.6 Field Conditions.....	21
3.3.7 High Pressure High Temperature Conditions	21
3.3.8 Stimulation Techniques	23
3.3.9 Frac Pack	23
3.3.10 Cement Performance	24
3.3.11 Cement Mechanical Properties	26
3.4 Shale Cement Performance Analogy.....	28
4 Failure Mode	29
4.1 OBJECTIVE	29

THIS REPORT WAS INADVERTENTLY DISSEMINATED IN THE PUBLIC DOMAIN/ONLINE SINCE 09/2015 WITHOUT A DISCLAIMER. DISCLAIMER HAS BEEN ADDED – “THIS INFORMATION IS DISTRIBUTED SOLELY FOR THE PURPOSE OF PEER REVIEW UNDER APPLICABLE INFORMATION QUALITY GUIDELINES. IT HAS NOT BEEN FORMALLY DISSEMINATED BY BSEE. IT DOES NOT REPRESENT AND SHOULD NOT BE CONSTRUED TO REPRESENT ANY AGENCY DETERMINATION OR POLICY

- 4.2 BACKGROUND 29
- 4.3 STUDY WELL CONDITIONS..... 30
- 4.4 FINDINGS FROM TASK 2 LITERATURE REVIEW 33
- 4.5 INVESTIGATION OF POSSIBLE FAILURE MODES AND RANGES OF STRESSES 33
 - 4.5.1 Stress-induced tensile failure of the cement..... 33
 - 4.5.2 Micro-annulus formation from repeated temperature and pressure cycling 36
 - 4.5.3 Shear failure of the cement/casing interface 37
 - 4.5.4 Inadequate quality control procedures/cementing practices prior to production 37
- 4.6 Summary 37
- 5 Physical Modeling 38
 - 5.1 Objective 38
 - 5.2 Background 38
 - 5.3 Test Conditions..... 38
 - 5.4 Results and Discussion 43
 - 5.4.1 Small Scale Physical Modeling..... 43
 - 5.4.2 Performance Properties 44
 - 5.4.3 Mechanical and Thermal Properties..... 45
 - 5.4.4 Annular Seal Testing..... 47
 - 5.4.5 Dimensionless Scaling Correlation Development 51
 - 5.4.6 Large Scale Annular Seal..... 54
 - 5.4.7 Large-Scale Test Results 55
 - 5.4.8 Dimensionless Scaling Correlation Evaluation 57
 - 5.4.9 FEA Results 62
- 6 FEA Report 65
 - 6.1 Summary 65
 - 6.2 Introduction and Background..... 66
 - 6.3 Technical Approach 67
 - 6.3.1 Key Assumptions 67
 - 6.4 Finite Element Model of Lab And Down-Hole System (Subtask 6.2-6.4) 69
 - 6.4.1 Boundary conditions and initial conditions 69
 - 6.4.2 Contact Interactions 70

THIS REPORT WAS INADVERTENTLY DISSEMINATED IN THE PUBLIC DOMAIN/ONLINE SINCE 09/2015 WITHOUT A DISCLAIMER. DISCLAIMER HAS BEEN ADDED – “THIS INFORMATION IS DISTRIBUTED SOLELY FOR THE PURPOSE OF PEER REVIEW UNDER APPLICABLE INFORMATION QUALITY GUIDELINES. IT HAS NOT BEEN FORMALLY DISSEMINATED BY BSEE. IT DOES NOT REPRESENT AND SHOULD NOT BE CONSTRUED TO REPRESENT ANY AGENCY DETERMINATION OR POLICY

6.4.3 Cement damage modeling	70
6.4.4 Thermal analysis approach.....	71
6.4.5 Thermal properties.....	72
6.4.6 Thermal boundary conditions	72
6.4.7 Pressure Loading	72
6.4.8 Combined Pressure and Thermal Loading.....	72
6.5 Results.....	73
6.5.1 Small Scale Pressure Cycling Results	73
6.5.2 Small Scale Thermal Cycling Results	74
6.5.3 Large Scale Results	76
6.5.4 Down-hole system results	76
Appendix A Literature Review.....	77
Appendix A.1 Shale Cement Performance	77
Appendix A.2 Cement Performance	78
Appendix A.3 Annular Pressure Build-up	85
Appendix A.4 Industry Trends.....	87
Appendix A.5 Well Architecture	91
Appendix A.6 Completion data	92
Appendix A.7 Field Conditions.....	94
Appendix A.8 HPHT	99
Appendix A.9 Stimulation Techniques.....	102
Appendix A.10 Frac Pack	104
Appendix A.11 Cement Mechanical Properties.....	106
Appendix A.12 Regulatory Information.....	111
Work Cited for Literature Review.....	111
APPENDIX B Physical Modeling	122
APPENDIX B.1 Testing Methods and Mechanical Properties.....	122
APPENDIX B.2 Anelastic Strain	126
APPENDIX B.3 Annular Seal	127
Appendix B.4 Large-Scale Laboratory Seal Performance Testing	130
Appendix B.5 Energy and Resistance Calculations	133

THIS REPORT WAS INADVERTENTLY DISSEMINATED IN THE PUBLIC DOMAIN/ONLINE SINCE 09/2015 WITHOUT A DISCLAIMER. DISCLAIMER HAS BEEN ADDED – “THIS INFORMATION IS DISTRIBUTED SOLELY FOR THE PURPOSE OF PEER REVIEW UNDER APPLICABLE INFORMATION QUALITY GUIDELINES. IT HAS NOT BEEN FORMALLY DISSEMINATED BY BSEE. IT DOES NOT REPRESENT AND SHOULD NOT BE CONSTRUED TO REPRESENT ANY AGENCY DETERMINATION OR POLICY

Works Cited for Failure Mode and Physical Modeling	139
Appendix C Finite Element Analysis	141
Appendix D Paper on Zonal Isolation	166
Table 1: Well Descriptions	31
Table 2: Deepwater Deep Target, BHST – 250°F, BHCT - 189°F	32
Table 3: Deepwater Shallow Target, BHST – 155°F, BHCT - 120°F	32
Table 4: Shelf, BHST- 275°F, BHCT - 195°F	32
Table 5: Well Conditions for OCS Well Types	39
Table 6: Deepwater Deep Target, BHST - 250°F, BHCT - 189°F	40
Table 7: Deepwater Shallow Target Conventional Design, BHST - 155°F, BHCT - 120°F	41
Table 8: Deepwater Shallow Target Resilient, BHST - 155°F, BHCT - 120°F	41
Table 9: Deepwater Shallow Target Low-Density, BHST - 155°F, BHCT - 120°F	42
Table 10: Shelf, BHST - 275°F, BHCT - 195°F	42
Table 11: Conventional Performance Properties	44
Table 12: Mechanical and Thermal Properties of Cement Compositions Cured at Atmospheric Pressure	45
Table 13: Mechanical Properties of Cement Compositions cured Under Pressure	47
Table 14: Mechanical Annular Seal Durability	49
Table 15: Thermal Annular Seal Durability	50
Table 16: Calculated Energy Application for Laboratory and Field. (Detailed Calculation Methods presented in appendix B)	53
Table 17: Energy Inputs for Field-Scale Tests of Energy Correlation	57
Table 18: Correlation Parameters	58
Table 19: Material Properties Assumed Tubing And Formations	68
Table 20: Comparison Of Fea Results And Lab Results For Small Scale Pressure Cycling	73
Table 21: Comparison Of Fea Results And Lab Results For Small Scale Thermal Cycling	74
Table 22: Comparison Of Fea Results And Lab Results For Large Scale	76
Figure 1: Cement Sheath Failure modes	26
Figure 2: Cement Sheath Failure Modes	26
Figure 3: Cement Sheath Failure Modes	34
Figure 4: Stresses Induced In The Casing-Cement-Formation System By Pressure Or Temperature Increases Inside The Casing	35
Figure 5: R_e vs E_a for Annular Seal Data	54
Figure 6: Annular Pressure Communication vs Pressure Cycle (magnified)	56

Figure 7: Annular Pressure Communication vs Pressure Cycle (overall).....	56
Figure 8: Large-Scale Annular Seal Failure Data	59
Figure 9: Field Data.....	60
Figure 10: Correlation Sensitivity	61
Figure 11: Displacement Gradients	62
Figure 12: Debonding	63
Figure 13: Shear Bond Test.....	123
Figure 14: Diagram of Tensile Test	124
Figure 15: Impact Setup	125
Figure 16: Pressure Annular Seal Apparatus	127
Figure 17: Thermal Annular Seal Apparatus.....	128
Figure 18: Thermal Annular Seal Apparatus.....	129
Figure 19: Large Scale Annular Seal Test (Temperature).....	131
Figure 20: Large Scale Annular Seal Test (Pressure).....	132
Figure 21: General View Of Small Scale Fea Model	141
Figure 22: View Of Meshing Of Small Scale Model.....	141
Figure 23: General View Of Large Scale Fea Model	142
Figure 24: View Of Meshing Of Large Scale Model.....	143
Figure 25: General View Of Down-Hole System Fea Model	143
Figure 26: View Of Meshing Of Down-Hole System Fea Model.....	144
Figure 27: Small Scale Model Boundary Conditions	145
Figure 28: Large Scale Model Boundary Conditions	145
Figure 29: Down-Hole System Model Boundary Conditions	146
Figure 30: Initial Vertical Stress State For Down-Hole System	146
Figure 31: Typical Contact Interaction Locations.....	147
Figure 32: Small Scale Thermal Boundaries.....	147
Figure 33: Large Scale Thermal Boundaries.....	148
Figure 34: Down-Hole System Thermal Boundaries	148
Figure 35: Small Scale Temperature Distributions (Cpvc Outer Pipe)	149
Figure 36: Small Scale Temperature Distributions (Steel Outer Pipe)	149
Figure 37: Large Scale Temperature Distributions.....	150
Figure 38: Down-Hole System Temperature Distribution.....	150
Figure 39: Small Scale Pressure Loading.....	151
Figure 40: Large Scale Pressure Loading.....	151
Figure 41: Down-Hole System Pressure Loading	152
Figure 42: Damage Of Elements In Small Scale Pressure Tests (CPVC).....	153
Figure 43: Contact Damage Of Surfaces In Small Scale Pressure Tests (CPVC).....	153
Figure 44: Small Scale Stress Contours At Estimated Failure For Pressure Tests (CPVC).....	154
Figure 45: Damage Of Elements In Small Scale Pressure Tests (STEEL)	155
Figure 46: Contact Damage Of Surfaces In Small Scale Pressure Tests (STEEL)	155
Figure 47: Small Scale Stress Contours At Estimated Failure For Pressure Tests (STEEL)	156
Figure 48: Damage Of Elements In Small Scale Thermal Tests (CPVC)	156
Figure 49: Contact Damage Of Surfaces In Small Scale Thermal Tests (CPVC)	157

THIS REPORT WAS INADVERTENTLY DISSEMINATED IN THE PUBLIC DOMAIN/ONLINE SINCE 09/2015 WITHOUT A DISCLAIMER. DISCLAIMER HAS BEEN ADDED – “THIS INFORMATION IS DISTRIBUTED SOLELY FOR THE PURPOSE OF PEER REVIEW UNDER APPLICABLE INFORMATION QUALITY GUIDELINES. IT HAS NOT BEEN FORMALLY DISSEMINATED BY BSEE. IT DOES NOT REPRESENT AND SHOULD NOT BE CONSTRUED TO REPRESENT ANY AGENCY DETERMINATION OR POLICY

Figure 50: Small Scale Stress Contours At Failure For Thermal Tests (CPVC) 157

Figure 51: Damage Of Elements In Small Scale Thermal Tests (STEEL)..... 158

Figure 52: Contact Damage Of Surfaces In Small Scale Thermal Tests (STEEL)..... 158

Figure 53: Small Scale Stress Contours At Failure For Thermal Tests (STEEL)..... 159

Figure 54: Large Scale Element Damage At Estimated Failure Under Pressure Loading 159

Figure 55: Large Scale Element Damage At Estimated Failure Under Thermal Loading 160

Figure 56: Large Scale Element Damage At Estimated Failure Under Combined Loading..... 160

Figure 57: Large Scale Contact Damage At Estimated Failure Under Pressure Loading 161

Figure 58: Large Scale Contact Damage At Estimated Failure Under Thermal Loading..... 161

Figure 59: Large Scale Contact Damage At Estimated Failure Under Combined Loading..... 162

Figure 60: Large Scale Stress Distribution At Estimated Failure Under Pressure Loading 163

Figure 61: Large Scale Stress Distribution At Estimated Failure Under Thermal Loading 164

Figure 62: Large Scale Stress Distribution At Estimated Failure Under Combined Loading..... 164

Figure 63: Down-Hole System Element Damage..... 165

Equation 1: Applied energy 51

Equation 2: Effective Resistance 51

Equation 3: Mechanical Applied Energy..... 52

Equation 4: Thermal Applied Energy 52

Equation 5: Mechanical Effective Resistance 52

Equation 6: Thermal Effective Resistance 52

Equation 7: Tensile strength equation 124

1 ACRONYMS AND ABBREVIATIONS

A:	Area (in ²)
BHCT:	Bottom hole circulating temperature (°F)
BHP:	Bottomhole pressure (lb _f /in ²)
BHST:	Bottomhole static temperature (°F)
BHT:	Bottomhole temperature (°F)
Bc:	Bearden Unit of measurement for Thickening Time
Bwoc:	By weight of cement
Bwow:	By weight of water
C:	Coefficient of Thermal Expansion (1/°F)
C _p :	Heat Capacity (in-lb _f /lbmF)
b/d:	Barrels per day
cc:	Cubic centimeters
DB:	Dry Blend
E:	Young's Modulus (lb _f /in ²)
FEA:	Finite element analysis
Ft ³ /sk:	Cubic feet per sack
gal/sk:	Gallons per sack
HTHP:	High Temperature High Pressure
k:	Thermal Conductivity (in-lb _f /hr in F)
KCL:	Potassium Chloride
m:	Mass (lbm)
MD:	Measured depth (ft)
Nu	Nusselt Number
OCS:	Outer continental shelf

OH:	Open Hole
P:	Pressure (lb _f /in ²)
ppg:	Pounds per gallon
psi:	Pounds per square inch
Pr:	Prandtl Number
PV:	Plastic Viscosity (centipoise cp)
Q:	Energy (in-lb _f)
Re:	Reynolds Number
S _c :	Compressive Strength (lb _f /in ²)
S _i :	Impact Strength (lb _f /in ²)
S _s :	Shear Bond (lb _f /in ²)
S _t :	Tensile Strength (lb _f /in ²)
T:	Temperature (°F)
t:	Time (hr)
TVD:	Total vertical depth (ft)
U:	Overall heat transfer coefficient
UCA:	Ultrasonic Cement Analyzer
V:	Volume (in ³)
YP:	Yield Point (lb/100ft ²)
w/c:	Water/Cement Ratio
v:	Poisson's Ratio
ε:	Anelastic Strain
ρ:	Density (lb _f /in ³)

2 INTRODUCTION

2.1 OBJECTIVE

The objective of this comprehensive final report is to fully document results and analyses completed during this investigation of wellbore integrity of OCS wells after stimulation operations. The work described here relates state of the art of cement seal integrity, failure modes of a cement sheath, physical modeling of cement system behavior under induced stresses, and finite element modeling of cement seal integrity. Several topics of cement design and well construction for which seal integrity may benefit from regulatory control will be identified.

A thorough evaluation of current state of well integrity regulation for wells undergoing stimulation and recommendations for regulation topics and structure will be the subject of a second final report.

2.2 CONCLUSIONS AND RECOMMENDATIONS

The major conclusions drawn from this work are that physical and numerical modeling of cemented wellbore durability under mechanically- and thermally-induced stress revealed that the complex progression of seal failure can be described and demonstrated. The trends identified by these two investigative methods are consistent and relatable to failure mode theory.

Cement seal failure is not a simple process governed by one or two physical properties. However, the failure trends identified by physical and FEA can be quantified using various groups of cement mechanical and thermal properties, casing and borehole geometry, geothermal conditions, and completion operations. These quantifiable trends present a basis for meaningful and specific regulations regarding wellbore design, cement design and placement, and stimulation treatment design.

Accuracy of these trends has not been tested in OCS operations. However, the results of this project indicate that cements currently used in OCS wells, both shelf and deepwater, will withstand current levels of stimulation without seal failure.

Specific conclusions drawn from each task of the project are presented below. These specific conclusions all support the general ones stated above.

2.2.1 LITERATURE REVIEW

Upon review of technical literature sources it was found that:

- Regulations vary greatly and a more proactive approach is needed to keep up with the changing deepwater drilling and completions environment.
- Studies in shale cement include cement performance in HPHT zones and seal durability related to fracturing. These studies can be helpful in addressing cementing issues related to HPHT and durability in OCS operations.
- Annular pressure build up is costly and time consuming. It is important to prevent it before it occurs. To achieve this, cement designs can be changed to improve the durability of the seal.
- As OCS industry trends toward hotter, deeper, longer wells, with various, challenging formations, the technology must change at a rapid pace to keep up.
 - This includes more difficult well architecture with non-standard casing and novel tools
 - Stimulation techniques are also changing with new fluids and materials that can affect the cement integrity.
 - HPHT and ultra-HPHT conditions further complicating the drilling and completions processes
 - Cementing designs need to be able to keep up with the rapidly changing deepwater drilling environment.
- Conventional cement systems are at times unable to maintain an effective seal under cyclic stressing conditions in the changing environment of the wellbore. These stresses are from thermal changes, and pressure changes such as stimulation activities like frac packs.
 - Computer simulations and models can help in the cementing design process for these challenges.
 - Cement to casing bond is dependent on numerous mechanical properties, not just compressive strength. To withstand these environments it may be necessary to develop more flexible cement systems.
 - Excellent cement job execution is also required to create a good bond. Mud removal, density control and other aspects of cement placement are important in creating a durable bond.
 - Mechanical properties needed for annular seal durability during cyclic loading in a deepwater environment need to be established.

2.2.2 FAILURE MODES

- Stresses induced on typical OCS wells by stimulation operations result from increased casing pressure and cooling of the casing by fracturing fluids. The magnitudes of these stresses are not generally sufficient to create damage to the production casing. However, the stresses can be sufficient to cause failure of the cement or to destroy the bond of cement to casing or cement to formation.

- Potential failure modes of cement during stimulation can be attributed to tensile stress, compressive stress, and shear stress. The casing-cement-formation system integrity depends on mechanical properties of the cement such as Young's Modulus, Poisson's Ratio, and tensile strength. Cement failure in tension due to hoop stress applied to the casing ID from bottom-hole treating pressure during stimulation is considered most common due to the intrinsically low tensile strength of most Portland cement systems.
- Additionally, the quality of cement placement and control of unwanted fluid migration in the cemented annulus after cement placement dictate the initial condition of the system and affect the potential for stress-induced seal failure. Finally, since Portland cement mechanical properties are governed by extent of chemical hydration occurring in the cement and this hydration rate depends on time, temperature and cement design, the mechanical properties of the cement component must be measured after curing for appropriate times at simulated down-hole conditions to accurately assess performance.
- In addition to time dependence, mechanical performance of Portland cement can degrade under cyclic stress that is far below failure stress for the material. This degradation is due to the porous nature of set Portland cement and localized failure of the pore walls that can result from stresses in the elastic region of the bulk material. Thus, stresses lower than failure strength of a cement can cause plastic strains. Stress repetition can result in additional plastic strain thus creating flow channels at lower-stresses than bulk mechanical failure would predict.
- In general, failure of the casing-cement-formation system as a result of hydraulic fracturing-induced stress is complex and is not accurately described by solely one or two cement mechanical property values. Primary failure points are within the cemented annulus. Failure is governed by cement composition, quality of cement placement, extent of hydration as governed by time interval between cement placement and stimulation treatment, and stimulation treatment temperatures and pressures.

2.2.3 SMALL SCALE PHYSICAL MODELING

- Small-scale laboratory testing of mechanical properties and seal durability of cement compositions representative of those used for cementing production strings of OCS wells produced data that were analyzed to develop a relationship between applied thermal and/or mechanical energy and seal failure as indicated by initiation of gas flow through the cemented annulus of the test fixture. This general relationship is not statistically precise, but it is scalable to field conditions. The trend described by the relationship when applied to representative conditions for stimulation of several OCS well types indicated that cements used in these wells constructed and stimulated according to standard methods should maintain viable seal. Specific conclusions based on analysis of these test results are:

- Mechanical and thermal stresses applied to the casing-cemented annulus-formation system during a fracture stimulation treatment are of sufficient magnitude to induce seal failure if cement designs with less mechanical integrity are used.
- Cements used for OCS production strings are designed to have excellent performance and mechanical properties.
- Initial estimates of energy magnitude indicate the major energy input from stimulation treatments is cooling of the wellbore by injection of fluid treatments.
- Seal failure timing and location measured by gas flow in laboratory models generally matched FEA predictions. The process is complex and rarely matches fundamental analytical predictions.

2.2.4 LARGE SCALE MODELING

- Mechanical failure on four of six large-scale fixtures originally constructed precluded their use. One pressure cycle test and one thermal cycle test were completed successfully.
- FEA results for each large scale test predicted failure energy and failure mode that compared well to actual results.
- Results of large scale model testing did not match well with the general dimensionless E_a - R_f scaling relationship. The effective resistance factor R_e was higher than the trend line would predict for both models at failure. The pressure cycling model was significantly closer to the trend line than the thermal result.

2.2.5 FINITE ELEMENT ANALYSIS

- A comparison of the FEA results with the physical lab tests showed some differences in failure mode and in the overall durability of the seal. The differences in the results can be attributed to multiple factors, one of which is that a failure or failure location in the FEA may or may not translate to a leak in physical testing or in actual well conditions.
- Currently FEA can be used to predict likely locations of failure and a general estimate of durability and further work is required to improve the correlation between laboratory test and simulation results. More extensive testing of cement mechanical properties will better define material inputs in the FEA models.
- In general, the more brittle cement is less durable, and failure will occur at fewer stress cycles. A high compressive or tensile strength does not indicate the ability to withstand a greater number of load cycles, but rather the ability for the cement to deform more before failure. This is especially true for deformation with regards to tension. It was also observed that more brittle cements are more likely to have radial

cracking and leak propagation at the outer pipe, while more ductile cement appears to be more likely to have crack propagation at the inner pipe.

- The stiffness of the formations (PVC or steel pipes) was found to have a varying effect on the overall durability of the systems. Generally overall the stiffer the outer pipe, the better the cement performed. However, a softer formation generally performed better with a more ductile cement.
- Several failure mode types identified in the Failure Mode analysis were predicted to occur. It was expected that formation of a micro-annulus at the inner pipe would be the predominant failure mode for all testing, however it was observed for both small and large scale pressure models that de-bonding at the outer interface was most likely to occur depending on cement properties. This was validated by the observed failure locations in lab testing. It was also noted that radial cracking was occurring along with the outer de-bonding in the FEA models. It is likely that radial cracking was occurring in the lab, but the leaks appeared at the outer pipe interface due to less resistance along that path and therefore noticed before any leaking at radial cracks occurred.
- Formation of a micro-annulus at the inner pipe was observed in most of the small scale and large scale thermal models. This was expected due to the nature of the thermal cycling and the difference between the expansion properties of the cements and steel. Additionally, the large scale model showed signs of “disking” failure as mentioned in Failure Mode analysis. This is from the tensile strains in the cement due to the thermal expansion and contraction cycles. In field conditions, a shear damage failure could also occur in addition to the “disking” due to the imperfections and irregularities of the wellbore.
- The field scale model did show some signs of damage in various locations along the height of the well, but complete failure did not occur after 10 stimulation cycles for the cement analyzed. Failure is likely to occur eventually, however it is likely that the number of cycles to failure would exceed the number of stimulation treatments over the life of the well. Although, it is not practical to model an entire wellbore system currently, it could prove to be useful for a comparative analysis to help better correlate lab testing to field use or aid in the validation of the dimensionless scaling. In order to further develop a field scale model, field testing/investigation study of field conditions is recommended. Such a study would give better insight of the behavior of wellbore conditions and which ones have the greatest impact on the system and aid in improving the accuracy and computational efficiency of the models.
- It is concluded that the use of FEA modeling of cements can successfully be used to validate lab testing further, aid in development of cement compositions prior to being tested in the lab and to gain a better understanding of performance in field conditions and perform comparative studies. Since only idealized models can be made of field conditions it is recommended that any modeling of field conditions be done

from a parametric perspective, meaning FEA could be used to do comparative analysis to aid in determining the performance of the seals when subjected to various conditions.

2.2.6 DESIGN AND PERFORMANCE TOPICS CONSIDERED FOR REGULATION

Regulations and standards were reviewed in a separate report. Categories such as Well Location, Well Construction, Stimulation & Fracturing, Fracturing Safety Rules, Waste Management, and Seismicity were compared. Two main factors to consider in ensuring viable seal stresses will not be exceeded were hole size and mechanical properties of the cement design.

2.2.7 RECOMMENDATIONS

The outcome of this study indicates that design and operational procedures during well construction and stimulation can affect the wellbore seal integrity of an OCS well. The hazards associated with seal failure warrant development of regulations pertinent to assuring that OCS well construction and stimulation is performed in order to establish and maintain wellbore integrity. Several specific, quantifiable design attributes can be incorporated into regulations to enhance the impact of the regulations.

The dimensionless scaling relationship shows promise, but it has no field confirmation. Field application of the method will improve accuracy and confirm its utility. While one set of shale field data along with example testing of predicted failure when substituting cement with lower mechanical integrity into OCS well conditions illustrate the method's potential, significant field testing is recommended. CSI plans to offer this testing service to its clients operating in the OCS to gather initial confirmation data. A concerted field study funded in a subsequent BSEE project would produce quicker confirmation.

2.3 BACKGROUND AND REPORT STRUCTURE

Creating and maintaining wellbore integrity is vital to safe, sustainable well operation to produce hydrocarbons. Uncontrolled flow of hydrocarbons through an unsealed annular space into another zone or to the surface signals a well control issue. Severity of this uncontrolled flow ranges from minor to potentially catastrophic. Loss in integrity most commonly occurs due to failure of a cement seal placed in the annulus between one of the well's casings and the borehole wall. Primary well cementing, a common well construction operation designed to create a sealed wellbore from the surface to the target producing zone(s), is aimed to establish wellbore integrity. However, the results of these construction operations are not always successful. At times, incomplete removal of drilling fluid during cement placement produces flow paths in the annulus. Formation fluid pressures combined with hydrostatic pressure decline of the cement column as it sets can allow fluid channeling through the unset cement, resulting in short-term fluid migration. Finally, cyclic stresses created in the cement annulus by

subsequent well operations such as casing integrity testing, perforation, or hydraulic fracturing can induce cement seal failure and subsequent fluid flow paths through the annulus.

The bond between the cement sheath and the formation rock is affected by temperature and pressure changes. Drastic changes in pressure or temperature in the casing as a result of fracturing or remedial operations can affect the integrity of the cement, the cement-casing bond, or the cement-formation interface. Cement-rock interface de-bonding can also occur due to shrinking of the cement. The presence of unremoved drilling fluid due to inefficient displacement in conjunction with cement shrinkage will result in the creation of annular gaps that creates paths for gas migration. Preventive methods include proper cement designs to ensure adequate mechanical properties and to prevent shrinkage. Additionally, completion design and operation optimization can maximize cement seal placement effectiveness and minimize the effects of stresses during hydraulic fracturing operations.

This project was structured to evaluate cement seal effectiveness when stimulating OCS wells from physical modeling as well as using FEA. Developing sufficient understanding of seal failure and the system variables that govern it would identify areas that could be controlled via regulation to reduce risk of seal failure. The project was structured into tasks designed to produce this outcome. A Project Work Group of interested operators and service company personnel was commissioned to provide practical guidance and critique results. In addition to the physical modeling and FEA, tasks included literature review of cement seal failure studies, theoretical evaluation of failure modes, and evaluation of regulations established in the US and internationally.

This report is a compilation of all the project work except the analysis of existing regulations. The task progress reports written throughout the investigation are included here more or less in tact with additional data and analysis included.

3 LITERATURE REVIEW

3.1 OBJECTIVE

The Bureau of Safety and Environmental Enforcement (BSEE) contracted CSI Technologies to perform a comprehensive study of well stimulation effects on annular seal of production casing in the outer continental shelf (OCS) oil and gas operations. A significant part of this study is a literature review of current publications pertaining to the subject. This review covers the impact of well stimulation on annular seals in the OCS.

A review of the literature revealed that there are several focus areas in current publications. As a result, the literature was broken down into these focus areas for review. They include an analysis of cement mechanical properties, well stimulation techniques, and high pressure high temperature (HPHT) conditions. To assess these issues, CSI has reviewed papers from the SPE, IADC, WCP, O&G Journal, Sciencedirect, and OTC among others. Papers were selected for review and inclusion based on relevant content with priority given to newer publications.

3.2 BACKGROUND

This literature review delivers a comprehensive assessment of well stimulation effects on annular seal of production casing in the OCS oil and gas operations. It focuses on the stimulation techniques, annular seal integrity, cementing operations, and well conditions in the OCS. Annular seal integrity of production casing in the OCS is important due to the potential economic and environmental losses associated with seal failure. The stresses endured by cement in the annulus during stimulation may result in cement-casing bond failure. The mechanical properties of the cement along with the construction materials used in the production casing also play a vital role.

For proper zonal isolation, the cement needs to bond to the casing and resist induced stresses. If cement with poor mechanical properties is used, the tendency for cracks and subsequent failures that lead to micro annuli formation results. This in turn leads to gas migration. There are different types of stimulation techniques employed in the OCS. A common technology is frac packing.

Frac packing involves utilizing hydraulic fracturing and placing gravel pack screens to create high permeability fractures in formations with sanding tendency. The cyclic stresses associated with the fracturing affect cement sheath integrity. This project will evaluate the fundamental stress-strain application associated with stimulation in the OCS, study the impact of frac-packing on cement-casing bond, quantify the mechanical properties of cement

and production casing materials, and recommend any necessary changes to current stimulation techniques to help reduce annular seal failure and prevent potential HS&E threats.

3.3 SUMMARY OF SELECTED LITERATURE

Below are technical summaries of each category outlined in the Objective section. These summaries are a combination of all papers reviewed on each topic. For a detailed perspective on each reviewed paper, please see the appropriate Appendix A.1 through A.12.

3.3.1 REGULATORY INFORMATION

Offshore regulations vary widely from one office to the next. Also, at the rate at which technology is advancing, it can be difficult for regulatory bodies to keep up. In this project a full search of regulatory information for all areas will be conducted. McAndrews (2011) investigated the changes to U.S. offshore drilling safety and environmental regulations post-Macondo. In this study, the authors compare prescriptive versus performance based regulations.

For the history of offshore regulations, the US OCS has had prescriptive regulations and performance based regulations, which take a more pro-active approach to safety. McAndrews (2011) notes that safety and environmental regulation is typically only revised in response to an accident. They give examples such as the Piper Alpha event causing major regulatory changes in the North Sea. Other accidents noted for causing major regulatory changes are Exxon Valdez, Bhopal, and Texas City. A more proactive approach will aid in preventing this occurrence.

3.3.2 ANNULAR PRESSURE BUILD UP

Annular pressure build up in this project refers to gas flow in the annulus leading to an increase in pressure on the annulus. Tinsley (1980) discusses the cost of annular flow remediation. The cementing costs for this remedial work in the High Island area can run from \$20,000-\$350,000 per well. These numbers show a need to prevent annular gas flow and pressure build up from the start. Hunter (2007) presents three keys to preventing sustained casing pressure. The first is to design and pump cement systems that can withstand the effect of cyclic stresses during the life of the well. The second is to include some self-healing additives in the cement. The third mechanism is to use a swellable packer. These three techniques need to be investigated further for successful implementation in a deepwater setting.

Annular pressure build up can be due to short term or long term issues, which have been discussed in many papers. Bannerman (2005) summarized the progress of the API Work Group on annular gas prevention and

remediation. In this paper, Bannerman (2005) highlights hole geometry and engineering design as some key cementing issues when preventing annular gas flow. Cement job execution, including density fluctuations in the cement slurry, and mud removal are vital to preventing annular gas flow. Levine (1979) discusses field application techniques for annular gas flow prevention after cementing. Some techniques include minimizing cement height, pressurizing the annulus, increasing the annular mud density, multistage cementing, and using modified cement slurries. According to Nelson (2006), the time from when cement gels up to 100lb per 100sqft till it reaches 500lbs per 100sqft is referred to as the transition time.

As a result, there is a potential for fluid migration when a slurry transitions. The imbalance between the formation pressure and the hydrostatic pressure provided by the slurry during the transition time can result in fluid migration. To prevent fluid migration, cement slurries are designed such that the transition time does not exceed the time it takes for the slurry hydrostatic pressure to balance formation pressure.

3.3.3 INDUSTRY TRENDS

As the demand for energy increases, the need for more effective technology also increases. It is becoming more important to have the ability to extract more hydrocarbons from existing reservoirs which requires more efficient wells and aggressive completion operations. The industry is also trending to hotter, deeper reservoirs resulting in long, extended reach wellbores in HPHT zones. Also, new tools are being developed and introduced to improve hydrocarbon recovery.

Rivas (2009) discusses the technology needed to drill and complete extended reach deepwater wells located in a Green Canyon block in the GOM. The typical well total depth was over 28,000' with a BHP of 20,000psi and temperature of 200°F. The water depth in this area is 4,100'-4,300'. To produce this well the fracturing treatment required a prototype fracturing tool with 150,000lbs of high strength 16/30mesh proppant and a 3.88" bore frac packer. At this time, the configuration was unusual since most frac packs used a 3.25" bore packer and 20/40 mesh intermediate strength proppant.

For a cement system to withstand an aggressive stimulation treatment, it must have certain properties. Ravi (2009) discusses the importance of elasticity in cement designs; especially in wells where a cyclic load is expected. Conventional cement can withstand a large amount of stress, but is brittle and cannot return back to the original dimensions under cyclic loading. Even though most cements designed for elasticity cannot withstand as high an overall stress as conventional cements, they tend not to de-bond as easily. Hamid (2013) investigated the efficiency of a nanoparticle used as an additive to enhance cement elasticity. The additive decreased the Young's

modulus of the cement but increased the Poisson's ratio significantly and can help cement elasticity while improving zonal isolation. Introducing cements with a better tensile strength and that maintain integrity better under a cyclic load is something the industry is looking for to prevent annular gas migration.

3.3.4 WELL ARCHITECTURE

Deepwater wells tend to be further on the cutting edge of technology when compared to wells in shallow water or on land. Sanders (2011), discusses deepwater wells in the Walker Ridge blocks of the GOM. The wells had water depths greater than 8000' and downhole pressures greater than 19,000psi. The maximum deviation was 20° with the production zone in the Lower Tertiary formation. In another study Chitwood (2011) identifies several conceptual well architectures for evaluating six major areas with technology gaps. These wells were in 6000'-10,000' of water with a TVD of 17,000' and 21,000'. The KOP is 500' below the 20" casing shoe with a 3°/100' build. Both wells used a 9 5/8" production casing with a 5 1/2" completion tubing.

Sometimes, non-standard casing sizes are used to increase the number of casing strings that can be set in an HPHT deepwater well; this is presented in a study by Miller (2005). Since number of casing set points is limited by the wellhead diameter and the desired production rate, non-standard casing is sometimes used and may allow one additional set point.

3.3.5 COMPLETION DATA

Deepwater completions have always involved several complex techniques. For instance, the extreme temperature and pressure under which the production and tie-back casing strings must function will require high strength and corrosion resistance. For successful well completions, several designs, procedures, tools, and safety concerns are addressed.

Ceccarelli (2009) states that when comparing currently available modes, cased-hole frac packs and open hole gravel packs are the most reliable deepwater completion methods. Both methods are more costly and time consuming than stand-alone screens, but are significantly more reliable. Frac packs are more costly due to large volumes and high-pressure pumping. According to Riberio (1993), another significant deepwater subsea completion technique involves the use of guidelineless (GLL) lay-away subsea tree that is designed to withstand stresses imposed by 6000' ft. completion riser string with direct hydraulic type control panel.

3.3.6 FIELD CONDITIONS

Formation stresses play an important role in the development and completion of deepwater wells. The direction and magnitude of these stresses are utilized in planning for borehole stability during fracturing, and selective perforation. Li (2005) conducted integrity studies on wells located in the Mississippi Canyon Block in the Gulf of Mexico with a water depth of 5,430' and a 9 5/8" 53.5# Q-125 production casing in a 12 1/4" cemented hole. The completion method was a cased-hole frac pack using a 4 1/2" 13Cr-95 production tubing, a telescoping joint, a 5 1/2" 23# 13Cr-95 blank pipe for the frac pack, a screen on 5" 18# 13Cr-85 base pipe, and a lower sump packer. The hole deviation was 29° as a 180' perforation interval, and the formation of the production zone was fine, unconsolidated and weak sands with a porosity between 25 to 38% and a UCS of approximately 200 psi.

Deepwater wells are considered to have a water depth over 1,000' with ultra-deepwater greater than 5,000'. HPHT wells are considered to have shut-in pressures greater than 10,000 psi and a bottom hole temperature greater than 302°F. Wendler (2012) implies that Ultra-HPHT wells are considered to have temperatures greater than 425°F and pressures greater than 15,000 psi. Additionally, many deepwater wells progress through salt zones. Salt formations have a much higher conductivity than the formation through the rest of the well. In a hot area, the salt formation has a lower temperature gradient, lessening the effects from the high temperature of the surrounding formation.

3.3.7 HIGH PRESSURE HIGH TEMPERATURE CONDITIONS

HPHT conditions in deepwater present additional challenges and potential issues that can occur are casing collapse and wellbore collapse. Sabins (2006) researched technological gaps in HPHT deepwater drilling and completions in the DeepStar project. Underlying issues such as the effect of high temperatures on equipment, access to real time data, and formation data were analyzed to identify gaps between existing capabilities and required capabilities for future HPHT deepwater oil and gas exploration. Cementing gaps identified include proper sealing agents for the annulus, proper cement system design, and cement testing procedures. For completions, gaps identified include modified completion fluids and equipment, laboratory testing capabilities, and flow assurance.

Another HTHP consideration is temperature and pressure limitation of downhole tools used for completions. Development and exploration of wells with increasing temperatures and pressures also requires increased capabilities of tools and technologies. According to Mazerov (2011), limitations and considerations for selection and use of tools such as packers or valves in HTHP conditions include metallurgy, exposure to CO₂ or H₂S, type of seals, stresses caused by cyclic loading of temperature or pressure, stresses from the combined loading of both temperature and pressure, type of elastomers used in seals, and the required ID for tools and tubulars. Also, tools

may be required to be tested at higher temps or pressures than expected operating conditions according to API or ISO requirements. Examples of current tools available on the market for HTHP conditions include packers with temperature ratings up to 475°F and 20,000 psi, and cement bond log (CBL) tools with temperature ratings up to 500°F and 30,000 psi.

Studies have been performed to correlate cement sheath integrity in HPHT environments. Considering properties of the cement sheath for long term integrity is important if the well is subjected to large changes in stress levels such as with HPHT wells. According to Griffith (2004) foamed cement is at least one order of magnitude more resilient than conventional cements and is resistant to both temperature and pressure cycling induced stresses. This feature permits the cement sheath to flex while the casing expands and then returns to its original condition. Because of the flexibility, the cement sheath is less likely to be damaged over a long period of time. Bour (2000) discussed the application of foamed cement on a geothermal well with temperatures above 400° F. The foamed cement was able to withstand the cyclic loading due to temperature fluctuations in the well. Upon application, there was no migration of vapor or H₂S to the surface, nor excessive casing movement or collapse.

Patterson (2007) researched HPHT completions in the continental shelf environment of the Gulf of Mexico and stated that they have extreme completion challenges with low permeability, the opposite of most Gulf of Mexico reservoirs. HPHT wells in this category are sorted into different categories:

- Green: BHP 17,000-22,000 psi, BHT 350-425°F
- Yellow: BHP 22,000-25,500 psi, BHT 425-485°F
- Orange: BHP 25,500-28,500 psi, BHT 485-515°F
- Red: BHP 28,500 psi and up, BHT 515°F and up

In HTHP wells, some considerations must be made during the slurry design process. If downhole temperatures in the cemented string exceed 230°F, silica must be included to prevent degradation and the development of permeability. According to Nelson (2006), in HPHT areas, cements tend to show signs of thinning as they are pumped downhole which can result in dynamic settling. This requires the cement to include a viscosifier that will perform at high temperatures. Lastly, it is important to use the correct type of retarder in an HPHT area. High temperature retarders are typically a blend of two or more chemicals such as sodium borate and lignosulfonates. Nelson (2006) states that hydroxycarboxylic acids are most effective in the 300°F range.

3.3.8 STIMULATION TECHNIQUES

Stimulation techniques serve as an important tool for enhancing production. The main stimulation techniques used for oil wells include hydraulic fracturing, acid injection, and the use of explosives. For deepwater stimulation, a higher focus is placed on fracturing and acid injection. Fracturing can help bypass formation damage, improve productivity, and alleviate sand production problems. To conduct fracturing in high permeability formations, larger proppants and higher proppant quantities are required. The proppants may be pre-coated with resin to alleviate flowback problems.

Viscoelastic surfactant (VES) based diverting fluids have two major applications due to their diverting ability and non-damaging properties. According to Zeiler (2004), one major application for VES is to divert the flow to targeted damaged zone so that the stimulation efficiency is maximized. The second major application for VES is in gravel packing which is often used in Gulf of Mexico for sand control. The placement of gravel comes with acid treatment, brines or completion fluids injection before and after placement. With sand control installed, traditional diverting methods such as high pump rate, HEC gel and mechanical methods are not suitable any more. Fluid properties of VES can be modified by additive adjustment to obtain maximum performance. Several cases ranging from BHST 140°F to 290°F in the Gulf of Mexico have been demonstrated.

3.3.9 FRAC PACK

Frac pack techniques which involve a combination of fracturing and gravel packing have been widely used for completions in a wide variety of conditions. The main challenge of frac packing is to create high conductivity fractures using the tip-screen out technique and to place proppant in these fractures. Marquez (2013) states that the key aspects of frac pack completion design and installation include reservoir characteristics, well design and preparation, job execution, mechanical equipment, post job analysis/diagnostics and well startup.

To properly design a fracturing program, Haddad (2011) infers that proper attention is given to high closure stress and potential formation failure. The optimum number of treatments, fracture geometry, conductivity, and perforation interval positioning are also accounted for in the fracture program design. Frac packs are often used to stop sand from entering the wellbore. Although frac pack placement strengthens the formation rocks near the fracture, they may also weaken the surroundings of the fracturing tip where stresses are increased. The increase in stress and subsequent rock failure results in frac packing causing skin increase and a degradation of productivity index.

To prevent formation damage and productivity loss, rock stability is given adequate consideration during frac pack job designs. Saldungaray (2002) conducted a case study involving frac packing openhole completions and noted

that while open-hole frac packing can yield higher production than cased hole frac packing, it is difficult to achieve for long intervals. In order to overcome this difficulty, gravel packing above fracturing pressures is suggested. Gottschling (2005) compared open-hole and cased-hole hydraulic fracturing methods and stated that long term production is better when case-hole frac treatments are used. With regards to short term production, open hole frac yields better results due to an immediate and uninterrupted flow back being used.

Advances in frac pack techniques show that it can be applied even with a poorly cemented liner. Vilela (2004) researched a four zone well with a bad cemented liner that was completed via a frack pack method that was new at the time. To frac pack all the four zones and control the sand production, the service company used a modified washpipeless isolation system together with a high pressure retrievable washpipeless isolation system (HPRWIS) to utilize a concentric string for isolation. Patterson (2011) describes a frac packing design that combines completion setting, perforating and frack packing into one trip. This deepwater cost saving method utilizes the rig to run tubing, demobilize, and then the completion process is finished with a frack pack down the production tubing without using the rig.

3.3.10 CEMENT PERFORMANCE

There are many facets to cement performance important to a successful deepwater well from when the cement is a liquid slurry, when it has set, and through the lifetime of the well. In deepwater wells, the cement system must be placed successfully in one of the most challenging environments in the world, and then must maintain a competent seal for the life time of the well. The cement used in deepwater wells varies from well to well, and from surface to production string.

The focus of this project is cement performance during stimulation; however this depends on good execution of the cement job. Ravi (2010) states that effective stimulation of a reservoir requires hole cleaning and slurry placement in the entire annulus. In the book, *Well Cementing* by Nelson (2006), mud removal is well documented. Sufficient mud displacement is required to provide complete and permanent isolation of the formations behind the casing with cement. One of the first steps is mud conditioning to modify the mud's properties, typically achieved by circulating two annular volumes of mud at the highest rate possible without experiencing losses. This helps to clean cuttings out of the hole, homogenizes the mud, and reduces the yield stress and plastic viscosity making it easier to displace the mud with another fluid.

Good cement performance requires good placement techniques. Cements placed in a horizontal section are susceptible to settling, leading to free water formation and solids settling out. It is important to optimize the rheology for the fluids to prevent settling and reduce the friction pressure. Also, pipe centralization and

movement are both critical to cement placement. Both aid in providing a cement sheath that covers the full annulus. Pipe movement can be helpful in the horizontal section where centralization is difficult. The use of centralizers help keep the casing away from the previous casing or open hole walls. Centralized casing allows for flow on all sides of the annulus. In an ideal centralized case with 100% standoff, the casing is centered in the middle of the hole or previous casing with a uniform annular space around the OD.

When the casing is in contact with the hole or ID of the previous casing, the standoff is 0%, and fluid flow occurs primarily in the wide sides of the annulus. Centralizers are used to increase the standoff as much as operationally possible to improve the quality of mud removal and cement. Since fluid velocity will be faster on the wide side of the annulus, increasing the standoff reduces the risk of channeling caused by slower flow in the narrow side of the annulus. API RP 10D-2 recommends a minimum of 67% standoff for casing bow-spring centralizer performance; however this specification is not a requirement for casing centralization in general. Within the industry, 75% minimum is often considered to be preferable for cementing. Centralizer placement to achieve desired casing standoff is calculated using centralizer spacing programs generally available in the industry. These algorithms consider factors such as wellbore geometry, deviation, type of centralizers used, and distance between centralizers to calculate casing standoff. Additionally, many placement simulators and models can estimate standoff and mud removal efficiency using these factors.

Other considerations for centralizer selection and placement include centralizer clearance, since the centralizer will need to pass through the ID of previous casing strings and provide standoff in larger diameter hole sections, and running force required to run the centralizers, since centralizers add friction while running in hole. Large friction or drag forces from running centralizers could prevent the casing from reaching the bottom of the hole, and also increases the hook load on the rig. Overall, the casing selection and placement process is a balance between operational considerations for cementing and installation consideration for the centralizers and casing.

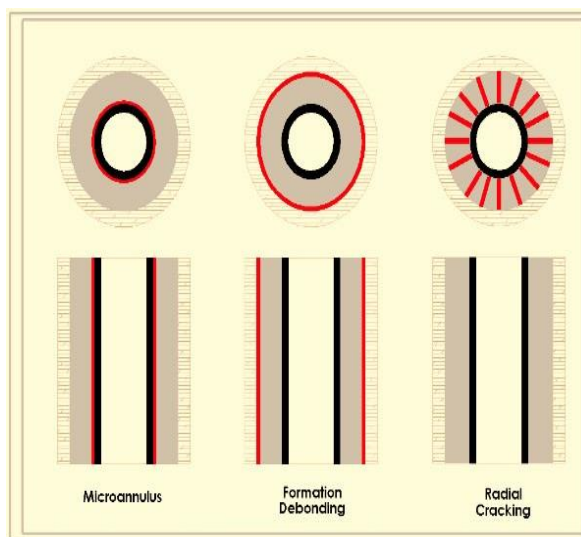
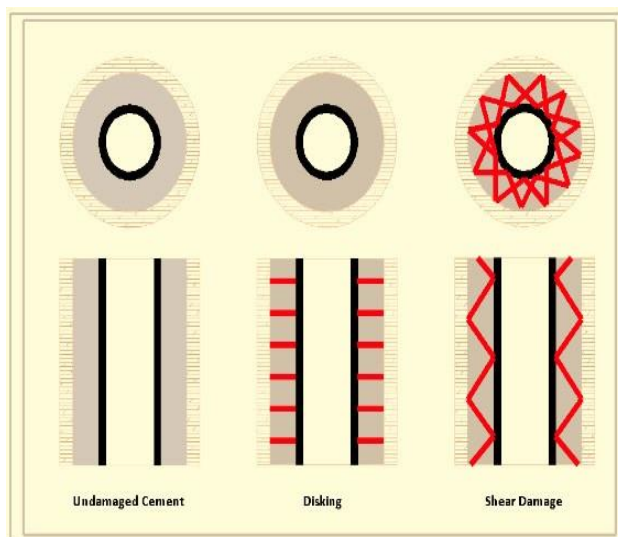
Long term cement performance is important to good cement integrity during stimulation. Hakan (2013) discusses the development of permeability in a cement sheath and how controlling gas flow through the sheath is important. Properties of cement that can lead to permeability include low density, excessive fluid loss, high shrinkage, and inconsistent mixing. These can lead to porosity and voids in the cement matrix creating a weak cement sheath around the casing, resulting in poor stimulation performance.

The cement bond to the casing is the major focal point of this project. Lecampion (2013) investigated a mathematical model fluid driven de-bonding of the wellbore annulus. De-bonding of this type has been

recognized since the 1960's to be the cause of leaks occurring from wellbores. Lecampion's paper recognizes and focuses on the de-bonding that occurs during injection. Lecampion (2011) discusses de-bonding during the injection of CO₂. This paper states that cement may de-bond from the casing or formation due to depressurization and thermal cooling that takes place after the cement placement or upon injection. Operations that induce pressure and temperature fluctuations can lead to three different defects: diskings cracks, radial cracks, and micro annulus as shown in Figures 1 and 2. Prevention of these defects can be achieved with careful cement placement, expanding cement systems and properly designed packers.

FIGURE 1: CEMENT SHEATH FAILURE MODES

FIGURE 2: CEMENT SHEATH FAILURE MODES



The casing to cement bond can also be analyzed using computer modeling. Teodoriu (2010) developed a model to predict the performance of the casing to cement bond under HPHT conditions during the life of the well. This model considers the casing as a thin wall cylinder while the cement and formation are thick walls. The authors studied the effect of temperature, pressure and casing/cement interactions on the integrity of different cement systems. They found some cements have improved annular seal under HPHT conditions than others.

3.3.11 CEMENT MECHANICAL PROPERTIES

For a proper zonal isolation and annular seal, the cement needs to be able to withstand stresses from various sources. The mechanical properties of cement determine how well the cement will bond to the casing and/or formation. As a result, the mechanical properties of cement can help determine effective annular seal bonds. According to Tellisi (2005), the information obtained from mechanical properties testing is just as vital to examine as the industry standard of compressive strength testing.

In the Minerals Management Service (MMS) report, Sabins (2002) studied the long term impact of stresses and compaction on cement integrity in deepwater wells. The ability of a cement system to provide proper zonal isolation and annular seal was evaluated. The project focused on the mechanical properties of the cement and induced cyclic stresses. CSI technologies performed laboratory testing while the University of Houston set up representative models. The annular seal tests were run using two different pipe configurations to simulate conditions in deepwater wells.

The Pipe-in-Soft configuration had cores made from plastisol surrounding the slurry while the Pipe-in-Pipe configuration used cores made inside iron pipes to provide an outer restrictive force on the core. According to Sabins (2002), results obtained indicated the Pipe-in-Pipe configuration had better stability at high loading. The Pipe-in-Soft configuration failed at high loading. The properties of the cement and its thickness influenced the stress distribution in the Pipe-in-Soft configuration but had negligible effects on the Pipe-in-Pipe configuration.

Due to changing well conditions, most deepwater wells require flexible cement slurry systems that withstand critical stresses. Mechanical properties such as Young's modulus, Tensile strength, Poisson's ratio and Compressive strength give an indication of cement sheath durability. Darbe (2008) states that due to exposure to high thermal and pressure stresses in deepwater, enhancing the mechanical properties of cement is critical to ensure zonal isolation and annular seal integrity. Other stresses on the cement include internal shrinkage during hydration which could result in cracking or a micro annulus.

Cement expansion due to temperature or pressure stresses can cause cement failure. Elasticity is very important to the life of a cement sheath especially with regard to wells that will undergo cyclic loading. Standard cement can withstand a large amount of stress. However, cement is brittle and does not easily deform or return back to original dimensions under cyclic loading. Cement can de-bond from either the casing or formation under these conditions. Additionally, cement cannot be cycled many times before failing. Ravi (2009) states that more elastic cement slurries cannot sustain as high of an overall stress as standard cement but due to elasticity the cement is less likely to de-bond while exposed to cyclic loading. Mechanical properties can be modified through the addition of elastomers to decrease the Young's modulus, which increases the cement's capability to deform elastically under stress, and the addition of fibers to increase tensile strength, which increases the cement's failure tolerance.

3.4 SHALE CEMENT PERFORMANCE ANALOGY

While not specifically deepwater, shale cementing requires highly engineered processes and fluids to be successful. Shale wells typically have long horizontal sections and many are in high pressure, high temperature (HPHT) areas that may require fracturing to achieve expected production. These challenges are reflected in deepwater drilling as well.

Cement stability is an important issue in HPHT shale wells. Under the HPHT conditions, cement systems tend to settle severely when compared to lower temperatures and pressures. Williams (2011) designed a system using particle size distribution technology to minimize settling in an HPHT horizontal well. This improves the cement coverage, giving consistent mechanical properties around the casing. Full cement coverage will ensure the cement sheath can perform to the highest of its potential.

Seal durability is also important in shale wells. This can be determined by evaluating cement mechanical properties. McDaniel (2014) identified several properties important in evaluating cement sheath durability. These properties included Young's modulus, Poisson's ratio, anelastic strain (a non-standard mechanical property describing the magnitude of plastic strain occurring due to cyclic stresses on the cement below the composition's elastic limit and discussed in detail later in this report), impact strength and tensile strength. This paper stated that mechanical durability cannot be based solely on compressive strength but needs to incorporate other facets of cement performance as well. The dimensionless variables developed in this study incorporated cement and wellbore properties to predict properties needed to prevent failure during post cementing operations.

Stated in both of the above referenced papers is the importance of good cement placement techniques. This includes several aspects related to good mud removal. Centralization needs to be adequate for even flow around the pipe, which helps lead to complete cement coverage. Mud should be adequately conditioned for displacement, and pipe movement should be incorporated into cement jobs as much as possible to removed gelled mud or settled solids.

4 FAILURE MODE

4.1 OBJECTIVE

The objective of this section is to evaluate possible failure modes of an Outer Continental Shelf (OCS) well casing-cement-formation system due to stresses applied during stimulation operations. The evaluation includes typical OCS well architectures, materials, and conditions. Stresses generated during stimulation operations and potential failure mechanisms resulting from those stresses are categorized and generally quantified. The potential impact of each failure mode is then assessed considering materials, well conditions and timing of stimulation operations. The resulting influence of failure on wellbore integrity is evaluated and categorized according to likelihood and degree of impact on the well.

4.2 BACKGROUND

Creating and maintaining wellbore integrity is vital to safe, sustainable well operation to produce hydrocarbons. Uncontrolled flow of hydrocarbons through an unsealed annular space into another zone or to the surface signals a well control issue. Severity of this uncontrolled flow ranges from minor to potentially catastrophic. Loss in integrity most commonly occurs due to failure of a cement seal placed in the annulus between one of the well's casings and the borehole wall. Primary well cementing, a common well construction operation designed to create a sealed wellbore from the surface to the target producing zone(s), is aimed to establish wellbore integrity. However, the results of these construction operations are not always successful. At times, incomplete removal of drilling fluid during cement placement produces flow paths in the annulus. Formation fluid pressures combined with hydrostatic pressure decline of the cement column as it sets can allow fluid channeling through the unset cement, resulting in short-term fluid migration. Finally, cyclic stresses created in the cement annulus by subsequent well operations such as casing integrity testing, perforation, or hydraulic fracturing can induce cement seal failure and subsequent fluid flow paths through the annulus.

The bond between the cement sheath and the formation rock is affected by temperature and pressure changes. Drastic changes in pressure or temperature in the casing as a result of fluid swapping, fracturing or remedial operations can affect the integrity of the cement, the cement-casing bond, or the cement-formation interface. Cement-rock interface de-bonding can also occur due to shrinking of the cement. The presence of unremoved drilling fluid due to inefficient displacement in conjunction with cement shrinkage will result in the creation of annular gaps that creates paths for gas migration. Preventive methods include proper cement designs to prevent shrinkage, and completion operations optimization to minimize the effect of pressure changes in the casing during hydraulic fracturing operations.

Mechanical properties of the cement systems govern cement reaction to cyclic stresses and impact. Parameters such as the Young's Modulus and Poisson's Ratio give a guideline as to how cement slurries will perform under these conditions. It must be emphasized, however, that failure of a cemented annular seal is a complex mechanism governed by more than just one or two mechanical properties of the cement. The nature and properties of all materials making up the casing-cement-formation system play a part in the system's integrity; e.g. casing and annular dimensions, annular dimensions, drilling fluid removal, drilling fluid filter cake deposits, formation stiffness, wetted state of formation and casing, and timing of casing integrity testing, perforation and stimulation. These many variables necessitate a systems approach to evaluation of mechanical integrity including numerical modeling and laboratory performance testing of the entire system.

4.3 STUDY WELL CONDITIONS

The literature review delivered three representative well descriptions for this study. The descriptions for these study wells are included below for reference in discussion of well conditions, casing-cement-formation system parameters, and stimulation effects. Information regarding bottom-hole treating pressure and bottom-hole temperature effects during typical hydraulic fracturing or frac pack treatments were added to this summary.

TABLE 1: WELL DESCRIPTIONS

Data Type	Shelf	Deepwater, Shallow target	Deepwater, Deep target
BHT (°F)	275	155	250
BHP (psi)	9500	8000	17000
MD (ft)	13900	14000	25600
TVD (ft)	12100	13500	25000
Water Depth (ft)	250	5000	5000
Deviation (°) and KOP	35°	25°	20°
Formation lithology	Sandstone, Shale	Sandstone, Shale	Sandstone, Shale
Formation properties	20% porosity	35% porosity	30% porosity
Production OH size (in)	8.50	12.250	12.25
Production Casing size (in)	7.00	9.875	9.625
Production Casing weight (lbs)	38.00	62.80	53.50
Production casing grade	Q-125	Q-125	Q-125
Production tubing size (in)	2.875	4.50	3.50
Production tubing weight (lbs)	6.500	12.75	9.30
Production tubing grade	N-80	HYP 13 Cr	13 Cr 110 BTS-8
Completion type	Frac pack, HRWP	Frac pack, Diesel	Frac pack, Matrix acid, Diesel
Completion fluid type	CaCl ₂ , ZnBr ₂	CaBr ₂ , CaCl ₂	CaBr ₂ , CaCl ₂
Completion fluid density (ppg)	10.40	11.80	15
Perforated section length (ft)	150	100	200
Number of completed stages	8	2	2
Treating Temperature Change(°F)	100 Cooler	40-50 Cooler	100 Cooler
Change in bottom hole pressure	Bottom Hole Treating Pressure starts at 1000 psi above hydrostatic and builds to 3000 psi		
Frac thru casing or tubing	Frac thru tubing, packer set 100' above pay zone, 150' of casing exposed to pressures		
Production string OH or cemented	Cemented	Cemented	Cemented

Cement designs for each example well type are listed below:

TABLE 2: DEEPWATER DEEP TARGET, BHST – 250°F, BHCT - 189°F

Materials	Concentration
Class H	
Silica Flour	20% bwoc (DB)
Silica Sand	15% bwoc (DB)
Antifoam	0.020 gal/sk
Dispersant	0.040 gal/sk
Fluid loss	0.120 gal/sk
Fluid loss	0.250 gal/sk
Free water	0.010 gal/sk
Retarder	0.060 gal/sk
KCL (3%)	3.000%bwow
Slurry yield	1.41 ft ³ /sk
Slurry Density	16.40 ppg

TABLE 3: DEEPWATER SHALLOW TARGET, BHST – 155°F, BHCT - 120°F

Materials	Concentration
Class H	
Antifoam	0.020 gal/sk
Retarder	0.040 gal/sk
Dispersant	0.120 gal/sk
KCL (3%)	3.000%bwow
Slurry yield	1.08 ft ³ /sk
Slurry Density	16.40 ppg

TABLE 4: SHELF, BHST- 275°F, BHCT - 195°F

Materials	Concentration
Class H	
Silica Flour	20% bwoc (DB)
Silica Sand	15% bwoc (DB)
Antifoam	0.020 gal/sk
Dispersant	0.040 gal/sk
Fluid loss	0.120 gal/sk
Fluid loss	0.250 gal/sk
Free water	0.010 gal/sk
Retarder	0.060 gal/sk
KCL (3%)	3.000%bwow
Slurry yield	1.41 ft ³ /sk
Slurry Density	16.40 ppg

Note that these designs which are representative of those currently used by operators in OCS, are normal density and designed to minimize settling and free fluid. The mechanical properties of these systems are representative of standard cement compositions used for these applications.

4.4 FINDINGS FROM TASK 2 LITERATURE REVIEW

Based on the literature review of published industry technical reports, papers and articles conducted in Section 2 of this report, it was found that cyclic stresses on conventional cement systems can lead to an ineffective seal. The lack of a proper seal for zonal isolation serves as a pathway for gas migration. The sources of these stresses include changes in temperature and pressure endured during production operations in the OCS. The tendency of the cement sheath to succumb to these changes is dependent on the mechanical properties of the designed slurry used in the production string and the magnitude of the cyclic stresses. Findings from the literature review show that while most conventional cements can withstand large stresses, they are brittle and often fail to regain normal design properties under cyclic loading. As a result, there is an increased potential for cement to de-bond from the casing after exposure to cyclic stresses. The addition of additives to make cement elastic in nature was shown to be an effective means of reducing the impact of cyclic stresses. The resulting increased tensile strength of the cement helps maintain wellbore integrity.

4.5 INVESTIGATION OF POSSIBLE FAILURE MODES AND RANGES OF STRESSES

The pressure and temperature changes occurring during a stimulation (hydraulic fracturing or frac-pack) treatment listed in the summary table indicate that stresses generated are too low to plastically deform the casing. Additionally, casing integrity tests performed prior to perforation would identify any weak points at connections. Thus, it can be assumed for this study that no structural damage to the casing will be created by a stimulation treatment. This assumption will be confirmed by numerical modeling and during lab-scale testing. The magnitude of stress imposed by the change in pressure and temperature can impart significant stress to the cement as well as the interfaces with casing and formation.

In the OCS, cement sheath failure can occur due to:

- Stress-induced tensile failure of the cement
- Micro-annulus formation from temperature and pressure cycling
- Shear failure of the cement/casing interface

These failure modes are illustrated and discussed below.

4.5.1 STRESS-INDUCED TENSILE FAILURE OF THE CEMENT

Stresses imposed on the cement sheath during post-cementing or pre-production operations can come from pressure testing the casing, perforating, well injection operations, and hydraulic fracturing operations. Due to the difference in deformation characteristics between cement, casing, and the formation, stresses generated tend to

concentrate at the boundaries between casing/cement/formation. The stresses can be propagated radially and tangentially along the cross-section. As stated by Mueller (2004), most tangential stresses are usually tensile while most radial stresses are compressive in nature. Production operations that involve pressure and temperature fluctuations can give rise to formation de-bonding, radial cracking and micro-annulus formation as depicted in Figure 3. Pumping operations during well intervention (stimulation, cementing, completion fluid placement, etc.) will induce thermal and mechanical stresses on the cementing casing. In fact, any intervention of production even without pumping operations (e.g. shut in for hurricane) will induce thermal and pressure gradients throughout the wellbore as pressure increases to shut-in pressure and temperature up the hole cools to static equilibrium temperature.

FIGURE 3: CEMENT SHEATH FAILURE MODES

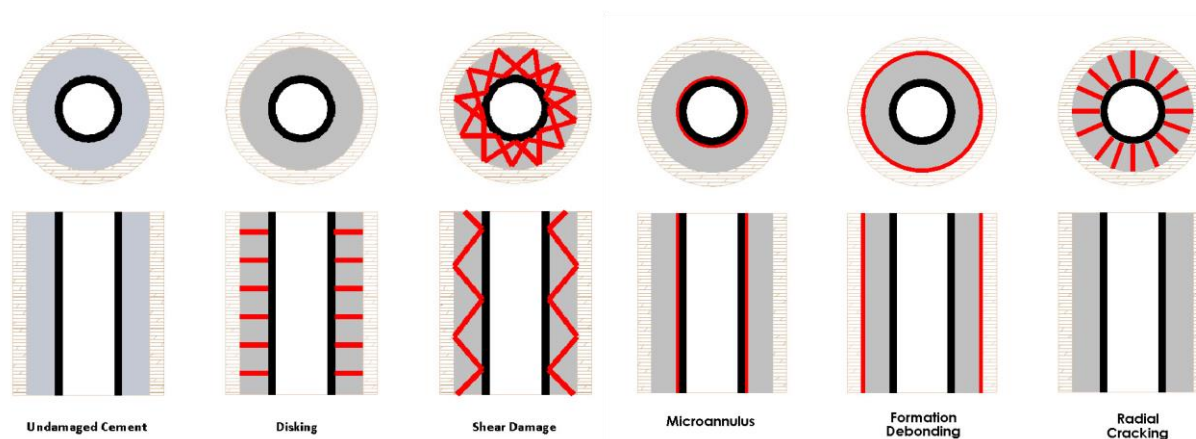
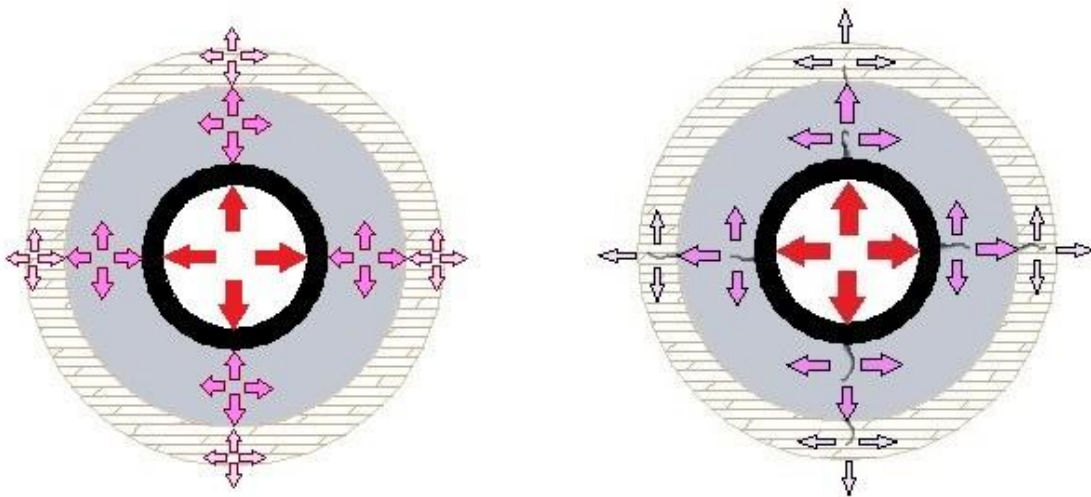


Figure 4 depicts stresses induced by increasing pressure or temperature. As stated stress gradients can occur at each interface due to contrasts in Young’s Modulus of the abutted materials. In the case of the study wells, it is significant to note that stiffness of the formations are similar to those of the cements designed for each production cementing application. Therefore, compressive stress concentration due to stiffness contrast will not be a factor under the study conditions. Thus, the radially-induced stress damage to the cement sheath will be tensile failure. The value of tensile strength must therefore be closely evaluated to ensure that it is sufficient to withstand the magnitudes of stress generated by stimulation. This evaluation must include early time strength development to account for stresses induced by casing integrity testing if performed after the cement sets.

FIGURE 4: STRESSES INDUCED IN THE CASING-CEMENT-FORMATION SYSTEM BY PRESSURE OR TEMPERATURE INCREASES INSIDE THE CASING



Hydraulic fracturing operations such as frac packing utilize high viscosity fluids that are pumped above the fracturing pressure. The high pressures involved and the number of cycles initiated to perforate the well can induce compressive and tensile stresses on the cement sheath. Wang (2014) stated that annular failures, transverse, and longitudinal fractures may occur during hydraulic fracturing operations that affect cement sheath integrity. The cement sheath is affected due to the presence of large fluids and a fluctuation in pressures at perforations. Depending on the mechanical properties of the cement such as the Young's Modulus and tensile strength, the cement may fail and the long term integrity of the cement sheath may be compromised. During cement slurry design, heavy emphasis is placed on the compressive strength development.

While a cement system may develop strength, set, and provide zonal isolation, the tensile strength of the slurry gives a better indication of how the cement sheath will respond to tangential stresses. Mueller (2004) developed correlations that model the stresses endured by the cement sheath during hydraulic fracturing. The simulation involved a 5500 psi hydraulic fracturing treatment on a well at 14,000 ft. and 290°F. The Young's Modulus of the cement was 12.4 GPa. Results showed a high stress concentration at the cement/casing boundary with radial stress of 1169 psi in compression and tangential stress of 530 psi in tension. Most cement slurries designed used in the production string have tensile strengths lower than 500 psi. An operation where the tensile strength of the slurry is constantly exceeded will lead to cement failure. Cement systems designed for OCS production strings

commonly have a recommended minimum Young's Modulus of 580 kpsi, Poisson's Ratio of 0.2 or higher and a tensile strength of 150 psi. Comparing with the results shown by Mueller (2004) indicates potential tensile failure for systems with tensile strengths lower than 500 psi.

Well deviation angle and timing of casing integrity testing also play a part in tensile failure of a cement sheath. Yuan (2012) conducted research that shows that the angle determines the magnitude of the stress impact. In the study it was shown that as angle increased from 0 to 40 degrees, the resultant stress and strain on the cement increased. Between 40 and 50 degrees, the highest stress was noticed and as such the potential for failure is highest at this point. As the inclination increases from 50 to 90 degrees the stress impact reduces.

Also, the process of pressure testing the casing after cementing can stress the casing-cement-formation system if wells are subjected to production casing integrity testing within 48 - 72 hours after cement is placed. While the minimum test pressures are usually limited to about 70% of the casings minimum internal yield, the pressures are large enough to affect long term cement integrity. Investigations conducted by Mueller (2004) in a specific case shows that pressure testing the casing to 4000 psi results in radial stress of 1061 psi in compression and tensile stress of 583 psi at the cement casing boundary. Since most field cement slurries are not designed with tensile strengths up to 583 psi, stresses incurred in such situations will lead to tensile failure. A second significant point to consider when assessing effects of casing integrity testing against set cement is that the test affects the entire cemented casing length. In contrast, the length of casing to which stimulation pressures are applied is limited to that below the packer depth. Thus, damage caused by casing integrity testing can affect the entire production casing annulus.

4.5.2 MICRO-ANNULUS FORMATION FROM REPEATED TEMPERATURE AND PRESSURE CYCLING

Seal failure resulting from cement plastic deformation caused by low-magnitude, cyclic stresses was first reported from the MMS project, "Long-term Integrity of Deepwater Cement Systems Under Stress/Compaction Conditions (Sabins, 2002). Since then, numerous investigators have discussed this behavior of Portland cement to plastically deform with stress application below its elastic limit. General theory for this behavior is that the plastic deformation results from micro failures of the cement matrix that form the pore walls of the composite material. Thus, the cement matrix does not appear to deform plastically, however strain hysteresis becomes evident with repeated stress cycling below the failure limit of the cement. This anelastic strain is exaggerated with decreased density and increased dilution of the cement.

When considering the effect of anelastic strain on integrity of a production casing-cement-formation annulus, it is easy to visualize that outward strain of the casing caused by pressure increase would strain the cement outwardly also. When stress is removed, the casing will contract elastically while the cement may not. The magnitude of this hysteresis can lead to micro annulus formation.

4.5.3 SHEAR FAILURE OF THE CEMENT/CASING INTERFACE

The bonding between the cement sheath and casing can be affected by temperature decreases occurring when fracturing fluid is injected down the wellbore. Cooling effects of this injection are estimated in the Well Conditions Table above. The coefficient of thermal expansion is much greater for steel than for cement. Thus cooling the casing will result in greater axial and radial strain for the casing than for the adjacent cement. The axial strain can be sufficient to break the bond of cement to casing. Radial casing strain will be countered by pressure increase. Magnitudes of these opposing strains and resulting stress are addressed in sections 4-6.

4.5.4 INADEQUATE QUALITY CONTROL PROCEDURES/CEMENTING PRACTICES PRIOR TO PRODUCTION

The design criteria and cementing procedures utilized for the production string have an effect on well integrity. The cement slurry design determines how the system will react to the stresses incurred during production. Mechanical properties of the cement such as the Young's Modulus, Tensile Strength, and Compressive strength development determine if a cement system will crack or fail under, tension, shear, or compression. Most field cement designs have tensile strengths lower than 500 psi. Research has shown that induced stresses on the cement sheath/casing interface can exceed 500 psi and will lead to tensile failure. Also, the time lag between initial production activities and when the cement sets is a crucial factor. With the exception of casing pressure testing, most fracturing and stimulation operations occur at least 2 weeks after cementing. Operations that occur earlier than the time required for the cement design to develop compressive strength will compromise the cement sheath integrity. Accounting for cementing placement practices and degree of success results in more realistic evaluation of induced stress effects.

4.6 SUMMARY

Integrity of the production-cement-formation system is crucial to optimum production over the well's life operationally, financially and environmentally. Stresses induced in the system by stimulation can result in seal failure in the cemented annulus. These failures can be tensile failure of the cement or de-bonding of the cement due to plastic deformation from micro-cracking or shear stress. These primary failure modes will be extensively explored for the subject well conditions and will be investigated via Small Scale Annular Seal testing and Finite Element Analysis (FEA) to expand the understanding of system conditions on cement durability.

5 PHYSICAL MODELING

5.1 OBJECTIVE

The objective of this section is to present and analyze results of both small and large-scale laboratory testing and analysis to evaluate the effect of stimulation treatments on cement and casing bond integrity.

5.2 BACKGROUND

The results from the Failure Mode Report quantified the potential failure modes of OCS well casing-cement-formation systems caused by stresses imposed by stimulation treatments. These results indicated most probable modes and locations of failure were in the cement at the casing cement interface or at the cement-formation interface. These locations along with the mechanically and thermally induced stresses generated during performance of a stimulation treatment are the focus of investigation for the remainder of this project.

Mechanical properties of the cement compositions govern cement reaction to cyclic stresses and impact. Parameters such as the Young's Modulus and Poisson's Ratio give a guideline as to how cement slurries will perform under these conditions. It must be emphasized, however, that failure of a cemented annular seal is a complex mechanism governed by more than just one or two mechanical properties of the cement. The nature and properties of all materials making up the casing-cement-formation system play a part in the system's integrity; e.g. casing and annular dimensions, annular dimensions, drilling fluid removal, drilling fluid filter cake deposits, formation stiffness, wetted state of formation and casing, and timing of casing integrity testing, perforation and stimulation. These many variables necessitate a systems approach to evaluation of mechanical integrity including numerical modeling and laboratory performance testing of the entire system.

This holistic, systems approach required incorporation of a broad array of mechanical properties testing of the cement compositions chosen for this investigation as well as cyclic mechanical and thermal stress testing of cement cast into a small-scale annulus. The results of this testing and engineering analysis of the resulting data are presented below.

5.3 TEST CONDITIONS

The Project Work Group provided well conditions for three types of OCS wells: Shelf, DeepWater, Shallow Target (DWST) and DeepWater, Deep Target (DWDT). These data supplemented with results from the Literature Review and Failure Mode reports, delivered three representative well descriptions for this study, including HTHP conditions. The descriptions for these study wells are included below for reference in discussion of well conditions, casing-cement-formation system parameters, and stimulation effects. Information regarding bottom-

hole treating pressures and temperatures during typical hydraulic fracturing and frac pack treatments on each representative well type were added to this summary.

TABLE 5: WELL CONDITIONS FOR OCS WELL TYPES

Well Conditions	Shelf	Deepwater, Shallow target	Deepwater, Deep target
BHT (°F)	275	155	250
BHP (psi)	9500	8000	17000
MD (ft)	13900	14000	25600
TVD (ft)	12100	13500	25000
Water Depth (ft)	250	5000	5000
Deviation (°)	35°	25°	20°
Formation lithology	Sandstone, Shale	Sandstone, Shale	Sandstone, Shale
Formation properties	20% porosity	35% porosity	30% porosity
Production OH size (in)	8.50	12.250	12.25
Production Casing size (in)	7.00	9.875	9.625
Production Casing weight (lbs)	38.00	62.80	53.50
Production casing grade	Q-125	Q-125	Q-125
Production tubing size (in)	2.875	4.50	3.50
Production tubing weight (lbs)	6.500	12.75	9.30
Production tubing grade	N-80	HYP 13 Cr	13 Cr 110 BTS-8
Completion type	Frac pack, HRWP	Frac pack, Diesel	Frac pack, Matrix acid, Diesel
Completion fluid type	CaCl ₂ , ZnBr ₂	CaBr ₂ , CaCl ₂	CaBr ₂ , CaCl ₂

THIS REPORT WAS INADVERTENTLY DISSEMINATED IN THE PUBLIC DOMAIN/ONLINE SINCE 09/2015 WITHOUT A DISCLAIMER. DISCLAIMER HAS BEEN ADDED – “THIS INFORMATION IS DISTRIBUTED SOLELY FOR THE PURPOSE OF PEER REVIEW UNDER APPLICABLE INFORMATION QUALITY GUIDELINES. IT HAS NOT BEEN FORMALLY DISSEMINATED BY BSEE. IT DOES NOT REPRESENT AND SHOULD NOT BE CONSTRUED TO REPRESENT ANY AGENCY DETERMINATION OR POLICY

Completion fluid density (ppg)	10.40	11.80	15
Perforated section length (ft)	150	100	200
Number of completed stages	8	2	2
Treating Temperature Change(°F)	62°F Cooler	58°F Cooler	87°F Cooler
Change in bottom hole pressure	Bottom Hole Treating Pressure starts at 1000 psi above hydrostatic and builds to 3000 psi		
Frac thru casing or tubing	Frac thru tubing, packer set 100' above pay zone,		
Production string OH or cemented	Cemented	Cemented	Cemented
Fracture treatment volumes (gal)	15,000	36,500	81,500
Fracture treatment rates (bpm)	16	30	40

Cement designs for each example well type are listed below along with results of normal design performance testing that illustrate the applicability of each composition to the well conditions.

TABLE 6: DEEPWATER DEEP TARGET, BHST - 250°F, BHCT - 189°F

Materials	Concentration
Class H	
Silica Flour	20% bwoc (DB)
Silica Sand	15% bwoc (DB)
Antifoam	0.020 gal/sk
Dispersant	0.040 gal/sk
Fluid loss	0.120 gal/sk
Fluid loss	0.250 gal/sk
Free water	0.010 gal/sk
Retarder	0.060 gal/sk
KCL (3%)	3.000%bwow

THIS REPORT WAS INADVERTENTLY DISSEMINATED IN THE PUBLIC DOMAIN/ONLINE SINCE 09/2015 WITHOUT A DISCLAIMER. DISCLAIMER HAS BEEN ADDED – “THIS INFORMATION IS DISTRIBUTED SOLELY FOR THE PURPOSE OF PEER REVIEW UNDER APPLICABLE INFORMATION QUALITY GUIDELINES. IT HAS NOT BEEN FORMALLY DISSEMINATED BY BSEE. IT DOES NOT REPRESENT AND SHOULD NOT BE CONSTRUED TO REPRESENT ANY AGENCY DETERMINATION OR POLICY

Slurry yield	1.41 ft ³ /sk
Slurry Density	16.40 ppg

TABLE 7: DEEPWATER SHALLOW TARGET CONVENTIONAL DESIGN, BHST - 155°F, BHCT - 120°F

Materials	Concentration
Class H	
Antifoam	0.020 gal/sk
Retarder	0.10 gal/sk
Dispersant	0.03 gal/sk
KCL (3%)	3.00%bwow
Slurry yield	1.08 ft ³ /sk
Slurry Density	16.40 ppg

TABLE 8: DEEPWATER SHALLOW TARGET RESILIENT, BHST - 155°F, BHCT - 120°F

Materials	Concentration
Class H	
Antifoam	0.050 gal/sk
Retarder	0.15% bwoc
Dispersant	0.10 gal/sk
Fluid Loss	2.00 gal/sk
Stabilizer	0.20 gal/sk
Slurry yield	1.14 ft ³ /sk
Slurry Density	15.9 Ppg

THIS REPORT WAS INADVERTENTLY DISSEMINATED IN THE PUBLIC DOMAIN/ONLINE SINCE 09/2015 WITHOUT A DISCLAIMER. DISCLAIMER HAS BEEN ADDED – “THIS INFORMATION IS DISTRIBUTED SOLELY FOR THE PURPOSE OF PEER REVIEW UNDER APPLICABLE INFORMATION QUALITY GUIDELINES. IT HAS NOT BEEN FORMALLY DISSEMINATED BY BSEE. IT DOES NOT REPRESENT AND SHOULD NOT BE CONSTRUED TO REPRESENT ANY AGENCY DETERMINATION OR POLICY

TABLE 9: DEEPWATER SHALLOW TARGET LOW-DENSITY, BHST - 155°F, BHCT - 120°F

Materials	Concentration
Class H	
Retarder	0.20% bwoc
Extender	2.50% bwoc
Extender	7.00% bwoc
Fluid Loss	0.40% bwoc
Fluid Loss	0.30% bwoc
Antisettling agent	0.20 gal/sk
Slurry yield	1.58 ft ³ /sk
Slurry Density	13.0 ppg

TABLE 10: SHELF, BHST - 275°F, BHCT - 195°F

Materials	Concentration
Class H	
Silica Flour	20% bwoc (DB)
Silica Sand	15% bwoc (DB)
Antifoam	0.020 gal/sk
Dispersant	0.040 gal/sk
Fluid loss	0.120 gal/sk
Fluid loss	0.250 gal/sk
Free water	0.010 gal/sk
Retarder	0.060 gal/sk
KCL (3%)	3.000%bwow

THIS REPORT WAS INADVERTENTLY DISSEMINATED IN THE PUBLIC DOMAIN/ONLINE SINCE 09/2015 WITHOUT A DISCLAIMER. DISCLAIMER HAS BEEN ADDED – “THIS INFORMATION IS DISTRIBUTED SOLELY FOR THE PURPOSE OF PEER REVIEW UNDER APPLICABLE INFORMATION QUALITY GUIDELINES. IT HAS NOT BEEN FORMALLY DISSEMINATED BY BSEE. IT DOES NOT REPRESENT AND SHOULD NOT BE CONSTRUED TO REPRESENT ANY AGENCY DETERMINATION OR POLICY

Slurry yield	1.41 ft ³ /sk
Slurry Density	16.40 ppg

Two cement compositions (resilient and low-density) were added to the Deepwater Shallow Target design scenario to broaden the testing beyond the basic cement compositions routinely employed. Resilient cement is used to reduce risk of cement mechanical failure. Chance of lost circulation can dictate the need for low-density cement. Both these compositions are designed to provide adequate handling time for placement, adequate fluid loss control, and to minimize settling and free fluid. Operators cementing an actual well may choose to design lower rheology depending on drilling fluid and spacer rheology as well as specific wellbore conditions. The mechanical properties of these systems are representative of the range of standard cement compositions used for these applications.

5.4 RESULTS AND DISCUSSION

5.4.1 SMALL SCALE PHYSICAL MODELING

Wellbore stresses experienced during stimulation treatments were simulated in the lab to determine how pressure and temperature cycling during stimulation affects bond and seal integrity. Testing for conventional performance properties included Density, Rheology, Fluid Loss, Free Fluid, Thickening Time and Compressive Strength (Table 11). Descriptions of these tests are found in Appendix B. Testing also included mechanical property evaluation including compressive strength, tensile strength, Young’s modulus and Poisson’s Ratio (Table 12). Coefficient of thermal expansion, heat capacity, and thermal conductivity were also measured for each cement as input for analysis of thermal cycling effects. Procedures followed for this mechanical and thermal property testing are described in Appendix B. A non-standard physical property, termed anelastic strain, was determined for each composition. This property describes the magnitude of plastic strain occurring due to cyclic stresses on the cement below the composition’s elastic limit. These strains most likely occur due to micro-failure of cement pore structure. Test procedure, raw test data, and more detailed description of the anelastic strain’s influence on seal durability under cyclic stresses are presented in Appendix B. Evaluations of cement-pipe bond and seal durability of the cement seal of the casing-bore hole annulus were performed by shear bond testing and specialized annular seal testing. These data are presented in Tables 13 through 15. The annular seal testing procedures and detailed test descriptions for both pressure and thermal cycling tests are presented in Appendix B. Energy input calculation methods and assumptions for data analysis are outlined in Appendix B.

The stress-bond data produced in this study are similar to the data set generated for a recent RPSEA-sponsored study of cement sheath durability for cemented intermediate casings in the Marcellus shale. The stress application in question for this study was drill pipe impact during drill out and drill ahead after cementing. Similar testing and analysis of stress effects on seal durability were performed with that data. The results of that study, summarized in paper URTeC 1913405, are compared to results of the current study as a check of the validity of the approach. This paper is included for reference in Appendix D.

5.4.2 PERFORMANCE PROPERTIES

Results of standard cement design tests for performance of OCS cement compositions, presented below in Table 11, indicate the compositions meet current design guidelines for OCS cements. Slurry rheology and stability, thickening time, fluid loss and strength development are all within acceptable ranges for general conditions. While minor adjustment might be necessary for application in the field, the compositions represent sound starting points for design of cements for OCS applications targeted in this study.

TABLE 11: CONVENTIONAL PERFORMANCE PROPERTIES

OCS Well Type		Density	BHCT	BHST	BHP	
		Lb/gal	°F	°F	Psi	
Deep Target		16.4	189	250	17000	
Shallow Target	Resilient	15.9	120	155	8000	
	low-density	13.0	120	155	8000	
	Conventional	16.4	120	155	8000	
Shelf		16.4	191	275	9500	
		Surface Rheology		Conditioned Rheology		API Fluid loss
		PV	YP	PV	YP	cc/30 mins
Deep Target		277	31	174	15	44
Shallow Target	Resilient	58	6	98	34	16
	low-density	286	45	244	49	36

THIS REPORT WAS INADVERTENTLY DISSEMINATED IN THE PUBLIC DOMAIN/ONLINE SINCE 09/2015 WITHOUT A DISCLAIMER. DISCLAIMER HAS BEEN ADDED – “THIS INFORMATION IS DISTRIBUTED SOLELY FOR THE PURPOSE OF PEER REVIEW UNDER APPLICABLE INFORMATION QUALITY GUIDELINES. IT HAS NOT BEEN FORMALLY DISSEMINATED BY BSEE. IT DOES NOT REPRESENT AND SHOULD NOT BE CONSTRUED TO REPRESENT ANY AGENCY DETERMINATION OR POLICY

	Conventional	37	6	50	21	no control	
Shelf		317	31	101	7	58	
		Free Water	Thickening Time		UCA Compressive Strength		
		%	40 BC	70 BC	500 psi	12 hrs	24 hrs
Deep Target		0	5:21	5:24	3:17	3845	4090
Shallow Target	Resilient	0	6:33	6:36	8:41	912	1664
	low-density	0	5:26	5:31	12:09	493	986
	Conventional	0.8	5:19	5:32	9:32	1974	3381
Shelf		0	5:57	6:19	3:29	3619	4240

5.4.3 MECHANICAL AND THERMAL PROPERTIES

Mechanical properties of the test compositions were measured after curing at two conditions. Test specimens cured in at temperatures up to 190°F in atmospheric-pressure water baths under the same conditions as the annular seal test specimens. These mechanical property data, reported in Table 12, are used in analysis of the laboratory and large-scale seal tests for this project. A second set of specimens was cured in a pressurized curing chamber at BHCT and BHP. These data are reported in Table 13 and are used for FEM.

Overall results presented in Tables 12 and 13 indicate that the cement systems generally exhibit superior performance than generic cements of similar density. Comparison of these data with those from the recent study as described in Appendix D indicate increased compressive strength, Young’s modulus, tensile strength, impact strength and reduced anelastic strain. Shear bonds are higher than would be predicted for general shear bond testing. Overall, these results along with the design properties presented in Table 11 demonstrate that a focus of OCS cementing is maximizing cement quality.

TABLE 12: MECHANICAL AND THERMAL PROPERTIES OF CEMENT COMPOSITIONS CURED AT ATMOSPHERIC PRESSURE

Property	Composition		
	Shelf	Deepwater Shallow Target	Deepwater Deep

		Conventional	Low Density	Resilient	Target
Compressive Strength (psi)	4900	6325	365	4485	3205
Young's Modulus (psi)	1.85×10^6	2.34×10^6	2.34×10^5	1.74×10^6	1.73×10^6
Poisson's Ratio	0.22	0.27	0.18	0.23	0.23
Tensile Strength (psi)	370	560	140	500	385
Anelastic Strain (in/in)	7.8×10^{-6}	3.5×10^{-6}	2.3×10^{-5}	6.6×10^{-6}	5.5×10^{-6}
Impact Strength (psi)	51	54	2	82	40
Shear Bond (psi)	315	325	455	605	460
Heat Capacity (in-lb _f /lb _m °F)	2975	3485	3820	3300	2990
Thermal Conductivity (in-lb _f /hr in °F)	626	441	297	374	603
Coefficient of Thermal Expansion 1/°F	4.6×10^{-6}	3.5×10^{-6}	2.8×10^{-6}	4.3×10^{-6}	4.4×10^{-6}

TABLE 13: MECHANICAL PROPERTIES OF CEMENT COMPOSITIONS CURED UNDER PRESSURE

Property	Composition				
	Shelf	Deepwater Shallow Target			Deepwater Deep Target
		Conventional	Low Density	Resilient	
Compressive Strength (psi)	6280	8120	1095	5130	5500
Young's Modulus (psi)	2.57×10^6	2.09×10^6	6.85×10^5	1.47×10^6	1.89×10^6
Poisson's Ratio	0.20	0.23	0.20	0.18	0.23
Tensile Strength (psi)	540	485	260	475	430
Anelastic Strain	8.5×10^{-6}	5.3×10^{-6}	7.2×10^{-6}	8.2×10^{-6}	6.6×10^{-6}
Shear Bond (psi)	295	280	370	525	350

5.4.4 ANNULAR SEAL TESTING

Cement seal durability for each cement composition was evaluated in the laboratory via a small-scale procedure named annular seal testing. The method involved constructing a scaled-down wellbore system consisting of an inner pipe (casing) fitted into the center of a larger pipe which created an annulus. The material of the outer pipe, which represented the borehole wall, was varied to investigate effects of formation mechanical properties on seal performance. Cements were mixed, poured into the annuli of these test fixtures, and cured. After curing to simulate cement hydration extent at time of general OCS stimulation treatment application, gas pressure was applied at the bottom of the cemented annulus and mechanical or thermal energy was applied to the system via the center pipe. The system was subjected to cyclic energy input until seal failure occurred. Cumulative energy required to initiate gas flow were recorded along with position of gas flow appearance in the annular space at the top.

It is important to note that failure is defined by actual establishment of gas flow through the cemented annulus. Mathematical analysis of failure induced in cement using only strength properties of the cement predicts failure always occurring at the inner pipe wall with lower energy input than observed. Testing in the laboratory with a range of cements, formation properties, and energy inputs produced a data set with which the aspects of the complex system can be compared.

Results of laboratory-scale annular seal testing for pressure cycling and thermal cycling are presented in Table 14 and Table 15. Thermal annular seal testing was delayed due to need to adjust test procedure from original plan. The testing was originally planned to be performed in a heated water bath with tap water circulated through the test fixture to generate thermal energy input. However, test fixture seals failed repeatedly before testing; probably due to the thermal and mechanical stresses introduced by removing each test fixture from the curing bath and plumbing in flow lines before returning it to the water bath for testing. Therefore, testing reverted to the standard curing and test method involving pressurization of the annulus at room temperature after curing each fixture in a heated water bath. Introducing thermal energy to the system by circulating chilled water through the center pipe produces the stress induced by cool fluid injection. This method worked satisfactorily. Energy input into each system at failure was calculated via the mechanical and thermal energy equations presented in Appendix B. Number of cycles required to fail each specimen were tracked and applied to the appropriate equations to yield the cumulative energy input information.

Preliminary evaluation of results of annular seal tests presented in Table 14 and 15 raises several interesting questions. Several systems failed while others maintained seal integrity during testing. Magnitudes of energy input for these observed failures varied with material property as well as formation. About half of the mechanical energy test specimens and one thermal test specimen that failed exhibited flow at the outer pipe. This physical behavior contradicts basic physical interpretation which predicts failure at the inner pipe wall. While no obvious trends emerged from results in Table 14, significant occurrence of failure at the simulated borehole wall did occur. These observations raise a significant question regarding definition of seal failure. The stresses predicted by fundamental physics undoubtedly indicate tensile failure occurring at the inner pipe interface. However, this failure does not always create a flow path; so physical loss of annular seal does not always occur. Increasing energy input beyond this initial numerically described failure does result in predicting failure at other points further out in the pipe-cement-formation system. Analysis of lab and FEM results in light of the system's energy resistance parameter, as illustrated in the paper in Appendix D, provided insight into calculated failure from numerical stress analysis in relation to seal failure manifest as gas flow. The basis for this analysis is the systems approach accounting for multiple variables and related effects. It is obvious from review of the failure data in Tables 14 and 15 that seal failure as indicated by gas flow is not a straightforward occurrence.

THIS REPORT WAS INADVERTENTLY DISSEMINATED IN THE PUBLIC DOMAIN/ONLINE SINCE 09/2015 WITHOUT A DISCLAIMER. DISCLAIMER HAS BEEN ADDED – “THIS INFORMATION IS DISTRIBUTED SOLELY FOR THE PURPOSE OF PEER REVIEW UNDER APPLICABLE INFORMATION QUALITY GUIDELINES. IT HAS NOT BEEN FORMALLY DISSEMINATED BY BSEE. IT DOES NOT REPRESENT AND SHOULD NOT BE CONSTRUED TO REPRESENT ANY AGENCY DETERMINATION OR POLICY

TABLE 14: MECHANICAL ANNULAR SEAL DURABILITY

Test Composition	Outer Pipe	Failure	
		Energy (in-lb _f)	Location
Shelf Sample 1	Steel	4.30x10 ⁶	Inner Pipe
Shelf Sample 2	Steel	4.08x10 ⁶	Outer Pipe
Shelf Sample 1	PVC	>6.78x10 ⁶	-
Shelf Sample 2	PVC	>5.23x10 ⁶	-
Deepwater Shallow Target Conventional Sample 1	Steel	3.90x10 ⁶	Outer Pipe
Deepwater Shallow Target Conventional Sample 2	Steel	3.59x10 ⁶	Outer Pipe
Deepwater Shallow Target Conventional Sample 1	PVC	2.28x10 ⁶	Inner Pipe
Deepwater Shallow Target Conventional Sample 2	PVC	1.86x10 ⁶	Inner Pipe
Deepwater Shallow Target Low Density Sample 1	Steel	4.12x10 ⁶	Outer Pipe
Deepwater Shallow Target Low Density Sample 2	Steel	3.79x10 ⁶	Outer Pipe
Deepwater Shallow Target Low Density Sample 1	PVC	4.74x10 ⁶	Inner Pipe
Deepwater Shallow Target Low Density Sample 2	PVC	5.45x10 ⁶	Inner Pipe

THIS REPORT WAS INADVERTENTLY DISSEMINATED IN THE PUBLIC DOMAIN/ONLINE SINCE 09/2015 WITHOUT A DISCLAIMER. DISCLAIMER HAS BEEN ADDED – “THIS INFORMATION IS DISTRIBUTED SOLELY FOR THE PURPOSE OF PEER REVIEW UNDER APPLICABLE INFORMATION QUALITY GUIDELINES. IT HAS NOT BEEN FORMALLY DISSEMINATED BY BSEE. IT DOES NOT REPRESENT AND SHOULD NOT BE CONSTRUED TO REPRESENT ANY AGENCY DETERMINATION OR POLICY

Deepwater Shallow Target Resilient Sample 1	Steel	$>7.94 \times 10^6$	-
Deepwater Shallow Target Resilient Sample 1	Steel	$>7.94 \times 10^6$	-
Deepwater Shallow Target Resilient Sample 1	PVC	$>7.94 \times 10^6$	-
Deepwater Shallow Target Resilient Sample 2	PVC	7.90×10^6	Inner Pipe
Deepwater Deep Target Sample 1	Steel	3.84×10^6	Outer Pipe
Deepwater Deep Target Sample 2	Steel	4.10×10^6	Outer Pipe
Deepwater Deep Target Sample 1	PVC	3.60×10^6	Inner Pipe
Deepwater Deep Target Sample 2	PVC	3.70×10^6	Inner Pipe

TABLE 15: THERMAL ANNULAR SEAL DURABILITY

Test Composition	Outer Pipe	Failure	
		Energy (in-lb _f)	Location
Shelf	Steel	4.45×10^7	Inner Pipe
Shelf	PVC	4.57×10^7	Inner Pipe
Deepwater Shallow Target Conventional	Steel	3.16×10^7	Inner Pipe
Deepwater Shallow Target Conventional	PVC	4.06×10^7	Inner Pipe
Deepwater Shallow Target Low Density	Steel	2.34×10^7	Outer Pipe
Deepwater Shallow Target Low Density	PVC	2.90×10^7	Outer Pipe

THIS REPORT WAS INADVERTENTLY DISSEMINATED IN THE PUBLIC DOMAIN/ONLINE SINCE 09/2015 WITHOUT A DISCLAIMER. DISCLAIMER HAS BEEN ADDED – “THIS INFORMATION IS DISTRIBUTED SOLELY FOR THE PURPOSE OF PEER REVIEW UNDER APPLICABLE INFORMATION QUALITY GUIDELINES. IT HAS NOT BEEN FORMALLY DISSEMINATED BY BSEE. IT DOES NOT REPRESENT AND SHOULD NOT BE CONSTRUED TO REPRESENT ANY AGENCY DETERMINATION OR POLICY

Deepwater Shallow Target Resilient	Steel	3.38×10^7	Inner Pipe
Deepwater Shallow Target Resilient	PVC	4.19×10^7	Inner Pipe
Deepwater Deep Target	Steel	4.12×10^7	Inner Pipe
Deepwater Deep Target	PVC	4.90×10^7	Inner Pipe

5.4.5 DIMENSIONLESS SCALING CORRELATION DEVELOPMENT

Having seal failure results from different physical models with a range of cements and energy application allows initial evaluation of the dimensionless Applied Energy-Energy Resistance correlation originally presented by McDaniel et al (2014) [1] presented in Appendix D for reference. The correlation is based on scaling theory and dimensionless variables. If data can be correlated via dimensionless variable relationships, the relationship can be scaled to larger or smaller systems and remain applicable. This method is the basis of many engineering methods such as friction pressure correlation using Reynolds Number. This concept can yield prediction methods for performance of complex systems based on relatively simple laboratory performance measurements (in this case, thermal and mechanical properties of cement coupled with hole dimensions and formation properties).

While the referenced correlation described the limited issues of drill pipe impact on casing at very early time after cementing, it proved too simplistic for description of the data from this project. An appropriate correlation required inclusion of both thermally and mechanically induced energy input. Additionally, significant variations in hole size, temperature, and stimulation treatment methods required a more generalized correlation of properties. The investigators had been unsuccessful in developing such a complex relationship in the past. However adoption of a simpler, segmented approach to the correlation proved successful.

The correlation started with the Applied Energy-Effective Resistance concept of the referenced paper. The two variables were split into mechanical and thermal components defined as:

EQUATION 1: APPLIED ENERGY

$$E_a = E_{am} + E_{ah}$$

EQUATION 2: EFFECTIVE RESISTANCE

$$R_e = R_{em} + R_{eh}$$

If only mechanical energy or thermal energy were applied, the other term is discarded. However, separate, additive terms for the two types of energy worked even for this complex correlation. The variables were further defined in terms of system dimensions and material properties to be:

EQUATION 3: MECHANICAL APPLIED ENERGY

$$E_{am} = \frac{Q_m}{E_s} \times \frac{E_f}{S_{T_t} \times p_f} \times \frac{1}{V_{annulus}}$$

EQUATION 4: THERMAL APPLIED ENERGY

$$E_{ah} = \frac{Q_h}{E_s} \times \frac{p_{steel}}{p_f} \times \frac{C_f}{C_{steel}} \times \frac{k'_f}{C'_t} \times \frac{E_f}{S_{T_t} \times p_f} \times \frac{1}{V_{hole}}$$

EQUATION 5: MECHANICAL EFFECTIVE RESISTANCE

$$R_{em} = \frac{L}{D_{hole}} \times \frac{S_{T_t}}{S_{T_c}} \times \frac{S_{I_c}}{E_c} \times \frac{1}{E_c \times W/c} \times \frac{p_c}{p_f}$$

EQUATION 6: THERMAL EFFECTIVE RESISTANCE

$$R_{eh} = \frac{C_{steel}}{C_c} \times \frac{C'_c}{k'_c} \times \frac{L}{50 \times D_{hole}} \times \frac{S_{T_t}}{S_{T_c}} \times \frac{S_{I_c}}{E_c} \times \frac{1}{E_c \times W/c} \times \frac{p_c}{p_f}$$

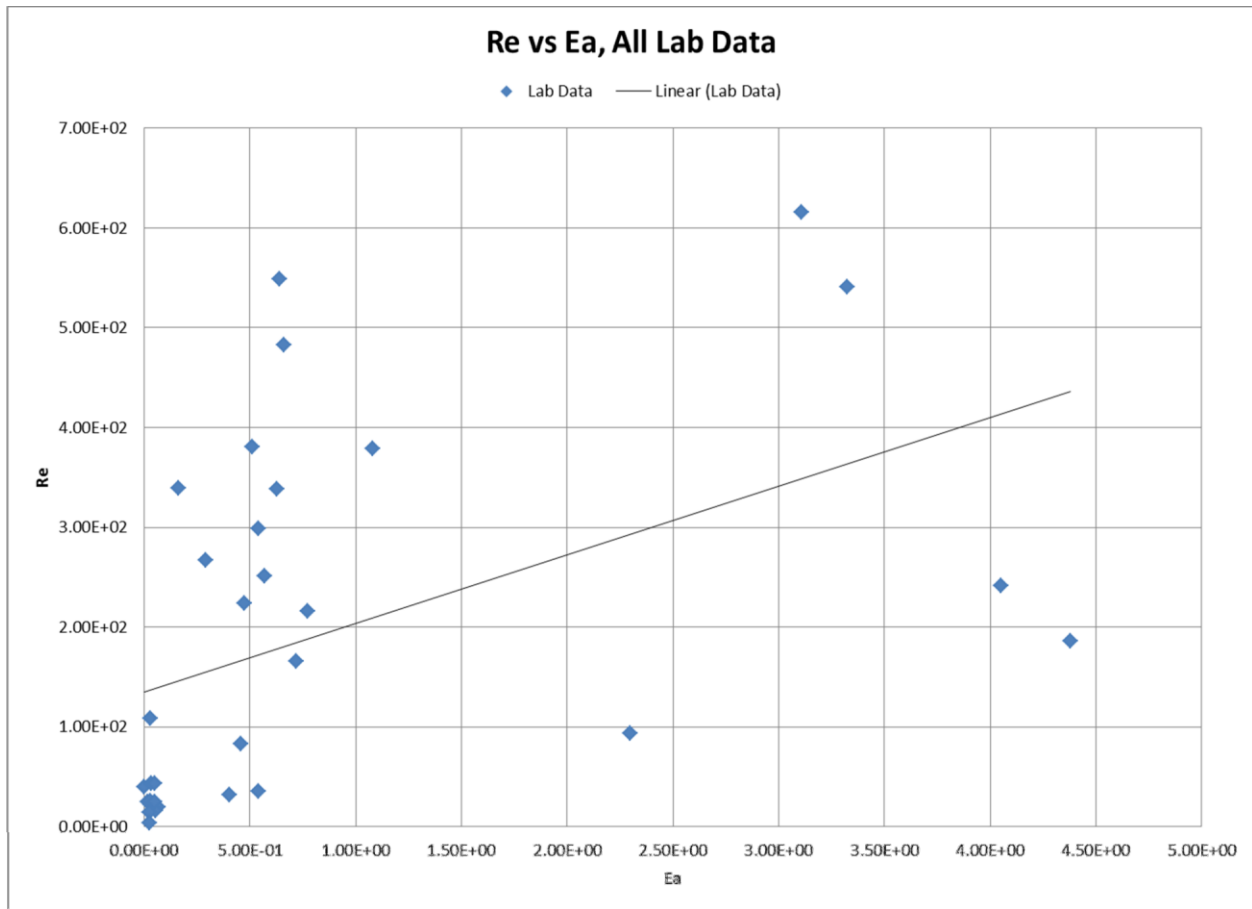
The variables are described in detail in Appendix B. Appropriate units, calculation methods, and real-world meaning behind each variable's inclusion are also presented. Note that each term in the relationship is composed of multiple parameters and that some variables are not immediately recognized as significant energy transfer or failure resistance. However, through trial and error, this relationship was found to correlate energy applied to failure of the sealed annulus. The energy applied in the lab scale annular seal tests along with the required properties of cement and other materials were analyzed along with annular seal data from the referenced paper. Results appear below in Table 16 and Figure 5.

TABLE 16: CALCULATED ENERGY APPLICATION FOR LABORATORY AND FIELD. (DETAILED CALCULATION METHODS PRESENTED IN APPENDIX B)

System	Formation	Eam	Rem	Eah	Reh
Shelf	PVC	4.74E-01	2.24E+02	-	-
DWSTC	PVC	1.63E-01	3.39E+02	-	-
DWSTL	PVC	4.02E-01	3.19E+01	-	-
DWSTR	PVC	6.25E-01	3.38E+02	-	-
DWDT	PVC	2.88E-01	2.67E+02	-	-
Shale 1	PVC	1.00E-03	3.98E+01	-	-
Shale 2	PVC	2.93E-02	2.22E+01	-	-
Shale 3	PVC	1.62E-02	2.47E+01	-	-
Shale 4	PVC	2.83E-02	2.59E+01	-	-
Shale 5	PVC	2.65E-02	1.09E+02	-	-
Shale 6	PVC	3.43E-02	4.36E+01	-	-
Shale 7	PVC	6.59E-02	1.97E+01	-	-
Shale 8	PVC	5.34E-02	1.64E+01	-	-
Shale 9	PVC	4.83E-02	2.48E+01	-	-
Shale 10	PVC	2.53E-02	1.45E+01	-	-
Shale 11	PVC	5.12E-02	4.34E+01	-	-
Shale 12	PVC	2.53E-02	4.01E+00	-	-
Shelf	Steel	5.70E-01	2.51E+02	-	-
DWSTC	Steel	5.10E-01	3.80E+02	-	-
DWSTL	Steel	5.38E-01	3.58E+01	-	-
DWSTR	Steel	1.08E+00	3.79E+02	-	-
DWDT	Steel	5.40E-01	2.99E+02	-	-
Shelf	PVC	-	-	7.19E-01	1.66E+02
DWSTC	PVC	-	-	6.39E-01	5.49E+02
DWSTL	PVC	-	-	4.56E-01	8.33E+01
DWSTR	PVC	-	-	6.59E-01	4.83E+02
DWDT	PVC	-	-	7.71E-01	2.16E+02
Shelf	Steel	-	-	4.38E+00	1.86E+02
DWSTC	Steel	-	-	3.11E+00	6.16E+02
DWSTL	Steel	-	-	2.30E+00	9.35E+01
DWSTR	Steel	-	-	3.32E+00	5.41E+02
DWDT	Steel	-	-	4.05E+00	2.42E+02

THIS REPORT WAS INADVERTENTLY DISSEMINATED IN THE PUBLIC DOMAIN/ONLINE SINCE 09/2015 WITHOUT A DISCLAIMER. DISCLAIMER HAS BEEN ADDED – “THIS INFORMATION IS DISTRIBUTED SOLELY FOR THE PURPOSE OF PEER REVIEW UNDER APPLICABLE INFORMATION QUALITY GUIDELINES. IT HAS NOT BEEN FORMALLY DISSEMINATED BY BSEE. IT DOES NOT REPRESENT AND SHOULD NOT BE CONSTRUED TO REPRESENT ANY AGENCY DETERMINATION OR POLICY.

FIGURE 5: R_e VS E_a FOR ANNULAR SEAL DATA



The correlation line depicted above represents the predicted failure line of the systems tested for OCS wells. Since the correlation is scalable, this failure line can be used to quantify the performance of a specific cement system in a given wellbore subjected to input energy. First E_a and R_e are calculated and plotted on the chart. If the point is above the failure line, the system will maintain its seal integrity. If the point lies below the line, failure is likely. The effectiveness of this correlation was tested with large scale data and field simulations. Results are presented below.

5.4.6 LARGE SCALE ANNULAR SEAL

Large-scale physical testing of pressure and thermal cycling effects on the seal effectiveness of a cemented annulus are described here. The physical model results are briefly compared to FEA results to determine the scalability of the ABAQUS model developed to predict small laboratory scale test results as well as to determine applicability of dimensionless scaling correlations being developed.

Large-scale testing of cement at elevated pressure or temperature requires considerable fabrication, plumbing, assembly, and process control. Preparation generally requires substantial time, and fixtures are not always fit to test. This project proved to be no exception. Six models were originally fabricated for this testing. The cemented annulus of four of the fixtures failed initial differential pressure application to confirm initially-sealed annulus. No reliable method exists to repair this failure, so the fixtures were discarded. Several improper fabrication procedures were uncovered and corrected as failures were discovered. These included exacting casing surface preparation by solvent washing and sandblasting as well as maintaining 1000 psi pressure on the cemented annulus while curing. Once these previously-known fabrication steps were reinstated, model fabrication success improved significantly.

Results of the two successfully completed large-scale test, one mechanical and one thermal, are presented and analyzed here. This test was a pressure cycling test performed on the Deepwater Shallow Target Conventional cement design. Test fixture and procedure are detailed in Appendix B.

The test cement composition was the Deepwater Shallow Target Conventional design with the set retarder removed. The composition, listed in Table 7, was chosen and modified for comparison to small-scale testing. Elimination of the retarder and curing the cement for seven days prior to testing produced a cement with properties similar to the same cement with retarder cured under the small-scale test conditions of 140°F. This was confirmed by comparison of compressive strength development curves for the two compositions at the respective temperatures.

5.4.7 LARGE-SCALE TEST RESULTS

The cemented fixtures, illustrated in Figures 18 and 19 in Appendix B, were tested with cyclic pressurization or heating/cooling of the inner pipe while a gas pressure of 40 psi was applied to the bottom of the cemented annulus. Pressure increases detected at the top annular space indicated seal failure. A pressure increase of 0.2 psi noted on the 75th pressure cycle was selected as initial indication of pressure communication resulting from seal failure for the pressure cyclic test. Pressure cycling continued to observe if increasing cycles resulted in increased communication. Results of annular pressure vs cycling are presented in Figure 6 and 7. The maximum pressure measured at the top of the model's annular space was roughly 35 psi. Accounting for the hydrostatic pressure of approximately 10 ft of water, this correlates to full communication to the source pressure of 40 psi. Similar results and interpretation were performed for the thermal cycling test.

FIGURE 6: ANNULAR PRESSURE COMMUNICATION VS PRESSURE CYCLE (MAGNIFIED)

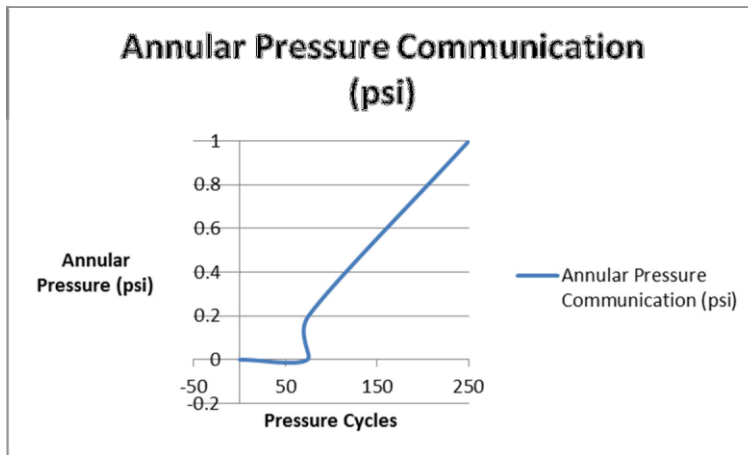
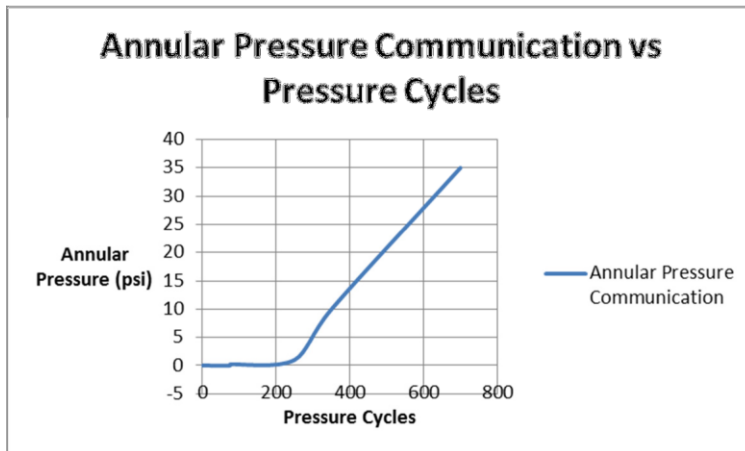


FIGURE 7: ANNULAR PRESSURE COMMUNICATION VS PRESSURE CYCLE (OVERALL)



The seal failure noted in large-scale testing is not catastrophic. Rather, it is noted by gradual pressure increase in the upper annulus as stress applications continue. This has not been observed on the small-scale tests due to test fixture configuration. The open top of the annulus on the small-scale fixture allows visual detection of gas flow when it first appears. Seal failure is noted as the time of first appearance of a gas bubble in the annulus. Flow rate acceleration is not detected or observed. This gradual gas flow increase with continued cycling is further indication of complex flow path development in the annulus as energy application increases.

Magnitude of applied energy for each test was calculated using the equations from Appendix B to be:

Mechanical	6.53×10^8 in-lb _f	outer pipe
Thermal	1.39×10^9 in-lb _f	inner pipe

5.4.8 DIMENSIONLESS SCALING CORRELATION EVALUATION

Applicability of the E_a-R_e correlation developed above was tested using large-scale lab data as well as estimates of field data for the three example well configurations. Estimates of thermal and mechanical energy imparted to the casing-cement-well bore system for stimulation treatments of the example wells was calculated via methods outlined in Appendix B. Additional field examples from the referenced paper were included in the evaluation. These data from the additional field example represent documented occurrence of seal failure that can be correlated to variation in cement composition.

Energy inputs for the field examples appear in Table 17.

TABLE 17: ENERGY INPUTS FOR FIELD-SCALE TESTS OF ENERGY CORRELATION

System	Thermal Energy (in-lb _f)	Mechanical Energy (in-lb _f)
Shelf	2.27×10^{10}	9.95×10^7
Deepwater-Shallow Target	6.68×10^{10}	2.11×10^8
Deepwater-Deep Target	8.07×10^{10}	2.07×10^8
Shale Example	-	4.00×10^9

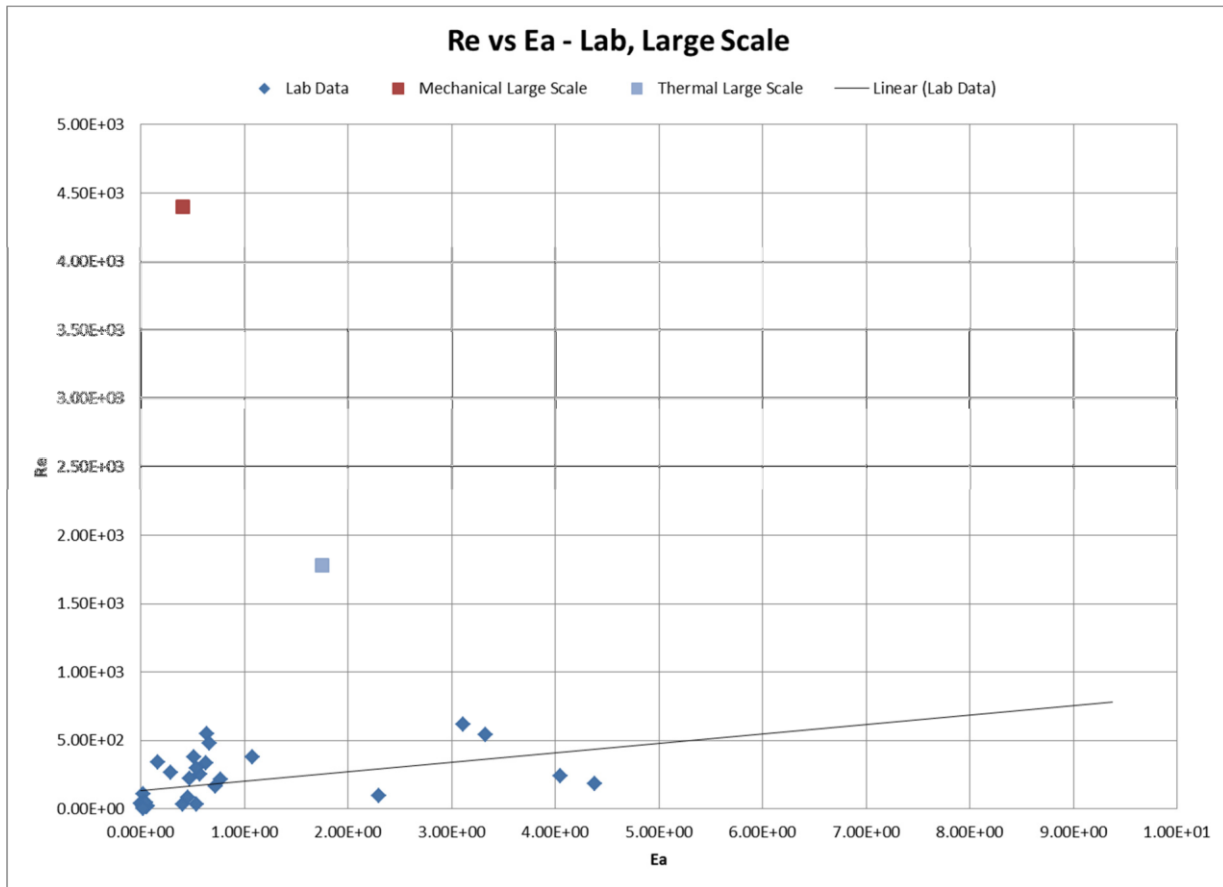
Resulting correlation parameters for each test system are presented in Table 18. As for earlier data, the calculation methods are described in Appendix D.

TABLE 18: CORRELATION PARAMETERS

System	Formation	Eam	Rem	Eah	Reh
Large Scale Mechanical	Steel	4.04E-01	4.40E+03	-	-
Large Scale Thermal	Steel	-	-	1.75E+00	1.78E+03
Shelf	Sandstone	7.21E-02	2.63E+03	3.67E+00	1.84E+03
DWSTC	Sandstone	6.76E-02	2.77E+03	4.61E+00	4.77E+03
DWSTL	Sandstone	6.76E-02	2.60E+02	4.61E+00	7.23E+02
DWSTR	Sandstone	6.76E-02	2.76E+03	4.61E+00	4.19E+03
DWDT	Sandstone	6.07E-02	2.18E+03	9.41E+00	1.11E+03
Shale Field 1	Sandstone	5.87E-02	7.09E+03	-	-
Shale Field 2	Sandstone	5.87E-02	6.51E+02	-	-
Low Strength DWST Field Example	Sandstone	6.76E-02	6.51E+02	4.61E+00	4.91E+01
Low Strength DWDT Field Example	Sandstone	6.07E-02	3.25E+01	9.41E+00	4.91E+01

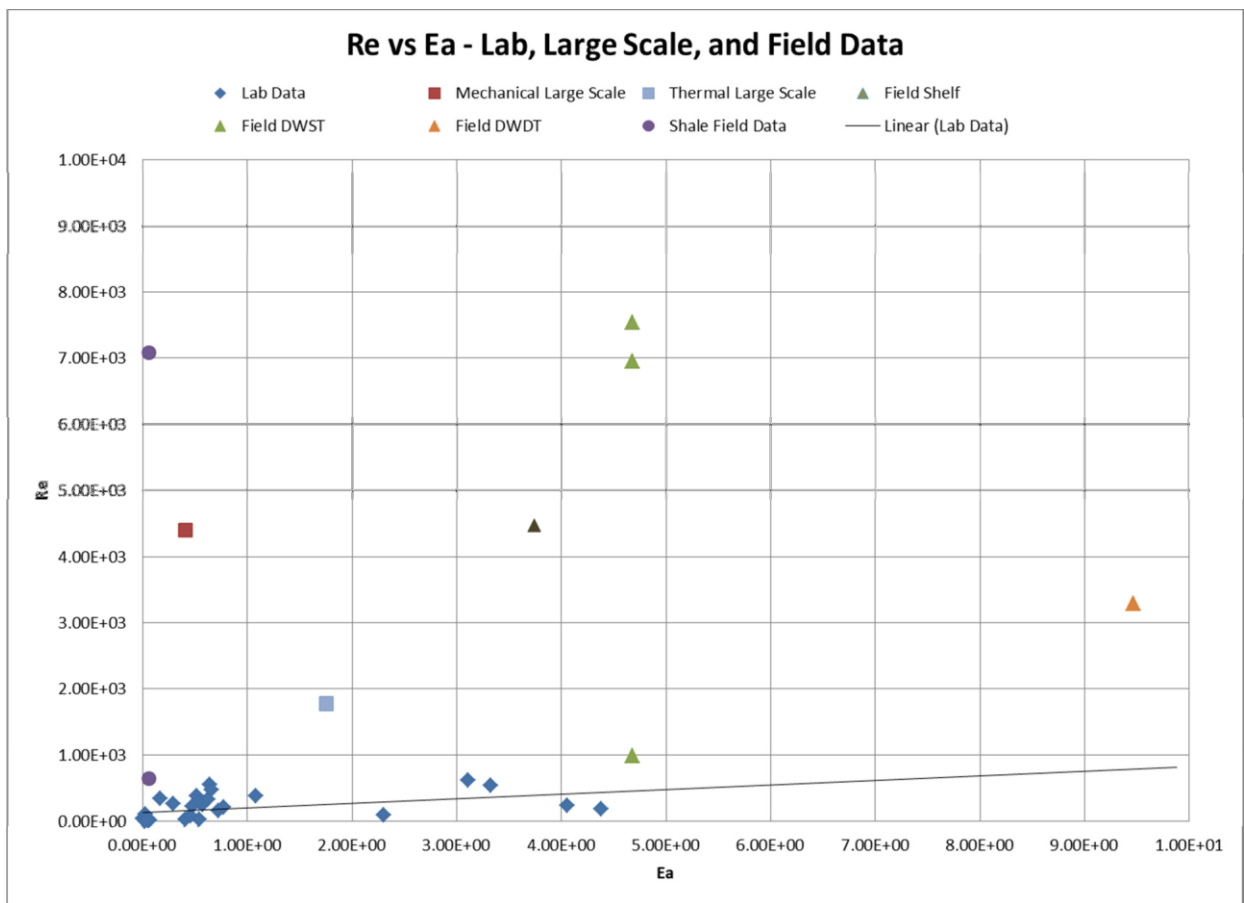
The results from the large-scale tests to failure appear in Figure 8 along with the same trend line from figure 7 and other lab data. These large scale data both lie above the trend line. This indicates that the failure prediction may be slightly optimistic in prediction of seal survival. So a correlation point residing just above the trend line has a significant probability of being in error. Therefore, data points falling just above the trend line should trigger design alterations to raise the point.

FIGURE 8: LARGE-SCALE ANNULAR SEAL FAILURE DATA



Next, the field examples for the OCS wells and the Shale well example with two different cements are added to the correlation plot in Figure 9. The OCS well data all lie well above the trend line indicating little chance of seal failure due to single stimulation treatments on properly cemented wellbores. This confirms the observation that OCS operators are investing in high-performance cement compositions. The two shale well points are significant in that they represent a well design that experienced seal failure 50% of the time with a specific cement design. Based on the results of the reference paper, the cement design was improved and failure was eliminated. Thus, the lower shale point (with poorer cement) represents actual field failure half the time. The higher data point depicts the improved cement design resulting in failure elimination. The lower point lies just above the trend line indicating suspect performance.

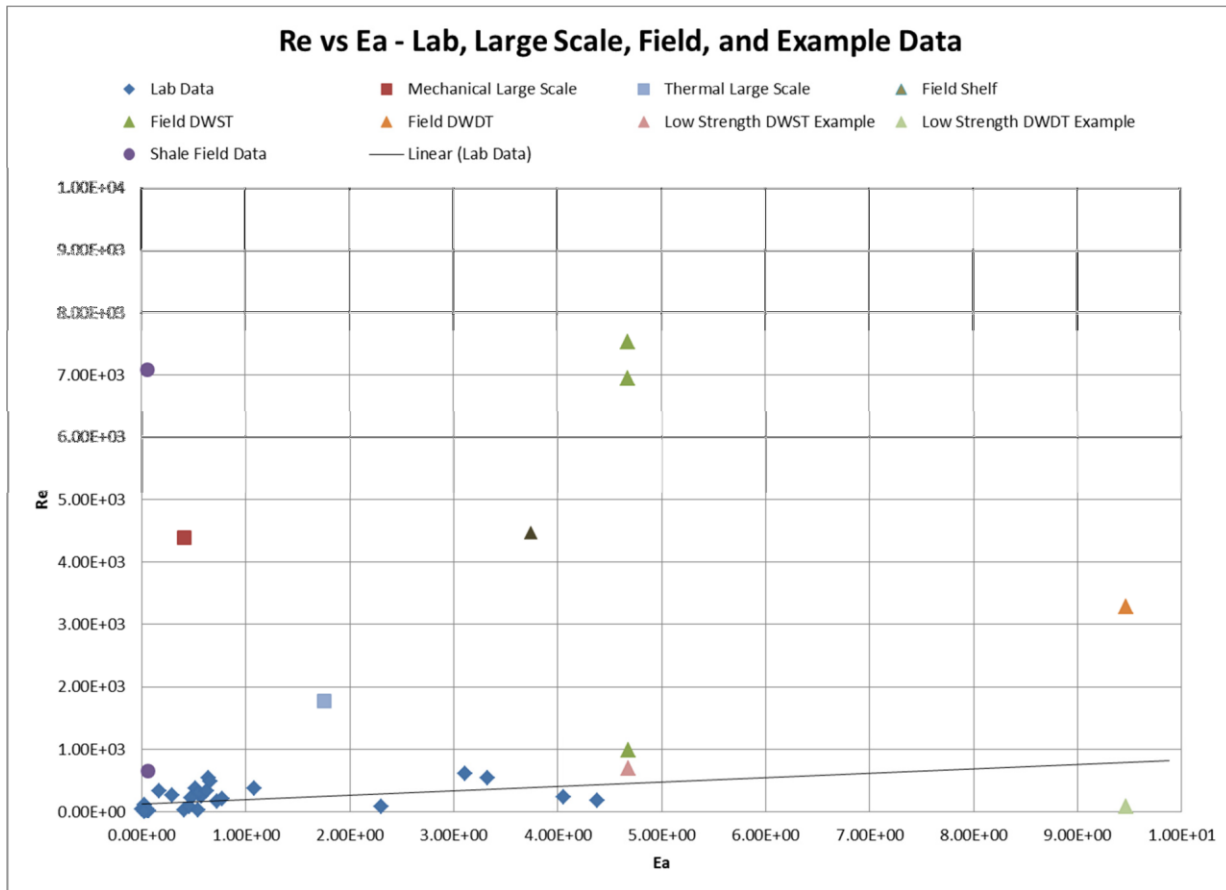
FIGURE 9: FIELD DATA



THIS REPORT WAS INADVERTENTLY DISSEMINATED IN THE PUBLIC DOMAIN/ONLINE SINCE 09/2015 WITHOUT A DISCLAIMER. DISCLAIMER HAS BEEN ADDED – “THIS INFORMATION IS DISTRIBUTED SOLELY FOR THE PURPOSE OF PEER REVIEW UNDER APPLICABLE INFORMATION QUALITY GUIDELINES. IT HAS NOT BEEN FORMALLY DISSEMINATED BY BSEE. IT DOES NOT REPRESENT AND SHOULD NOT BE CONSTRUED TO REPRESENT ANY AGENCY DETERMINATION OR POLICY.

Finally, the sensitivity of the correlation is evaluated by substituting the performance data for the unsuccessful cement form the Shale Study into the DWDT and DWST wells in Figure 10. Note that stimulating these wells cemented with the poor performing cement is predicted to result in seal failure as expected.

FIGURE 10: CORRELATION SENSITIVITY



The correlation defined herein appears to describe performance trends for cement systems in OCS wells. However, significant corroboration of the method through field trial is required to develop confidence in the method's applicability. Additionally, the imprecise nature of the annular seal physical test apparatus and methods, both small- and large-scale, are recognized. So, the correlation must be recognized for what it is: a scalable relationship describing annular seal durability in terms of materials, dimensions, and performance properties of a cemented well system. The correlation is based on empirical combinations of multiple properties and experimental errors have not been quantified. However, the initial data indicate that the correlation does relate meaningful trends between wellbore stresses and cement seal durability. The current form is considered a starting point requiring refinement and validation.

5.4.9 FEA RESULTS

Note that the FEA modeling of the large-scale tests, discussed in detail below, agrees well with the results. This outcome is encouraging in that predicted failure locations for both mechanical and thermal tests matched actual results. Additionally, predicted energy inputs required to induce failure were similar to actual results. Figures 11 and 12 illustrate the predicted behavior of the cement sheath during mechanical stress application. These illustrations from ABAQUS confirm that a flow path should result at the outer cement surface:outer casing interface. Figure 11 depicts displacement gradient. Steeper gradients occurring on the outer surface of the cement represent crack origination points. Similarly, debonding of cement from the outer pipe is depicted on the outer cement surface in Figure 12.

FIGURE 11: DISPLACEMENT GRADIENTS

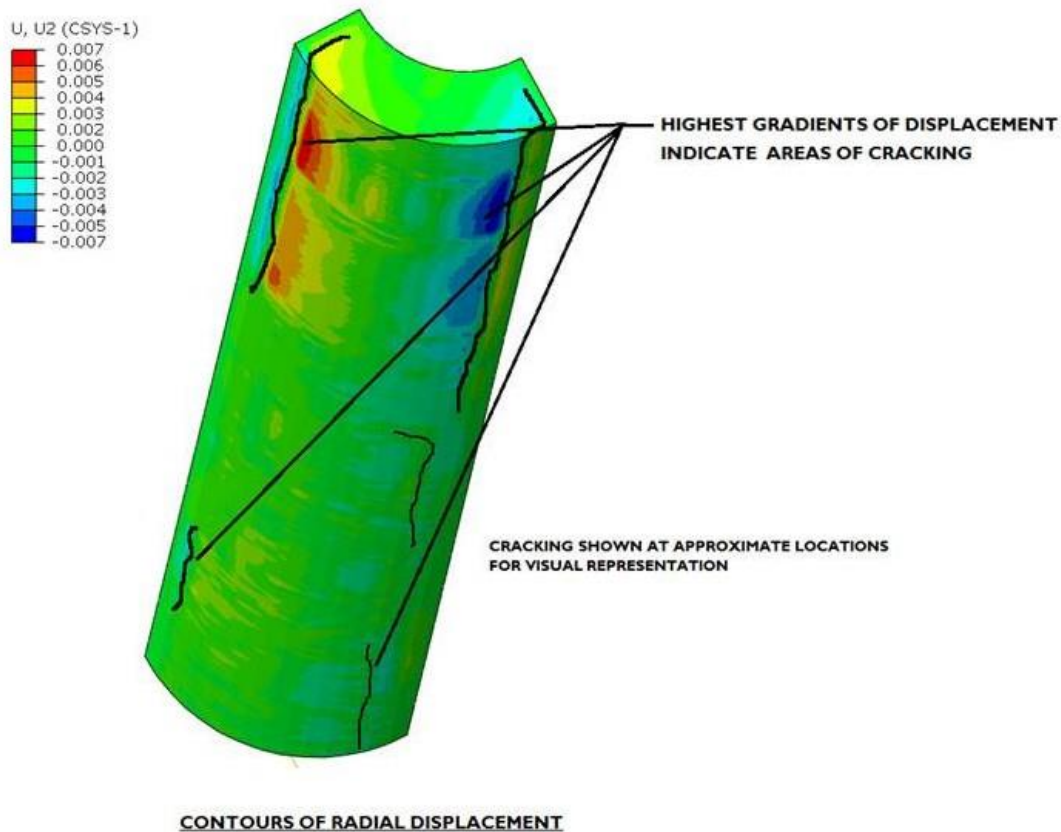
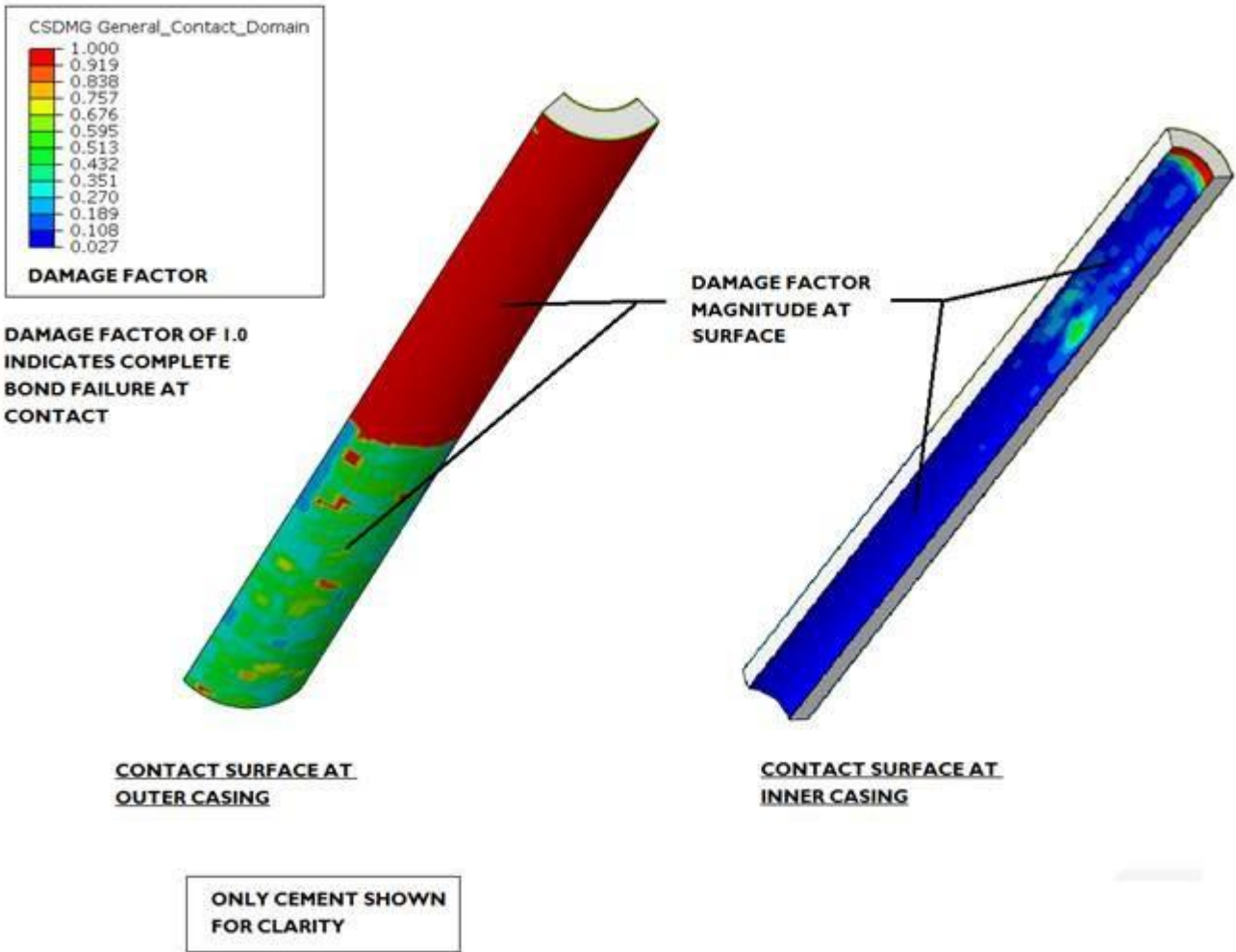


FIGURE 12: DEBONDING



BOND FAILURE AT CEMENT TO CASING INTERFACE

THIS REPORT WAS INADVERTENTLY DISSEMINATED IN THE PUBLIC DOMAIN/ONLINE SINCE 09/2015 WITHOUT A DISCLAIMER. DISCLAIMER HAS BEEN ADDED – “THIS INFORMATION IS DISTRIBUTED SOLELY FOR THE PURPOSE OF PEER REVIEW UNDER APPLICABLE INFORMATION QUALITY GUIDELINES. IT HAS NOT BEEN FORMALLY DISSEMINATED BY BSEE. IT DOES NOT REPRESENT AND SHOULD NOT BE CONSTRUED TO REPRESENT ANY AGENCY DETERMINATION OR POLICY.

While the data contradict logical correlation behavior, they are insufficient to conclude that no correlation exists. This discrepancy could be caused by any of a number measurement issues. Failure of both the small-scale tests occurred at energy input values much lower than predicted by FEA. Additional large-scale tests may indicate the necessity of repeating the small-scale tests for this composition and fixture construction. Also, the definition of failure point is different for the two tests. Failure for the small-scale test is noted as the cycle at which the first bubble appears. For the large-scale test, failure is defined as a significant increase in annular pressure arbitrarily chosen as 0.2 psi. The first gas bubble may have appeared many cycles earlier without significantly increasing measured pressure. Thus energy input would be overestimated. Again, additional data should allow these issues to be addressed.

6 FEA REPORT

6.1 SUMMARY

CSI Technologies is performing a research study for the Bureau of Safety and Environmental Enforcement (BSEE) to better understand the effects of well stimulation on the annular seal of production casings in the outer continental shelf (OCS) during oil and gas operations. The scope of work for the study includes:

- Laboratory testing to simulate casing-cement behavior in response to typical stimulation effects such as pressure and temperature, carried out by CSI Technologies.
- Development of Finite element analysis (FEA) models to analyze the cement bond and casing pressure integrity, performed by Wild Well Control's Advanced Engineering group (formerly known as Prospect).

The latter is discussed in this section of the report .

The objective of the FEA is to examine how the well stimulation techniques affect the cement bond behind the production casing and the pressure integrity of the production casing due to pressure and temperature cycles.

Initially the laboratory test results were compared to FEA models of the test arrangement to establish the best approach for the FEA. Thereafter the findings and FEA techniques were then applied to the large scale models and the down-hole simulation.

A comparison of the FEA results with both the small and large scale physical lab tests showed some differences in failure mode and in the overall durability of the seal. The differences in the results can be attributed to multiple factors, one of which is that a failure or failure location in the FEA may or may not translate to a leak in physical testing or in actual well conditions. In addition, the small scale lab results and FEA modeling revealed the need for additional mechanical property testing to refine the material inputs used in the FEA. Time constraints of the project did not allow for additional material testing to refining the inputs for the FEA model. Thus, the material inputs and assumptions defined in the small scale tests were used for all FEA modeling.

Although there are some variations with the seal durability (no. of cycles to failure) between the FEA and lab results; there was a strong match of failure location and likely failure mode. Thus, the FEA results can indicate where the failure is likely to occur, but not precisely when. Further development of material inputs through a stringent material testing program could lead to greater accuracy for determining seal durability. A summary of the comparisons between the lab testing and FEA modeling are shown in Table 20, 21 and 22.

6.2 INTRODUCTION AND BACKGROUND

The overall objective of this project is to evaluate technological and safety impacts of well stimulation processes on the cemented production casing annulus of an OCS well. Specific technical objectives are to:

- Evaluate fundamental stress-strain application associated with stimulation of OCS wells including HPHT wells
- Quantify mechanical properties of the materials of OCS well construction (formation, steel, drilling fluid filter cake, cement that govern the well bore's structural integrity during stress application)
- Investigate how stimulation techniques including frac-packing affect the cement bond to the production casing and the associated annular seal effectiveness
- Analyze induced stresses from stimulation on cement strength, cement/casing bond and micro-annulus formation
- Compare casing pressure integrity and cement strength zonal isolation pre- and post-stimulation
- Conduct a regulatory analysis of well stimulation techniques domestically and internationally to identify gaps and draft modifications aimed to reduce risk of HSE threats due to well integrity failure

The work has been broken into a series of Tasks. The work reported herein concerns Task 6, subtasks 6.1 through 6.4.

The objective of Task 6 was:

- To use Finite Element Modeling to examine how the well stimulation techniques can affect the cement bond behind the production casing and the pressure integrity of the production casing due to temperature and pressure cycles

As part of Task 6 CSI has contracted Wild Well Control's Advanced Engineering group with developing finite element analysis (FEA) models to simulate the tests performed in the laboratory. The non-linear finite element (FE) code ABAQUS was used to examine how the well stimulation techniques can affect the cement bond behind the production casing (i.e. cement strength, formation of micro annuli within the cement column) and the pressure integrity of the production casing due to temperature and pressure cycling.

6.3 TECHNICAL APPROACH

Using data acquired from mechanical property tests, the ABAQUS non-linear finite element code was used to generate the required FEA models. Factors taken into consideration include cement strength and the formation of a micro-annulus within the cement column. A breakdown of the subtasks is provided below.

- Subtask 6.1: Data processing from information acquired from mechanical property testing conducted in earlier tasks.
- Subtask 6.2: Finite Element model construction & testing will be done. Various models were required to accommodate the failure modes being explored.
- Subtask 6.3: Finite Element simulations were run to replicate laboratory testing to calibrate finite element modeling approaches
- Subtask 6.4: Finite Element simulations were run on to model full scale section of a down-hole system to determine likelihood of various failure modes identified in the Failure Mode section. These included cracking of cement or formation, development of a micro-annulus between cement and casing, delamination of the cement/casing bond or cement/formation bond, and the cyclic response of casing.

6.3.1 KEY ASSUMPTIONS

The cement sheath is subjected to damage each time it is subjected to pressure and/or temperature loads. Due to the material properties of Portland based cements; degradation and damage leading to cracks or de-bonding at interfaces may occur below the failure stress of the material.

Several failure modes were assumed to occur within the cement sheath system; radial cracking in the cement due to the tensile forces from the applied loads, de-bonding at the cement to formation and the micro-annuli formation at the coil tubing to cement interface. In addition, shear cracking or diskings from temperature induced loading may occur.

True stress-strain compression curves were available for the cement. Tension stress-strain curves or failure crack widths were not available; therefore the tensile stress-strain curves were assumed. Development of the tensile stress-strain curves and damage modeling for the cements are further discussed in Section 6.4.3.

Tensile bonding strength of the cement was not provided; therefore the maximum bond strength in direct tensile loading was assumed to be 10% of the tensile strength of the cement. The bond strength is highly dependent on the surface profiles. Cement bonding and bond damage is discussed further in Section 6.4.1.

Material properties of the cements were provided by CSI and are shown in Table 12. Material properties for the steel and CPVC pipes are shown in Table 19 below. The coil tubing and casing used in the down-hole model is assumed to have a yield stress of 70,000psi and is modeled elastic-perfectly plastic, however both the steel and CPVC pipes used to simulate the formations were assumed to stay in the elastic regime under the pressures anticipated.

TABLE 19: MATERIAL PROPERTIES ASSUMED TUBING AND FORMATIONS

Material	E [ksi]	N	g [pcf]	f'c [psi]	Thermal Conductivity [W/mK]	Specific Heat [J/(kg °K)]
Coil Tubing	29,000	0.30	490	70,000	46	499
Steel Pipe (elastic)	29,000	0.30	490	-	46	499
CPVC Pipe (elastic)	450	0.30	95	-	0.195	900
Rock Formation	1740	0.22	120	5,500	0.833	1700

E – Young’s modulus

n – Poisson’s ratio

f'c-Compressive strength

g -Density

6.4 FINITE ELEMENT MODEL OF LAB AND DOWN-HOLE SYSTEM (SUBTASK 6.2-6.4)

3D finite element models of the test setups were created using Abaqus v6.14-1 [3] and solved using the Explicit solver. The explicit solver was chosen as modeling unreinforced concrete/cement materials can sometimes cause convergence problems in the Standard solver due to the extreme non-linearity caused by cracking. The Explicit solver is computationally efficient for the analysis of extremely discontinuous events, such as cracking in cement and can be used to perform quasi-static analyses with complicated contact conditions. Time increments in the Explicit solver are influenced by the overall event time scale, element shape and mass of the system; therefore in order to reduce solve time a combination of mass scaling and reduction of step times were used. To ensure that this method did not influence the solution, energy histories for the systems were checked and the mass scaling used was varied as required.

Geometry of the assemblies was provided by CSI. The small scale assembly is shown in Figure 17 and the large scale assembly is shown in Figures 19 and 20. Where possible, 8 node reduced integration brick elements (C3D8R) were used. General views of the mesh used in the models are shown in Figure 22, Figure 23 and Figure 26. To reduce computational expense, a one-fourth of the test setup was modeled by using symmetry planes in both the small and large scale models. In addition, the coil tubing was modeled to extend just slightly past the faces of the cement sheath to help with model convergence. The sand bed at the bottom of the cement was omitted as it is to allow for the placement of cement in the pipes and have some compressibility to allow movement. It is not anticipated that the exclusion of the coil tubing ends or the sand bed will have a significant effect on the analysis results.

The computational expense of the down-hole full scale model was reduced by modeling a 500ft x 1,000ft diameter section of soil assumed to be 5,000ft below the ocean floor. To further reduce computational expense symmetry planes were used to model a 15 degree “slice” of the system. The well was assumed to have a production casing size of 7-5/8” outer diameter with a wall thickness of 3/8”. The diameter of the hole was assumed to be 9-5/8” diameter with the casing placed concentrically.

General views of the FEA models are shown in Figure 21, Figure 23 and Figure 25.

6.4.1 BOUNDARY CONDITIONS AND INITIAL CONDITIONS

The small scale large scale models were restrained by fixing the base of the outer pipe in the vertical and horizontal directions. Symmetry planes were used in the X and Y planes. Boundary conditions for the small and large scale models are shown in Figure 27 and Figure 28 respectively.

The down-hole system was modeled using boundary conditions to best approximate actual down-hole conditions. To reduce computational expense symmetry planes were used and only 500ft of well bore was explicitly modeled. The system was restrained in the vertical direction using a zero velocity condition and was restrained horizontally by using zero velocity conditions in the X and Y directions around the perimeter. In order to capture the boundary condition at the top of the system and capture the initial stress state of the soil, the geostatic stress state was predefined to approximate the initial stress in the soil from the weight above as would be seen in situ conditions. Initial and boundary conditions for the down-hole system are shown in Figure 29 and Figure 30.

6.4.2 CONTACT INTERACTIONS

The assembly of parts used to create the test model was held in space using contact interactions true to how the parts interact in reality. Surface to surface contact definitions were defined at the cement to coil tubing interface and at the cement to formation pipe interface. The contacts were assigned a cohesive behavior utilizing a traction separation based contact enforcement method. Maximum tensile bonding strength at the interface was assumed to be 10% of the tensile strength of the cement slurry analyzed. Shear bond strength at the contact surfaces were provided by CSI and are shown in Table 12.

In order to simulate the de-bonding of the contact surfaces damage initiation was defined using the maximum nominal stress criteria interaction property. Once the contact stresses reach the tensile or shear bond strength separation is allowed to begin. After damage is initiated, damage evolution was modeled using mixed mode fracture energy with exponential softening behavior.

See Figure 31 for typical contact pairs in the small scale model. It should be noted that the large scale and down-hole system model are similar.

6.4.3 CEMENT DAMAGE MODELING

The cement sheaths were modeled using the concrete damaged plasticity model in ABAQUS. It provides a general capability for modeling concrete and other quasi-brittle materials in all types of structures by using the concepts of isotropic damaged elasticity in combination with isotropic tensile and compressive plasticity to represent the inelastic behavior of concrete. It consists of the combination of non-associated multi-hardening plasticity and scalar (isotropic) damaged elasticity to describe the irreversible damage that occurs during the cracking process.

The model is a continuum, plasticity-based, damage model for concrete and cements. It is based on the assumption that the main two failure mechanisms are tensile cracking and compressive crushing of the material. The evolution of the failure surface is controlled by two hardening variables, tensile and compressive equivalent plastic strains that are linked to failure mechanisms under tension and compression loading, respectively.

The fracture energy criterion was used to model the cements brittle behavior by using a stress-displacement relationship. The stress-strain behavior of the cement in uniaxial compression outside of the elastic range is modeled by using compression hardening and strain softening.

The concrete compression damage and concrete tension damage optional parameters were used to simulate the loss of stiffness of the cement as damage occurs. Maximum compressive stiffness reduction was set to 99% and 90% for tension. Once these values are reached a complete loss of stiffness is assumed to occur. Element deactivation was enabled to remove these elements from the stiffness matrix at complete failure.

6.4.4 THERMAL ANALYSIS APPROACH

Thermal loads were applied by means of a sequentially un-coupled thermal stress analysis. To accomplish this, a transient heat transfer analysis was first solved. The nodal temperature values from the heat transfer analysis were then mapped onto the structural solution model. The material definition in the structural model included a thermal expansion coefficient and thus the model developed thermal strains with the addition of a ΔT and thermal stresses when expansion was resisted by the stiffness of the structure. Since the heat transfer analysis and stress analysis are in different time period thermal properties and convection coefficients were converted into the appropriate time scale.

Two heat transfer analyses were performed for the small scale models, one for the steel outer pipe and one for the CPVC outer pipe. In order to simulate the cycling of cold and hot water, the temperature was varied over time using the load amplitude feature within ABAQUS. A complete thermal cycle consisted of 140°F for 10 minutes and then 38°F for 5 minutes, 325 complete cycles were performed to be imported into the structural model. The initial temperature of the model was assumed to be an ambient temperature of 72°F. The thermal cycling represents the circulation of hot and cold water through the inner pipe in the lab tests.

One heat transfer analysis was performed for the large scale model. The temperature was varied over time using the load amplitude feature within ABAQUS similar to the small scale model. A complete thermal cycle consisted of 150°F for 90 minutes and then 50°F for 90 minutes, 85 complete cycles were performed to be imported into the structural model. The initial temperature of the model was assumed to be an ambient temperature of 72°F. The thermal cycling represents the circulation of hot and cold water through the inner pipe in the lab tests.

One heat transfer analysis was performed for the down-hole system model. An initial temperature of 155°F was assumed down-hole with a temperature of 80°F applied for 180 minutes.

6.4.5 THERMAL PROPERTIES

Thermal expansion coefficient, conductivity and specific heat values for the cement mixes were provided by CSI and are shown in Table 12. In order to reduce computational time, average values of the cement thermal properties were used to reduce the number heat transfer analysis required. A sensitivity check was performed to ensure that this method was an acceptable approach.

The thermal expansion coefficient for steel was assumed to be 6.7×10^{-6} in/in-°F, 3.5×10^{-5} in/in-°F for CPVC pipe and 4.4×10^{-6} in/in-°F for the soil. Assumed thermal conductivity and specific heat values used for the steel, CPVC and soil are shown previously in TABLE 19.

6.4.6 THERMAL BOUNDARY CONDITIONS

The external boundary conditions were defined by giving the outer surfaces a convection coefficient and a sink temperature (water temperature or ambient air temperature). The circulated water was applied to the interior surface of the inner pipe with a film coefficient that was set to $580 \text{ W/m}^2\text{K}$ and for surfaces exposed to air a film coefficient of $15 \text{ W/m}^2\text{K}$ was used, both of which are considered appropriate.

See Figure 32 to Figure 34 for thermal boundary conditions and Figure 35 to Figure 38 for results of the heat transfer analysis.

6.4.7 PRESSURE LOADING

The models were pressurized by applying a surface pressure on the face of the interior wall of the inner tubing/pipes for all cases. For the small scale models the pressure was applied in increasing intervals of 1,000psi up to 10,000psi max. Each pressure interval up to 9,000psi was cycled 25 times; once 10,000psi was reached it was cycled up to a maximum of 650 cycles or until a failure. In addition, an upward constant pressure of up to 50psi was applied to the bottom of the cement sheath. These loads are applied as shown in Figure 39. A pressure of 2,000psi was applied cyclically to the large scale model until failure. In addition, a constant upward pressure of 20 psi was applied to the bottom. Large scale model pressure loads are shown in Figure 40.

A pressure load of 10,000psi was cycled to on the down-hole system.

6.4.8 COMBINED PRESSURE AND THERMAL LOADING

The large scale model was subjected to thermal loading and cyclic pressure loading combined. The loads were applied simultaneously so that the same number of thermal and pressure cycles were applied.

The down-hole model was loading such that multiple pressure cycles were applied while one thermal cycle was applied.

6.5 RESULTS

6.5.1 SMALL SCALE PRESSURE CYCLING RESULTS

The results for the pressure cases and a comparison to laboratory testing are shown in TABLE 20. Results showing typical cement damage and contact damage are shown in Figure 42 and Figure 43 for the CPVC outer pipe respectively and Figure 45 and Figure 46 the steel outer pipe case respectively. Results showing typical stress distributions at estimated failure are shown in Figure 44 and Figure 47 for the CPVC outer pipe and the steel outer pipe case respectively.

TABLE 20: COMPARISON OF FEA RESULTS AND LAB RESULTS FOR SMALL SCALE PRESSURE CYCLING

Case	Lab results		FEA Results	
	N_{TEST}	Location	N_{FEA}	Estimated location
Deepwater Shallow Target Low-Density	193	Inner pipe	153	Partial Inner Pipe Area and Outer Pipe
Deepwater Shallow Target Low-Density	153	Outer pipe	91	Radial Cracking/Outer Pipe
Deepwater Deep Target	120	Outer pipe	89	Radial Cracking/Outer Pipe
Deepwater Deep Target	135	Outer pipe	76	Radial Cracking/Outer Pipe
Deepwater Shallow Target Resilient	407	Inner pipe	128	Inner Pipe Area
Deepwater Shallow Target Resilient	No failure	None	None	None
Shelf	No failure	None	450	Radial Cracking/Outer Pipe
Shelf	165	Outer pipe	None	None

THIS REPORT WAS INADVERTENTLY DISSEMINATED IN THE PUBLIC DOMAIN/ONLINE SINCE 09/2015 WITHOUT A DISCLAIMER. DISCLAIMER HAS BEEN ADDED – “THIS INFORMATION IS DISTRIBUTED SOLELY FOR THE PURPOSE OF PEER REVIEW UNDER APPLICABLE INFORMATION QUALITY GUIDELINES. IT HAS NOT BEEN FORMALLY DISSEMINATED BY BSEE. IT DOES NOT REPRESENT AND SHOULD NOT BE CONSTRUED TO REPRESENT ANY AGENCY DETERMINATION OR POLICY.

Deepwater Shallow Target Conventional	105-115	Inner pipe	135	Radial Cracking/Outer Pipe
Deepwater Shallow Target Conventional	218	Outer pipe	None	None
N_{TEST} - No. of Cycles at 10,000psi to failure N_{FEA} - Estimated no. of Cycles at 10,000psi to failure				

6.5.2 SMALL SCALE THERMAL CYCLING RESULTS

The results for the pressure cases and a comparison to laboratory testing are shown in TABLE 21. Results showing typical cement damage and contact damage are shown in Figure 48 and Figure 49 for the CPVC outer pipe respectively and Figure 51 and Figure 52 the steel outer pipe case respectively. Results showing typical stress distributions at estimated failure are shown in Figure 50 and Figure 53 for the CPVC outer pipe and the steel outer pipe case respectively.

TABLE 21: COMPARISON OF FEA RESULTS AND LAB RESULTS FOR SMALL SCALE THERMAL CYCLING

Case	Lab results		FEA Results	
	N_{TEST}	Location	N_{FEA}	Estimated location
Deepwater Shallow Target Low-Density	200	Inner pipe	>325	None
Deepwater Shallow Target Low-Density	161	Outer pipe	115	Radial Cracking/Outer Pipe
Deepwater Deep Target	338	Inner pipe	>325	None
Deepwater Deep	284	Inner pipe	107	Inner Pipe Area

Target				
Deepwater Shallow Target Resilient	289	Inner pipe	91	Inner Pipe Area
Deepwater Shallow Target Resilient	233	Inner pipe	194	Inner Pipe Area
Shelf	315	Inner pipe	126	Inner Pipe Area
Shelf	305	Inner pipe	107	Radial Cracking/Outer Pipe
Deepwater Shallow Target Conventional	280	Inner pipe	130	Inner Pipe Area
Deepwater Shallow Target Conventional	218	Inner pipe	124	Inner Pipe Area
N_{TEST} - No. of Cycles at 10,000psi to failure N_{FEA} - Estimated no. of Cycles at 10,000psi to failure				

THIS REPORT WAS INADVERTENTLY DISSEMINATED IN THE PUBLIC DOMAIN/ONLINE SINCE 09/2015 WITHOUT A DISCLAIMER. DISCLAIMER HAS BEEN ADDED – “THIS INFORMATION IS DISTRIBUTED SOLELY FOR THE PURPOSE OF PEER REVIEW UNDER APPLICABLE INFORMATION QUALITY GUIDELINES. IT HAS NOT BEEN FORMALLY DISSEMINATED BY BSEE. IT DOES NOT REPRESENT AND SHOULD NOT BE CONSTRUED TO REPRESENT ANY AGENCY DETERMINATION OR POLICY.

6.5.3 LARGE SCALE RESULTS

The results for the pressure, thermal and combined cases and a comparison to laboratory testing are shown in Table 22 below. Cement damage is shown in Figure 54, Figure 55 and Figure 56 for the pressure, thermal and combined cases respectively; contact damage is shown in Figure 57, Figure 58 and Figure 59 for the pressure, thermal and combined cases respectively. Results showing stress distributions at estimated failure are shown in Figure 60, Figure 61 and Figure 62 for the pressure, thermal and combined cases respectively.

TABLE 22: COMPARISON OF FEA RESULTS AND LAB RESULTS FOR LARGE SCALE

Case	Lab results		FEA Results	
Large Scale Deepwater Shallow Target Conventional	N_{TEST}	Location	N_{FEA}	Estimated location
2,000psi Pressure Cycles	75	Outer Pipe	85	Outer Pipe Area
Thermal Cycles	31	Inner Pipe	40-50	Inner Pipe Area/Disking
Combined	Not tested	Not Tested	14	Inner Pipe Area/Disking
N_{TEST} - No. of Cycles at 10,000psi to failure N_{FEA} - Estimated no. of Cycles at 10,000psi to failure				

6.5.4 DOWN-HOLE SYSTEM RESULTS

The results for the down-hole system are shown in Figure 63 after 1 pressure cycle was applied and after 10 pressure cycles and an 80°F temperature applied.

APPENDIX A LITERATURE REVIEW

APPENDIX A.1 SHALE CEMENT PERFORMANCE

Williams et al. (2011): the authors developed cement using particle size distribution technology to minimize settling in an HPHT horizontal well in the Haynesville shale. In a horizontal HPHT environment, settling or free fluid cannot be tolerated. The authors also discuss best practices for cementation of Haynesville wells. This includes uniform borehole geometry, good pipe centralization, pipe movement to aid in mud removal, maintaining a rheological and density hierarchy between the fluids during mud removal prior to cementing, and a stable cement system. Testing for the cement system should include a GO/NO-GO test and a dynamic settling test. Other considerations highlighted are to include stresses on the cement sheath based on changing downhole conditions such as thermal fluctuations, additional drilling, or stimulation. The findings of this research indicate less sedimentation in the horizontal section during placement due to the particle size distribution in the cement system. Benefits include increased surface area, reducing the need for anti-settling additives, improved dynamic stability over a wide range of temperature, ability to maintain rheological hierarchy and improved fluid loss control.

APPENDIX A.2 CEMENT PERFORMANCE

Bannerman et al. (2005): the authors summarize the progress API Work Group on Annular Flow Prevention and Remediation in studying the causes and prevention of deepwater shallow water flows (SWF) and annular flow incidents in other wells. Loss of well control (LWC) incidents can sometimes occur when cementing or after. API RP-65 Part 2 provides guidelines for preventing and or controlling flows, and preventing SCP. Some findings of this research show that often when an LWC incident occurs, the cement slurry was not designed to prevent flow and mud removal and zonal isolation practices were not followed.

Some good practices for adequate zonal isolation are highlighted as follows: proper mud conditioning, stable wellbore, adequate annular clearances, spacer design, casing centralization, well monitoring, sufficient WOC time, and use of mechanical barriers where appropriate. Highlighted in the well design and drilling plan section is that a cement plan should provide short and long term control and isolation of potential flow zones. Some key cementing issues are listed:

- Hole geometry – including centralizer requirements, casing running conditions and ability to move pipe and achieve mud removal.
- Engineering design – cementing objectives determine cement design and coverage needed. Performance requirements include gas control, fluid loss, free fluid, thickening time and compressive strength. Tensile strength and elasticity can also be included.

Cement job execution is also important. Slurry density fluctuations can adversely affect a cement sheath, pipe movement and reciprocation can assist in effective mud removal, spacers can help to remove mud, water wet the cement contact surfaces, and provide a buffer between the cement and drilling fluid. Post cementing operations should include maintaining a full hole, proper WOC time, and a top job if needed.

Bois et al. (2011): This articles lists the different studies performed since the 1990's to understand long term fluid migration. Before that all the studies focused on fluid migration during cementing while cement is still in liquid or gel state. It details the investigation procedures used by three research teams,

Goodwin & Crook (1992), Jackson & Murphy (1993) and Boukhalifa (2005), to investigate long term fluid migration. It also compares the results of these investigations with the different theoretical models .At the end the authors present a new mechanistic analysis of micro annuli formation to explain their mode of formation and detail the conditions under which they appear.

Bosma et al. (2000): This article describes a new cement analyzer developed to determine the setting behavior, elastic/viscosity properties and volume changes of cement and other sealant materials (resins). The apparatus is used to measure the expansion and shrinkage phenomena in either closed or open systems as per API 10TR2. It helps overcome the limitations of API procedures and equipment such as the impossibility to perform the tests under high pressures and temperatures and the inability to measure shrinkage/expansion while monitoring the cement reaction.

Brandl et al. (2013): the authors studied a cement spacer based on a micro emulsion technology and a cement design using a multifunctional polymer. The authors also describe a case history where this was applied in the South China Sea successfully. In this paper, the authors describe cementing as a critical aspect during deepwater well construction with unique considerations for fluid placement, design, and performance. Some common problems include poor mud removal which can leave a mud channel and result in an incomplete cement sheath which is not an effective barrier.

The slurry designed for this project was light weight, easy to mix, stable with zero free fluid and fluid loss of 32mL API. The transition time was 6 minutes. These are all effective properties according to the authors. One finding from this study is micro emulsion technology effectively cleans NAF and water wets the surface as verified by goniometer. Another important fluid design aspect is the spacer and lead cement slurry were engineered to match the density, friction and minimum pressure gradient hierarchy which is needed for effective displacement according to the authors.

Doherty (2011): In this article, the author describes the four key factors that should be considered in designing cement jobs for riserless deep water wells. The first key factor is shallow water flow. This flow occurs when the cement starts gelling and does not transmit hydrostatic pressure. To prevent this, specialized additives to plug the slurry pores or to control its fluid loss can be used; pumping foam slurries is another option. The second factor is to know the formations we are cementing and to use the

actual conditions of temperature and pressure when testing cement slurries. The third factor is the tight window between the formation pressure and fracture pressure.

The engineer must use software modelling to dynamically simulate the cement job and ensure that the ECD stays within the pore pressure/frac pressure window and that all the best practices such as mud removal and casing centralization are implemented. The last factor is lost circulation issues when drilling through salt. High tech materials are available to prevent and cure these losses. Finally, proper pre job planning and optimized spacers and cement slurries are best defense against casing failures caused by corrosive fluids, creeping salt formations and stresses induced by fluid changes, tests, stimulation operations and formation depletion.

Kinzel (1993): The author of this article discusses the considerations for centralizer selection for high-angle and horizontal wells. Centralizers are required for effective mud removal for cementing. Selection requirements include the ability to rotate/reciprocate, a high restoring capacity and a low moving force. Other considerations discussed included cementing liners, centralizer placement, and types of centralizers such as bow-type, rigid or downhole activated centralizers.

Mueller (2012): This article gives the list API standards and their area of applicability in deepwater cementing: API RP65, API RP 65-2, API Standard 65-2, API RP 10B-3 and API-RP 10B-4

Fioanini et al. (2014): This paper discusses the recent use of epoxy resins in primary cement jobs as a substitute for conventional cements because of their high compressive strength, enhanced ductility and their ability to avoid contamination. To ensure that the industry will accept these resins as a proven means of zonal isolation, it was necessary to find a method to identify their presence behind the casing and determine the strength of their bond. The authors present a new evaluation method that combines visual and analytical methods to interpret sonic and ultrasonic cement logging data. This method was used to determine the exact location of a resin slurry that was part of a multistage cementing job.

Hakan et al. (2013): the authors discuss the development of permeability in a cement sheath and how controlling gas flow through the cement sheath is important. There are many different phenomena that let gas pass through the cement. Wrong density, poor mud filter cake removal, premature gelation, excessive fluid loss, high permeable cement, high shrinkage, cement failure under stress, and poor

interfacial bonding are all reasons that gas may flow through cement. Inconsistent mixing also results in non-uniformity in the cement sheath, which can lead to gas percolation. This study examined a magnesium complex with carbonate as a cement additive to investigate its prevention of permeability development within the cement sheath. At 3% it can create impermeable cement.

Hunter et al. (2007): This article is about the three key mechanisms that can be used to prevent and stop sustained casing pressure (SCP). The first mechanism is to design and pump reliable cement systems that can withstand the effect of cyclical stresses during the life of the well. The second mechanism is to include auto-seal chemicals in the cement sheath matrix. In case of formation hydrocarbon influx, these chemicals will activate and seal the micro annuli or cement sheath cracks. The last mechanism is a swellable packer that can be run as a part of the casing string. If the rubber elements of these packers come in contact with liquid hydrocarbons, they will swell to more than twice their original size and reestablish zonal isolation.

Jiang et al. (2012): This paper discusses using bond logs to determine whether zonal isolation was achieved or whether remedial cementing is required. The paper covers the use of bond logs in a 35 year old depleted field where several new wells were to be drilled to evaluate zonal isolation.

King et al. (2013): the authors amassed a large collection of information on well construction failure. In the conclusions, the authors highlight several notes about failure occurrence. Failure rates vary widely with type of well, geographical location area and maintenance culture of the operator. Gas migration potential varies primarily with geography and appears to be highest where natural seeps of gas or oil are present. Current well design with nested cemented casing strings are effective in sharply reducing pollution potential from oil and gas wells.

Laws et al. (2006): This paper discusses some of the issues faced while cementing in Oman. The paper reviews general good practices for achieving a successful cement job.

Lecampion et al. (2013): the authors investigate and experimentally demonstrate a mathematical model fluid driven de-bonding of the wellbore annulus to provide a fundamental basis for well design. De-bonding of the cement/casing or cement/rock interfaces has been recognized since the 1960s to be the cause of leaks occurring from wellbores. This could be due to pressure and temperature fluctuations

and cement shrinkage. The focus of this paper is during injection. Fluid driven depending of the cement interfaces is not uncommon, as it has been observed during well stimulation by hydraulic fracturing. These experiments confirm the predicted scaling relationship that estimates the grown in the de-bonding length in the zero-buoyancy case and that the annular de-bonding will reach a stable value wherein the fracture extends over $\frac{1}{2}$ - $\frac{3}{4}$ the circumference of the annulus.

Lecampion et al. (2011): The authors discuss de-bonding of the cement sheath on CO₂ injection wells. The authors cite the low permeability of cement as a prime reason it is selected to hydraulically seal well bores to protect upper formations and groundwater from hydrocarbon bearing zones. However, the cement may de-bond from the casing or formation due to depressurization and thermal cooling taking place after cement placement or upon injecting a new fluid into the wellbore. The thickness of the cement sheath may be up to 5000 times thinner than the length of the casing section. When the casing is centered in the openhole well, the problem is reduced to a one dimensional problem. Once the cement of one section has hardened the next section is drilled, cased and cemented.

These operations can induce pressure and temperature fluctuations to damage the cement annulus. Three types of defects can occur due to these actions: Disking cracks, radial cracks, and micro annulus. De-bonding was first recognized in the 1960s as a result of fracturing. This paper investigates that defects in the cemented annulus of a well are important only if hydraulically connected. The fluid only needs to overcome the clamping stress in order to open the micro annuli. A number of things can be done to help prevent this: careful cement placement, expanding cement systems, and properly designed packers are highlighted.

Levine et al. (1979): the authors discuss field application techniques for annular gas flow prevention after cementing. Some techniques include minimizing cement height, pressurizing the annulus, increasing the annular mud density, adjusting thickening time, multistage cementing, increasing cement mix water density and modified cement slurries. This paper highlights some common techniques used when preventing gas flow. Limit primary cement column height, vary thickening times within a column of cement, apply surface pressure on the annulus, increase annular mud density prior to cementing, multistage cementing, increase density of cement slurry mix water, utilize modified cement slurry.

Ravi et al. (2010): the authors studied the challenges faced when drilling through depleted, weak zones and how the design of the spacer fluid and cement slurry can help prevent losses. The paper discusses how to prevent losses, how to lower cement slurry density, and the importance of fluid loss control in cement and spacer fluids. When discussing cement slurry placement the authors highlight several aspects. Effective stimulation of a reservoir requires hole cleaning and slurry placement in the entire annulus. Horizontal sections are vulnerable to cement slurries settling. This can lead to free water formation and solids settling out. It is important to optimize the rheology of the fluids to prevent settling and reduce the friction pressure. Pipe centralization and movement are both critical to cement placement. Both aid in providing a cement sheath that covers the full annulus at points along the well where isolation is critical. Pipe movement can be especially helpful in horizontal sections where centralization is difficult.

Teodoriu et al. (2010): This paper is about a new analytical model developed to predict the performance of casing-cement bond under HPHT conditions during the life of a well. The model considers the casing as a thin wall cylinder while the cement and formation are considered as thick walls. The authors studied the effect of temperature, pressure and casing-cement-formation interactions on the integrity of different cement slurry systems. They also presented a comparison between conventional cements and new non-Portland based cement slurries (Epoxy resin). These new cements have improved annular seal under HPHT conditions and better mechanical shear and hydraulic bonding.

Tinsley et al. (1980): The authors discuss annular gas flow in various fields and an experiment conducted to analyze annular gas flow. Houston Offshore (High Island) commonly has gas flow 0.5-1.5hrs after cementing. Remedial cementing cost can be \$20,000-\$350,000 per well. Previous annular gas flow studies highlight adequate fluid loss control as a way to prevent cement slurry dehydration and in turn, help to prevent annular gas flow. They also study a compressible cement system. The conclusions state that during transition state, cement slurries have a decrease in internal volume due to chemical hydration and fluid loss, and during this time, slurries do not transmit full hydrostatic pressure. Free water is not a primary factor in gas flow. They also found the new compressible cement system to be effective in the field.

Talabani et al. (1993): This article talks about the mechanisms and causes of gas migration and the use of new cement additives to prevent this migration. The authors propose the addition of some readily available additives such as ironite sponge powder, Anchorage clay and synthetic rubber powder to the cement slurry to eliminate the risk of gas channeling. They also recommend the use of ultra-sonic laboratory measurement to check for micro-fractures before the cement is pumped in the field.

APPENDIX A.3 ANNULAR PRESSURE BUILD-UP

Alves et al. (2006): The authors in this paper developed a model to predict two phase annular flow in gas wells. The model developed was correlated with data obtained for 75 wells and evaluated for conformity. The results indicated that the model correctly predicts gas flow properties which include pressure gradient and liquid film thickness. When compared to most empirical correlations, the model better represented flow characteristics in the chosen field wells.

Alves et al. (2006): This paper focused on developing a model to predict casing annular temperature and pressure in deepwater wells. Since a rise in annular pressure and temperature may result in potential damage to casing, the authors derived a model to help predict and mitigate the problem. The model is based on the volumetric change of annular fluid during production, due to temperature and pressure. The annular fluid increases in pressure due to a heat transfer between rising production fluids and the casing walls. The model was successfully applied to a deepwater well in West Africa and used to predict annular pressure. The well was 4265ft below sea level.

Brooks et al. (2008): The authors present a study on using two stage cementing to prevent gas flow. The flow of annular gas has proven to be very difficult to prevent, dangerous, and challenging and costly to remediate. The authors cite cost in the Middle East as being \$200-\$250K to remediate and in the range of \$1M in the North Sea. This paper focuses on short term gas migration. The authors say around 50% of casing string exhibiting SCP are production casing strings, while the rest are spread among the intermediate, surface and conductor strings. The conclusions of this paper state that understanding the mechanisms which cause gas migration can be used to help mitigate it. Proper drilling techniques, gas blocking systems, and casing annulus packers can all be used to prevent gas migration

Eaton et al. (2006): This paper discusses annular pressure build up due to increased temperature and reduced nitrogen hydrostatic pressure in the annulus of an un-cemented liner hanger in a production well in the Gulf of Mexico. The paper focuses on the possible collapse of the production casing and considers underlying factors such as completion design and equipment modification. The authors analyzed data for eight wells and identified the possible causes of hanger collapse during production. To

prevent collapse, the authors suggest changes in completion techniques such as making sure cement is placed across the liner hanger during the initial cement job.

Garcia et al. (1976): This paper focused on the loss of hydrostatic pressure in the cement column due to cement setting from top to bottom. The authors developed procedures to promote more uniform setting of the cement column. The fluid loss and mix water of the cement should be as low as possible, and if possible, cement setting time should be tailored to set from the bottom up. Also displacement efficiency can be increased by conditioning mud prior to removal and moving the pipe during cementing operations.

Kadry (1999): The author describes a blow out on a well in the Mediterranean caused by annular gas flow during cementing operations. The blow out occurred after second stage cementing operations had been completed but prior to the final cut of a 9 5/8" casing. The author attributed the annular gas flow and consequently the blow out, to the cementing procedures utilized at the location. Emphasis is made on the lack of control on mud losses, free water, unrepresentative thickening time of cement, and inaccurate hydrostatic pressure predictions.

APPENDIX A.4 INDUSTRY TRENDS

Bowersock et al. (2014): This article discusses the results of some case studies and reports where mechanical devices such as packers were used at the time of, or shortly after cementing operations had been completed to help isolate zones that would be produced. The paper cites a study where 7 out of 11 wells in a region, all were completed without a mechanical barrier, required remedial operations to be able to control placement of frac fluids. The next 37 wells were completed with a packer set 50-100ft above the desired production zone and did not need any remedial work. The paper also discusses the use of multiple mechanical tools, such as packers and multi-stage tools, together to improve cement sheath integrity.

Chitwood et al. (2011): This paper identified six major areas where technology gaps have large potential impacts for deepwater drilling and completions; well testing, early production systems, underbalanced drilling, dual gradient drilling, tender assisted drilling and a well intervention/completion vessel. Each of these areas was reviewed. For evaluation purposes, conceptual well architecture and drilling programs were used. The wells were in 6,000' and 10,000' of water with a TVD of 17,000' and 21,000', a KOP 500' below the 20" casing shoe with a 3^o/100' build. The various casing sizes, setting depths and well trajectory used are shown in the paper. Both well used a 9 5/8" production casing with a 5½" completion tubing.

Dooply et al. (2013): This paper discusses the benefits of using a foamed fluid placement simulator during pre-job planning and evaluation of a cement job as well as post job evaluation.

Morris et al. (2012): This paper discusses the use of epoxy resin in place of cement. Positive factors of resin are that the resin density is easily adjusted as well as rheological properties. Resin tends to have higher strengths, bond properties (to casing and formation) and chemical resistance when compared with cement. Resin is easily adjusted to allow for use in a wide range of temperatures.

Parcevaux et al. (1990): the authors explain in great detail several methods for preventing annular gas migration. Proper mud removal is highlighted as a major player in the prevention of gas migration. Mud conditioning, casing centralization, casing movement namely rotation and reciprocation, proper pre-

flushes and spacers, proper fluid volumes for contact time, and adequate flow rates are all important in promoting good mud removal. There is a section on gas migration after cement setting and relating it to shear or hydraulic bond strengths.

Cement to formation and pipe bonds have been a subject of discussion for a long time. Good bonding is the principal goal of primary cementing, with few papers published on the subject. Shear bond is related to cement tensile strength and the surface condition of the casing. They did not find a correlation between bond strength and compressive strength. Hydraulic bond failure is primarily a function of pipe expansion or contraction and the viscosity of the pressurizing fluid. Downhole deformations can occur as a result of thermal stresses or hydraulic stresses (such as fracturing). The effect of pressure changes on casing dimensions and stability is well documented, and well known. The results of the studies detailed in this paper show that downhole deformations resulting from thermal and hydraulic stresses constitute a major drive for gas migration at the hard cement casing and formation interfaces. These factors are not generally taken into account and should be carefully considered.

Ravi et al. (2009): This paper discusses the importance of elasticity in cement slurry designs. Elasticity is very important to the life of a cement sheath especially with regard to wells that will undergo cyclic loading such as those used as storage wells. Standard cement can withstand a large amount of stress. However cement is brittle and does not easily deform or return back to original dimensions under cyclic loading. Cement can de-bond from either the casing or formation under these conditions. Additionally, cement cannot be cycled many times before failing. More elastic cement slurries cannot sustain as high of an overall stress as standard cement but due to elasticity the cement is less likely to de-bond while exposed to cyclic loading. Elastic cements can be cycled more times than standard cement as they are less brittle.

Reddy et al. (2002): This paper discusses the use of liquid additives and a single type of neat cement for cementing in the GOM to help improve cementing, especially in the presence of SWF zones. The paper covers the versatility of this method to be able to cement multiple casing strings. The versatility is due to the fact that cement blends from previous jobs do not need to be sent back to shore to make room

for a new blend as all necessary cement and additives can be maintained on the rig and mixed when needed. The paper covers several case studies to make the authors point and by citing case studies.

Rivas et al. (2009): This paper discusses the required technology to drill and complete extended reach deepwater wells located in a Green Canyon Block of the Gulf of Mexico. The typical well total depth was over 28,000', a bottom hole pressure of 20,000 psi, a bottom hole temperature of 200°F, and a water depth of 4,100' - 4,300'. The formation contained an 8,000 – 15,000' thick salt canopy with the base around 20,000' TVDSS, and Middle to Lower Miocene sands in the production zone around 23,000' to 28,000' TVDSS. The intermediate liner was a 13 5/8" casing set above the base of salt, the production liner was a 9 7/8" 62.8# Q-125 in a 12 1/4" hole and there was a contingency plan for a 7" 38# HCQ-125 liner. While VIT, burst discs, and nitrogen were considered for APB mitigation, the technique selected was to drill a vent hole into the wellhead that was plugged and connected to a continuous monitoring system for the B annulus and to install burst discs for the C annulus in the 22" casing string.

The completion tubing was 5 1/2" 23# 110 ksi, the completion method used in the production zone was a stacked frac-pack located at 25,800' TVDSS in the 9 7/8" liner, the completion fluid was a ZnBr (14.8 – 15.2ppg) and the design production rate was up to 25,000 bopd. A prototype 7" frac tool was used 6 times in the field with 150,000 lbs. of 16/30 mesh high-strength proppant and a 3.88" bore frac packer. This configuration was unusual at the time; most frac packs used a 3.25" bore packer and 20/40 mesh intermediate strength proppant. The minimum treating rate was 30 bpm with a cross-linked frac fluid.

TVDSS = Total vertical depth subsea.

Sanders et al. (2011): This paper focuses on planning, tool functions and features and operational considerations for perforating deepwater high-pressure wells located in the Walker Ridge Blocks of the Gulf of Mexico. The wells had water depths greater than 8,000', downhole pressures greater than 19,000' psi, a temperature of 260°F, a maximum deviation of 20°, a production zone in the Lower Tertiary formation and a planned perforation interval of 800' from about 25,170 – 26,000' with 3-6 frac-pack intervals. The completion fluid was a 14.7ppg Ca/Zn/Br brine. These wells were perforated using a single-trip multi-zone frac-pack system run in on a 3.5" 13.3# drill pipe; since all tools and components were run at once and all zones simulated in the same trip, 15.5 days of rig time was saved compared to a conventional stacked frac-pack. As part of the planning process, gun shock loads were modeled since

these loads are a risk for high-pressure deepwater wells. Loads included wellbore pressure waves, fluid re-pressurization, and deformation of tubing and guns. The maximum pressure on the firing head gauge was 19,000 psi, which changes over time to about 12,000 psi after 1.5s.

APPENDIX A.5 WELL ARCHITECTURE

Miller et al. (2005): This paper covers use of non-standard sizes of casing to increase the number of casing strings that can be set in a HPHT deepwater well. Since number of casing set points are limited by the wellhead diameter and desired production casing diameter to accommodate high-rate production tubing, reverting to non-standard casing size to allow one additional casing set point and increasing wall thickness to increase casing strength is a proven design method. Having the non-standard casing manufactured is not a problem. However, applicable liner hangers are not available to accommodate non-standard diameters and close clearances.

Liner hangers must be rotatable to allow casing movement during cementing to ensure optimum cement coverage in the narrow annulus. The authors note that operators routinely drill oversized holes to improve annular geometry. In the overlap, small clearance may dictate use of polymer squeezes rather than cement to achieve a seal in the liner lap. While acknowledging tight clearance and difficulty of placing cement, they conclude that this traditional approach is a proven and direct method to add an extra casing point or increase casing wall thickness.

APPENDIX A.6 COMPLETION DATA

Aldridge et al. (1996): Cooler wellhead inlet temperatures caused by chilling of cement and stimulation fluids pumped to the well may result in unusual stress imposition of the tubulars. The paper generally discusses mechanical improvements and chemical injection systems.

Burman et al. (2005): This paper presents frac pack completion of 6 wells in the Marco Polo deepwater development project in Green Canyon. A total of 17 frac-packs were done in 4300 ft. water depth from a TLP. The operation is much different from today's completion practice since the wells were drilled with WBM and completed with risers. However, well conditions and procedures indicate several sources of wellbore stress induced during deepwater frac-pack completions.

Wells were perforated overbalanced. A total of 51 sliding sleeves were installed. Mudline temperature was 38°F at 4300 ft. Reservoir depth ranged from 11,000 ft. to 13,500 ft. tvd-ss with reservoir temperature of around 120°F and pressure of around 7300 psi. Tip screenout designs called for a net pressure increase of 500 psi indicating a bottom hole fracturing pressure of 8000 to 8500 psi. Frac fluid was conventional borate cross-linked fluid with gel concentrations adjusted to account for increased proppant carrying efficiency due to cold riser temperatures. Minimum frac rate was 10 BPM.

Ceccarelli et al. (2009): It addresses use of project management tools to help reduce cost and time as well as to increase reliability. The authors discuss 6 deepwater completion issues that benefit from cost-reliability-efficiency analysis (triple constraint). Three are sand control type, barriers, and components materials. Ancillary information regarding each topic is included here. The authors state that cased-hole frac-packs and openhole gravel packs are most reliable deepwater completion methods. Both methods are more costly and time consuming than stand-alone screens, but they are significantly more reliable. Frac-packs are more costly due to large volumes and high-pressure pumping. Barrier analysis relates to mechanical barriers run in along with gravel pack or frac-pack strings and does not relate to cemented casing integrity. Materials specification analysis indicates that deepwater default material of choice is 13CR-80 steel due to its corrosion resistance.

Copeland et al. (2005): This PowerPoint presentation covers issues of drilling and completing deep shelf wells in the GOM. First is the extreme temperature and pressure under which the production and tie-back casing strings must function will require high strength and corrosion resistance. Second, the presentation noted that sand control in deep shelf wells will induce significant pressure in the work string as well as high surface treating pressure.

Procyk et al. (2009): This article describes completion design for the Magnolia field. Eight wells, completed in 2004, were developed from a TLP in 4673 ft. of water. The producing formation undergoes compaction with extreme depletion (>8,000 psi decrease in reservoir pressure). Wells were completed with cased hole frac packs using viscoelastic surfactant gelled fluid. No information was provided about cementing or actual frac pack treatment conditions. However, a few pertinent bits of information regarding the well design and operations were noted in the article. Viscoelastic surfactant gel was used due to compatibility issues with borate cross-linked guar and the CaBr completion fluid. Heavy-walled casing was used for compaction resistance. Perforation of this casing was therefore a concern. Final perforating scheme was 21 shots/ft. with a 0.667 diameter perforation charge.

Ribeiro et al. (1993): the authors describe the state of the art deep water subsea completion techniques. One piece of equipment is a guidelineless lay-away subsea tree: this is designed to withstand stresses imposed by 6000' ft. completion riser string with direct hydraulic type control panel. The authors cover several innovations but the main message is subsea completion will continue to play a key role in the offshore arena, however all new technologies developed must be innovative and simple. Standardization will be key in the future.

APPENDIX A.7 FIELD CONDITIONS

Al-Thuwaini et al. (2010): The authors investigate a fit-for-purpose sealant for HPHT wells. The generally accepted definition of HPHT used is undisturbed temperature of 300°F or greater than the hydrostatic pressure gradient of 0.8psi/ft. This investigation is on high performance light weight slurries (HPLW). To achieve this, the authors use particle size distribution (PSD). To prevent gas migration in the short term casing is properly centralized, mud removal is adequate, and slurry is prepared and designed adequately. However, long term failure can expose the cement column to unwanted annular hydrocarbon migration leading to sustained casing pressure.

To prevent this, a self-healing cement was introduced. Long term isolation challenges are related to temperature and pressure cycles and well testing. In HPHT wells the cement sheath is subjected to an extreme range of temperature and pressures through drilling, fracturing and testing phases. This can create a large amount of stress and lead to de-bonding issues. Rock properties taken into account were young's modulus and Poisson's ratio. During a hydraulic fracturing job the applied pressure would induce a high Mohr Coulomb stress of 20.44 MPa or 2964 psi, and a maximum tangential tensile stress of 10.55KPa (1.53psi). In that situation, a conventional cement would crack.

When this HPHT well is fractured, the temperature can decrease from 340°F to 199°F which leads to a contraction of the casing. Again, this would lead to a conventional system de-bonding from the casing. The solution is to analyze the stress for the well during its lifetime and design a cement that can withstand that stress without de-bonding. The properties of the cement to optimize are Young's modulus, Poisson's ratio, and tensile strength. Best cement practices should still be used: good centralization and good mud removal techniques.

Bastos (2008): in this article, the author elaborates on the need for advances in drilling and completion for deepwater due to deeper, longer, hotter wells. The history of deepwater technology development is covered. High oil prices should translate to more money for R&D to continue developing new technology in all areas of drilling and producing. New technology fronts are downhole on board intelligence, with new directional steering and LWD/MWD capabilities and producing more technical

data. Real time operation remote monitoring and delivering this data from remote location to a central base; this permits the allotment of intelligence and specialized knowledge to the well location. Computer modelling and simulation: this is used during planning and engineering phase and with extra data available in real-time can be used to confirm or alter well construction plan.

Biezen et al. (1999): the authors present methods to help design and execute effective cement jobs for HPHT and deepwater wells. Successful zonal isolation requires good engineering practices, and consideration of the slurry design and slurry placement techniques and best practices of the field. Typical requirements for deepwater low temperature cements are a short transition time, excellent compressive strength at low temperature, low fluid loss, good slurry integrity and long term properties such as sealing and bonding to casing and formation. Good displacement is required for good bonding. Foam sealants are often chosen for their compressibility, good displacement efficiency, long term sealing ability, ductility, and good bonding to formation and casing.

HPHT wells require cement that can perform well in both short term and long term. To evaluate the slurry, a settling test must be run at HPHT conditions. All other standard tests should be run at actual temperature and pressure schedules to get representative results. The long term sealant requirements are to add silica flour to prevent strength retrogression, mechanical properties such as tensile strength and Young's modulus need to be determined to withstand downhole operations, and the sealant should be resistant to any chemicals present in the well. Stresses the cement may see are thermal, and pressure during testing, stimulation, production and injection.

Heathman et al. (2006): The authors evaluated the use of finite element analysis to couple casing and cement designs for HPHT wells. The challenge for this study was that many cement sheaths are under designed for the extreme stresses they are exposed to once placed. Stresses include: continued drilling, completion operations, well testing, access to various annuli for pressure control during thermal changes, and the effects of gradual drawdown during long term production. The traditional focus of the cementing job is designing the slurry to be placed properly.

However, the wellbore longevity depends on how it behaves when coupled to the casing and formation during all subsequent operations. This model system was composed of the formation material, cement, and casing divided into a finite number of parts or elements so that the governing equations could be solved. Solutions ranged from simple modifications to operational procedures or wellbore design to a complex cement sheath redesign or any combination of those. To solve the problems identified by this analysis, a more elastic cement was developed using a copolymer elastic bead in conjunction with a gas producing additive. A month after placement, a CBL was run and showed good bonding where required.

Cordeiro et al. (1999): The authors of this paper gave an overview of drilling, completion and workover operations in the Marlim Field in Brazil. Wells were drilled in water depths between 1,968' to 3,608', the production casing used was a 9 5/8" casing and either a 7" liner or 9 5/8" casing for injector wells, and the production zone formation is an Oligocene unconsolidated sandstone. Three methods to install the wellhead for completions were used; the first method required a lay vessel and a completion vessel on location at the same time, the second used a dummy completion base and the lay and completion vessels were not required to be on location at the same time, and the third did not require a completion vessel. Due to sand production, a gravel-pack open-hole completion method was used. After research to improve production, a frac-pack technique was used, which used the gravel pack for sand control and high rate water packing with brine instead of a viscous fluid. To remove the drilling filter cake from the formation, chemicals were used while flowing the well. According to the authors, the way a horizontal production hole is drilled in unconsolidated sandstone determines a good completion job.

Li et al. (2005): The authors of this paper conducted studies on long-term well integrity with regards to completion design, and formation loads on the casing such as reservoir movements, compaction loading, and sea floor subsidence. The wells were located in the Mississippi Canyon Block in the Gulf of Mexico with a water depth of 5,430' and a 9 5/8" 53.5# Q-125 production casing in a 12 1/4" cemented hole. The completion method was a cased-hole frac pack using a 4 1/2" 13Cr-95 production tubing, a telescoping joint, a 5 1/2" 23# 13Cr-95 blank pipe for the frac pack, a screen on 5" 18# 13Cr-85 base pipe, and a lower sump packer.

The hole deviation was 29° as a 180' perforation interval, and the formation of the production zone was fine, unconsolidated and weak sands with a porosity between 25% -38% and a UCS of approximately 200 psi. The authors estimated that the reservoir pressure would decrease from 5,320 psi to 2,700 psi over 9 years of production. Numerical models simulated a 600' section of the formation and casing for predictions of compaction, subsidence and reservoir deformation assuming a 10' radius of formation around the completion equipment. Sea floor subsidence was estimated to be 0.33', vertical compaction was estimated to be 1', and lateral movements were estimated to be 1' south and 1.2' east.

The ratio of the ultimate damage limit to the simulated compaction strain is the mechanical well life safety factor, and in the model the safety factor given was 1.7. Cement integrity in the areas just above, below and at the completion interval needs to have integrity to support the casing and provide isolation. As the formation compacts loads transfer to casing and then to the completion, plastic strains on the cement were 5% -7%, and strains of the casing were below 1%. Damage to the cement was limited to the area near the formation where sands become shale. The telescoping joint was intended to reduce the transfer of compressive stresses to the inner tubing and pipe. The authors note that this effect is changes when there is gravel, poor gravel placement, or no gravel. In the case of poor gravel placement, cement integrity is needed to prevent buckling or premature screen damage.

Sinha et al. (2008): The authors analyze and estimate the near wellbore condition after drilling. Formation stresses play an important role in prospecting and development of oil and gas fields. Both the direction and magnitude of these stresses are required in planning for borehole stability during drilling, fracturing, and selective perforation. Near wellbore stresses can be caused by several sources including borehole stress concentrations, drilling mud pressure, plastic yielding of rock prior to breakouts, shale swelling, drilling induced fractures, and invasion of monomer and resin materials. The formation may be weakened or strengthened by these forces.

Wendler et al. (2012): The authors of this paper discuss issues related to well testing for producing reservoirs in deepwater and ultra-deep water environments. Deepwater wells are considered to have a water depth over 1,000' with ultra-deepwater greater than 5,000'. HPHT wells are considered to have shut-in pressures greater than 10,000 psi and a bottom hole temperature greater than 302°F . Ultra-HPHT wells are considered to have temperatures greater than 425°F and pressures greater than 15,000

psi. HPHT conditions in deepwater present additional challenges to testing, and potential issues that can occur are casing collapse, wellbore collapse and a breakdown of drilling fluids. High temperatures can affect elastomer performance and metal yield strength in packers and seals.

The cement bond and components such as tubulars or packers need to resist thermal cyclic loading or other stresses. The authors include a list of other primary considerations for planning, including contingency planning. The inverse Joule-Thompson effect on HPHT wells is also discussed where the temperature of a gas will change with a pressure reduction while flowing through a restriction. Heating will occur either in the near wellbore region with a pressure drop across the perforations or in the wellbore itself, which can result in a surface temperature close to the downhole temperature or an apparent reservoir temperature higher than the static reservoir temperature. This paper also discusses fluid selection for HPHT environments, hydrate prevention, coiled tubing applications, and perforating considerations.

Wu et al. (2011): This paper detailed a study on wellbore stability during drilling in non-reactive shale using a thermo-poroelastic 2D model on a HPHT well located in the South China Sea. Drilling results in changes in near-wellbore stress, pore pressure, temperature, and chemistry. Wellbore instability can occur when the stress in this near-wellbore area becomes greater than the formation rock strength. Data for the model was acquired or calculated, such as dynamic Young's modulus, dynamic Poisson's ratio, compressional slowness, shear slowness, rock bulk density, overburden stress, and reservoir pressure. The authors assumed that shear failure in the wellbore occurs when the maximum/minimum Terzaghi effective stress meet the Mohr Coulomb strength criteria, and that tensile failure occurs when the minimum Terzaghi effective stress equals the tensile strength of the wellbore wall.

APPENDIX A.8 HPHT

Carter et al. (2005): In this paper, the authors study stress corrosion cracking and how it can be related to different chemicals and metallurgies. Often metallurgy for production tubing is selected based on the produced fluids. However, many instances of corrosion cracking are due to the completion or packer fluids. In an HPHT situation, this can be exaggerated. Small differences in composition can have a large impact on corrosion cracking.

Griffith et al. (2004): The authors studied foam cement properties in an HPHT environment. In this study, the mechanical properties of the foamed cement sheath are examined. The long term integrity of cement depends on the material/mechanical properties of the cement sheath such as young's modulus, tensile strength and resistance to downhole chemical attack. Considering properties of the cement sheath for long term integrity is important if the well is subjected to large changes in stress levels such as with HPHT wells.

Foamed cement is at least one order of magnitude more resilient than non-nitrified cements and is resistant to both temperature and pressure cycling induced stresses. This feature permits the cement sheath to flex while the casing expands and then return to its original condition. Because of the flexibility, the cement sheath is less likely to be damaged over a long period of time. Foamed cement if properly designed is likely to provide better long term zonal isolation at extreme conditions than conventional cement systems through improved mechanical properties. These improved features are: hydration volume reduction is compensated for due to compressibility, and cement sheath elasticity is improved compared to conventional cement sheaths.

Maldonado (2005): In this article, the author discusses HTHP completions and associated risks, design requirements, success factors and new technology. Potential effects of HTHP conditions on tools include pipe movement, packer compression, increased fluid friction, thermal cycling, tubing stresses, and elastomer performance. For high pressure requirements, the cross-section of downhole tubulars or equipment can be increased, high-strength materials can be used, and materials such as corrosion-

resistant alloys can be used it here is risk of corrosion. Other technical challenges include reliability, seals, metallurgy, and well fluid compatibility.

Mazerov (2011): This article covers existing challenges for completions in HTHP environments both onshore and offshore, including the Haynesville and Gulf of Mexico shelf. Various operators and service company representatives were interviewed. While the definition of HTHP has expanded over time, in this article HTHP is considered to be temperatures greater than 302°F and shut-in pressure greater than 10,000 psi, ultra-HTHP is greater than 400°F and 20,000 psi, and extreme-HTHP is greater than 500°F and 35,000 psi. These HTHP conditions increase operating risk and cost. Downhole tools can require expensive metallurgy, and high pressures require increased horsepower on the surface for stimulation operations. Temperatures can affect the stability and lifespan of downhole electronics, and the presence of CO₂ and H₂S can increase risk for corrosion and cracking. Wall thickness can be increased to provide the required pressure resistance, however this reduces the ID available for flow.

Patterson et al. (2007): The authors examined HPHT completions in the continental shelf environment of the Gulf of Mexico. These formations tend to have extreme completion challenges with low permeability, the opposite of most GOM reservoirs. HPHT wells sort into 4 main categories:

- Green: BHP 17,000-22,000psi, BHT 350-425°F
- Yellow: BHP 22,000-25,500 psi, BHT 425-485°F
- Orange: BHP 25,500-28,500 psi, BHT 485-515°F
- Red: BHP 28,500psi and up, BHT 515°F and up

The completion concept for the well in the case study was a 4.5" monobore natural completion because sand control was not necessary. High production rates were anticipated, and the potential to frack was realized. This would not be a normal GOM soft rock frac pack for stimulation.

The wells reviewed for this stimulation were from south Texas where HPHT hard-rock fracturing was more common. A challenge was finding a fluid that can effectively open the formation at high temperatures and finding a proppant that could withstand the conditions. As the reserves in the deep GOM shelf are pursued, the formations can get extremely tight and these completions will need to have optimized fracturing methods. More wells are falling in the HPHT category. The well studied here required high pressures, frac fluids that could withstand high temperatures and proppant that could

withstand the maximum stress of 14,000psi at the end of its life. By designing the frac job this way, the authors were able to achieve the desired post frac production rates.

Thompson et. Al (2012): This article reviews design and development considerations for subsurface safety valves in HTHP environments. Tier 1 HTHP conditions are defined as pressures up to 20,000 psi and temperatures up to 400°F. Tier 2 pressure and temperature extends to 25,000 psi and 450°F, and Tier 3 conditions are up to 30,000 psi and 500°F. Considerations for design include cyclic loads, internal and external loads, fatigue, life-cycle testing, vibrations, rates of flow, thermal gradients, and fluid incompatibility with non-metal materials. For subsurface safety valves specifically, technical challenges include materials, method of device control, and sealing. They are also subject to a minimum level of design and verification per API 14A or ISO 10432. PER 15K recommended practice also gives additional considerations for these valves.

APPENDIX A.9 STIMULATION TECHNIQUES

Elphick et al. (1993): This paper describes using fracturing as an effect stimulation method to high permeability formations and compares the difference between fracturing high permeability formations and conventional fracturing. Although fracturing are more likely to be applied to low permeability formations, fracturing of high permeability formations is still attractive because less wells are needed to fully explore the field. Fracturing can help bypass the formation damage, improve the productivity and alleviate the sand producing issue. To conduct fracturing in a high permeability formation, larger proppants and higher proppant quantities are required. Since large proppants tend to have flowback problems, they may be pre-coated with resin to reduce the flow. Fluid loss control additives are also often used in fracturing fluids for high permeability formations. High viscosity fracturing fluids are required to better carry the proppants and prevent proppant bridging.

Haddad et al. (2011): This article outlines the approach to conduct ultra-deepwater fracturing jobs depths between 8200 ft. and 8900 ft. For ultra-deepwater jobs, there are a wide range of factors to be considered when designing the fracturing pack program, including rock mechanics, fracturing fluids, proppant, design approaches, sand control issues, wellbore volume effects and tool. Challenges of the design include completion hardware, perforation designs and geological conditions. There are also some limitation such as stimulation vessel capacity, service tool erosion, completion equipment spacing and logistics. The authors conducted pre-frac and post-frac analysis to determine the parameters of fracturing and evaluate the treatment after a frac job. Possible issues and causes of failure were also summarized in the article.

Morgenthaler et al. (1995): The authors in this paper demonstrate how real time stimulation evaluation should be conducted and how it can help improving the efficiencies of stimulation jobs in deepwater well completion. Traditionally, stimulation was evaluated based on production performance after the treatment was done. During the real time monitoring, treating rate and pressure will be used for acid composition adjustment and diversion design. As a result, real time evaluation collects pressure and rate data, calculates treating pressure and injectivity, predicts damage removal effectiveness, and eventually leads to precise adjustment and higher efficiencies.

Nunes et al. (2009): This article discusses the development of an analytical model to estimate the size of a formation damage zone caused by flow of particulate suspensions, and apply it in well stimulation planning. When particulate suspension flow through porous media like formation, the capture of particulates will result in a lower permeability of the media. The probability of particulate retention can be quantitatively characterized as filtration coefficient. By calculating filtration coefficient from well injectivity history, the radius of formation damage zone can be therefore estimated and incorporated to numerical reservoir simulators for further stimulation design.

Scoppio et al. (2014): The authors in this paper describe a corrosion testing program that can be used to evaluate high strength corrosion resistant tubing alloys. For deep water high pressure well, the tubing need to withstand corrosive environment cause by acid stimulation. In addition, the minimum yield strength of the tubing should be no less than 125 ksi to maintain its mechanical integrity. The authors employed an acid package that would be typically used for stimulation and ran corrosion tests at temperatures between 70 to 130°C for 6 hours. Mass loss, selective and localized corrosion were evaluated with optical microscope and scanning electronic microscope (SEM). 17% Cr tubing material demonstrated a better overall performance than 25% CrW. Although the corrosion rates of 25% CrW were acceptable under regular conditions, the selective dissolution of ferrite phase in 25% CrW were much more severe at 100 and 130°C. In addition, it's far less resistant to HF than 17% Cr counterpart.

Zeiler et al. (2004): The paper describes the case studies of viscoelastic surfactant-based diverting fluids applications in Gulf of Mexico (GOM). Viscoelastic surfactant (VES) based diverting fluids have two major applications due to their diverting ability and non-damaging properties. First of all, acids tend to enter high permeability regions when they are injected to remove formation damage or inorganic scaling. VES can be used to divert the flow to targeted damaged zone so that the stimulation efficiency could be maximized. In addition, gravel packing is often used in Gulf of Mexico for sand control. The placement of gravel comes with acid treatment, brines or completion fluids injection before and after placement. With sand control installed, traditional diverting methods such as high pump rate, HEC gel and mechanical methods are not suitable any more. VES emerged as a good alternative that is not limited by sand control. Fluid properties of VES can be modified by additive adjustment to obtain maximum performance. Several cases ranging from BHST 140°F to 290°F in GOM were demonstrated in the paper. Improved diversions were achieved with VES based agents.

APPENDIX A.10 FRAC PACK

Haddad et al. (2011): The authors describe the designing of fracturing stimulation programs for Lower Tertiary Wilcox formation. For this ultra deepwater formation, fracturing programs need to deal with complex geological conditions, high closure stress and potential formation failure. The design is also required to comply with tool spacing limitations as well as tool erosion limitations. Optimum number of treatments, fracturing geometry, conductivity, and perforation interval positioning are included in the program. This article shed lights to multi-stage frac program designing in other ultra deepwater fields that face similar.

Han et al. (2011): This paper outlines how frac packs will affect rock stability and sand production. Frac packs are often used to prevent sand from entering the wellbore. The placement of frac-pack often strengthens the formation rocks near the fracture; however, they may also weaken the surroundings of the fracturing tip where stresses are increased. As a result of stress increase and rock failure, frac packs may cause skin increase and degradation of productivity index. The authors apply geomechanical/fluid flow modeling to analyze the mechanism of formation damage and productivity loss. Rock strength testing and core flow testing confirm the rock failure mechanism. It is recommended to take rock stability into consideration when designing frac pack jobs, in order to avoid undesired production reduction.

Lizak et al. (2010): In this paper, the authors discuss the methods of bottom-hole pressure calculation that may affect deepwater frac-pack treatment selection. Conventional Pmax calculation is proved to be over conservative. New calculation with annulus Pmax instead of reservoir supporting pressure is more accurate and allows a number of frac-pack candidates to be reconsidered. The authors review the estimation methods and confirm their conclusion with the support of post-job gauge data and the success of a large amount of actual job.

Marquez et al. (2013): The authors present a Microsoft Excel –based completion scoreboard tool that evaluate the key aspects of frac-pack completion design and installation. The key parameters consist of six main categories: reservoir characteristics, well design and preparation, job execution, mechanical

equipment, post job analysis/diagnostics and well startup. The assessment is completed by assigning a relative score from 0 to 5 to each category.

Vilela et al. (2004): The authors demonstrate how a new frac-pack technology is used to complete a four zone well with bad cemented liner. In this completion job, poorly cemented liner affects live annulus monitoring and increases the complexity to gravel packing and squeeze job. To frac pack all the four zones and control the sand production, the service company uses a modified washpipeless isolation system together with a high pressure retrievable washpipeless isolation system (HPRWIS) to utilize a concentric string for isolation. This technology helps the service company successfully accomplish the completion job without unscheduled events.

Weirich et al. (2013): This article provides worldwide case histories of different frac-packing systems installed under extreme conditions with improved efficiency and higher rate of success. The main challenge of frac-packing is to create high conductivity fractures using the tip-screen out technique and to place proppant in these fractures. The paper reviews best practices, lessons learnt, engineering implementations and the challenges related to the frac-packing process since 1997.

APPENDIX A.11 CEMENT MECHANICAL PROPERTIES

Darbe et al. (2008): The authors of this paper discussed ways to modify mechanical properties of cement slurries and secondary effects on the overall design. Enhancing the mechanical properties of cement is important because the cement will be exposed to thermal and pressure stresses downhole, and a loss of zonal isolation from high stresses is detrimental to the environment and increases costs for the operator through decreased production and the price of remedial work. Other stresses on the cement include internal shrinkage during hydration, especially if any volume changes continue after the cement becomes solid, which could result in cracking or a micro annulus.

Another failure mode of cement can occur at the cement and casing interface if pressure or temperature stresses cause the casing to expand more than the cement. Mechanical properties can be modified through the addition of elastomers to decrease the Young's modulus, which increases the cement's capability to deform elastically under stress, and the addition of fibers to increase tensile strength, which increases the cement's failure tolerance. Other modifiers include gas and foamed cement. Adverse secondary effects that can occur when these additives are used are increased rheology and decreased slurry stability, which should be avoided when designing for improved mechanical performance. High rheology will result in increased pump pressures or reduced pump rates, which can result in difficulties during placement.

Elastomers can also result in a lower overall compressive strength, and a high volume of fibers can result in fiber agglomeration into balls. The specific gravities of many elastomers are different from cement, and the addition could result in non-homogeneous slurries. The standard best practices for placement still apply to mechanically enhanced cement slurries: drill fluid conditioning, pipe movement, centralization, pumping at the highest possible displacement rates, pumping spacer to prevent intermixing between the cement and mud, and following a density hierarchy between fluids. Centralization allows for adequate flow around the pipe, and will minimize the stress on the cement at the narrow point if the thickness is adequate.

De la Roij et al. (2012): The authors of the paper state that use of nanotechnology additives may greatly improve the characteristics of oilfield cements. The paper claims that the improvement is done by using nanotechnology to bridge between the crystalline structures of the cement through all phases of the cement hydration process and a bit beyond. The nano additive appearance is a very fine grain sized powder that contains alkali minerals, synthetic zeolites, and a complex activator.

The paper begins with base line information of the cement hydration process with a neat cement then goes on to discuss how improvements are made by the addition of nanotechnology. It is claimed and shown by the authors using electron microscopes that the nanotechnology additive creates long chained crystalline structures which use only additional water (even sea water) within the cement slurry prepared. The authors finish off by writing about how the nano additive improves issues within the areas of density, permeability, shrinkage, bonding with steel casing, chemical resistance, pump time, flexibility (Young's Modulus), High temperatures $>300^{\circ}\text{C}$, compressive strength, and handling safety with environmental impact.

Murtaza et al. (2013): This paper outlines the results of testing to evaluate the physical properties of Saudi cement class G with silica flour and admixed with different additives under high temperature and pressure conditions. Initially, experiments were conducted on class G cement slurry without additives to establish a baseline. Then testing was performed on cement slurry with additives and silica flour. The addition of silica flour resulted in a substantial increase in compressive strength as compared to type G slurry. The addition of silica flour also reduced the porosity and permeability of the cement producing a free water content of almost zero. A microstructural analysis showed that the silica flour admixed slurry created a uniform pore structure with few voids in it. XRD analysis revealed the addition of silica flour transformed the CH phase to calcium silicate hydrate and tobermorite at high temperature preventing strength retrogression and providing low permeability to the cement.

Nasvi et al. (2012): This paper outlines the results of a study to investigate the suitability of geopolymer as well cement and the mechanical behavior of geopolymer and Class G cement was compared under different down-hole temperatures. It was found that geopolymer possesses higher uniaxial compressive strength (UCS) values at elevated temperatures (above 50°C) and Class G cement possesses the highest values at ambient conditions. It was also observed that the peak strength of both geopolymer and Class

G cement was attained at curing temperatures of 50-60 °C. Class G cement showed higher values of Young's modulus at lower curing temperatures, while geopolymer had higher values at elevated curing temperatures, meaning the cement is stiffer at ambient conditions compared to geopolymer, while geopolymer is stiffer at elevated temperatures.

Acoustic emission testing revealed that Class G cement has highest values of crack propagation stress thresholds at ambient conditions, while geopolymer had the highest values at elevated temperatures (above 40 °C). Photogrammetric results of strain measurement showed that geopolymer underwent shear failure at lower curing temperatures, whereas the failure was splitting at elevated temperatures. Additionally, the class G cement revealed no major changes in the failure strain of the sample with the curing temperature, and the type of failure was shear failure for all the curing temperatures.

Reddy et al. (2007): This paper describes the importance of preserving cement integrity in a well with complications arising from testing cement slurries at atmospheric conditions. Even though the cement may be cured under wellbore or laboratory conditions, the samples are actually tested at atmospheric temperatures and pressure. A recent commercially made instrument, the Chandler Model 6225 MPro, uses shear and compression ultrasonic waves to measure mechanical properties of cement samples at elevated temperatures and pressures. While testing under downhole conditions, the 6225 MPro eliminates the inherent problems of atmospheric testing with depressurization and cooling effects of testing under atmospheric conditions that cause micro defects.

Since shear waves do not travel through liquids or gas, this new model allows for long term acoustic testing while the slurry is still in the liquid phase up through transit to a solid phase giving a more complete evaluation under downhole conditions. The resulting elastic modulus, shear modulus and Poisson's ratio data, gives a more thorough view of the slurry as opposed to the current method of removing the sample and running a one-time test under atmospheric conditions. Currently the UCA is the only commercially available instrument that measures compressive strengths at downhole temperatures and pressures. However, the UCA's tested properties are only useful for comparing different formulations during the selection process and does not hold up well in correlations between compressive strength and cement integrity.

Reveth et al. (2014): This paper uses present day examples from a deepwater development field to show how cement systems with advanced mechanical properties counter the critical stresses during the lifecycle of a well while maintaining zonal isolation. The solution to most of the common cementing challenges today requires a flexible cement system. This is determined by its mechanical properties such as Young's modulus, tensile strength, Poisson ratio and compressive strength. But in other job profiles a SHC system may be necessary. As with other systems the flexible cement system also has an upper limit after which it fails. In such a case, the SHC system mitigates the loss of zonal isolation.

Furthermore, the SHC system has advanced additives that react to hydrocarbon (HC); i.e. the system swells when the HC comes in contact and thus restores well integrity by sealing the annulus. In conclusion long term isolation can be achieved by using advanced flexible cementing systems with engineered mechanical properties, compressive strength, an SHC system or a combination of the two. Due to the high cost of remedial operations in deepwater drilling it would be most advantageous to use one or both of these methods together. This could provide long term well integrity and prevent HC flow in the case of micro-fractures or micro-annulus.

Tellisi et al. (2005): The authors propose that more extensive study needs to be done in the analysis of long term life of the well cement sheath. It is proposed in the paper that well cement selection should include the longer term needs of the cement and not just the short term benefits such as optimum thickening time and density. Longer term issues within the life of the well include varying temperature and pressure as well as the stresses of various down hole operations to ultimately provide long term zonal isolation for the life of the well. The paper covers the additional testing that can be completed before the cement is placed in the well to help insure the long term viability of the cement job.

The first of test suggested is a Hydration Volume Reduction Test(HVR). Hydration Volume Reduction test examines how much a well cement sample changes in volume while it is undergoing its hydration reaction. The document states that too much shrinkage would cause unwanted channeling within the annulus. The second test suggested is a tri-axial mechanical properties test. Mechanical properties testing evaluate how well a cement sample resists physical stresses placed upon it. The paper states that the information taken from mechanical properties testing is just as vital to examine as the industry

standard of compressive strength testing. The paper states by the authors that HVR issues as well as mechanical properties may be resolved with slurry optimization.

Thomas et al. (2012): The authors investigated the effects of high temperature on the microstructure and hydration products of mixtures of silica and Class G cement using small-angle neutron scattering, transmission electron microscopy, nanoindentation, XRD, and micro scratch testing. Above 110°C the morphology of the hydration products undergoes a change and the C-S-H phase converts to alpha-dicalcium silicate hydrate, which results in an increase in permeability and a decrease in compressive strength. When 35% BWOC of silica is added to cement, these adverse effects are mitigated through the formation of tobermorite and xonotlite crystals.

Slurries were cured at various combinations of temperatures (30°C, 175°C and 200°C) and times (17 hours, 6-8 days, and 1 year) under the same curing pressure. After 1 week of curing at 200°C, XRD indicated that the silica was fully converted into hydration products. Micro scratch tests indicated that at 200°C the fracture toughness decreased by 30% between 1 week and 1 year of curing. Varying the initial curing times and temperatures before increasing the final curing temperature to 200°C indicated that the initial cure conditions affected the hydration and silica reaction, since the silica flour used began to react above 100°C. An initial cure at lower temperatures resulted in more xonotlite formation after the curing temperature was increased, and a high initial curing temperature resulted in more tobermorite formation. In general, higher temperature curing resulted in a higher cement elastic modulus and hardness which was attributed to increased crystallinity of the hydration products.

APPENDIX A.12 REGULATORY INFORMATION

McAndrews et al. (2011): The authors in this paper looked at changes to U.S. offshore drilling safety and environmental regulations post-Macondo and speculate on further changes. They compare prescriptive versus performance based regulations. In October 2010 the Department of the Interior enacted new offshore drilling regulation including the Drilling Safety Rule and the Workplace Safety Rule. These rules combine both prescriptive and for the first time, performance-based regulation. Just as the Piper Alpha explosion in 1988 had a profound impact on the regulations in the North Sea, the US Gulf of Mexico has and will experience significant changes to regulations.

Unfortunately, safety and environmental regulation is typically only revised after an accident has occurred. Prescriptive regulation is easier to implement and monitor, but might not prevent new types of accidents related to new challenges or new technology related to developments in deepwater drilling. Prescriptive regulation can also cause operators to feel the need to only comply with regulation, rather than taking proactive action with offshore safety. The flexible performance based regulation may be more effective in operational areas with new technical challenges and rapid changes in technology are anticipated.

WORK CITED FOR LITERATURE REVIEW

Acorda, A. E., T. Ellis, and T. Bray. "Improving Mud Removal and Simplifying Challenging Cement Design: A Deepwater Case History in the South China Sea." *IPTC-16761-MS*. Presented at the International Petroleum Technology Conference, 26-28 March, Beijing, China 2013

Agbasimalo, N., and M. Radonjic. "Experimental Study of Portland Cement/Rock Interface In Relation to Wellbore Stability For Carbon Capture And Storage (CCS)." *ARMA-2012-206*. Presented at the 46th U.S. Rock Mechanics/Geomechanics Symposium, 24-27 June 2012, Chicago, Illinois

Aldridge, D., and P. Dodd. "Meeting the Challenges of Deepwater Subsea Completion Design." *SPE-36991-MS*. Presented at the SPE Asia Pacific Oil and Gas Conference, 28-31 October 1996, Adelaide, Australia

Al-Thuwaini, J., M. E. Abdulaziz, J. Epke, and M. F. Fayyaz. "Fit-for-Purpose Sealant Selection for Zonal Isolation in HPHT Deep Tight Gas Wells." *SPE-137774-MS*. Presented at the SPE Deepwater Drilling and Completions Conference, 5-6 October 2010, Galveston, Texas, USA

Alves, I. M., E. F. Caetano, K. Minami, and O. Shoham. "Modeling Annular Flow Behavior for Gas Wells." *SPE Production Engineering - SPE-20384-PA* (1991): 435-40.

Armstrong, J. L., P. Jean, and G. Puz. "Deepwater Development Environmental Issues and Challenges." *SPE-73873-MS*. Presented at the SPE International Conference on Health, Safety and Environment in Oil and Gas Exploration and Production, 20-22 March 2002, Kuala Lumpur, Malaysia

Bannerman, M., J. Calvert, T. Griffin, J. McCarroll, D. Postler, and R. Sweatman. "New API Practices for Isolating Potential Flow Zones During Drilling and Cementing Operations." *SPE-97168-MS*. Presented at the SPE Annual Technical Conference and Exhibition, 9-12 October 2005, Dallas, Texas

Bassett, J., J. Watters, K. N. Combs, and M. Nikolaou. "Lowering Drilling Cost, Improving Operational Safety, and Reducing Environmental Impact through Zonal Isolation Improvements for Horizontal Wells Drilled in the Marcellus Shale." *SPE-168847-MS*. Presented at the Unconventional Resources Technology Conference, 12-14 August 2014, Denver, Colorado, USA

Bastos, Braulio. "Advanced Drilling And Completion." *WPC-19-4867*. Presented at the 19th World Petroleum Congress, 29 June-3 July 2008, Madrid, Spain

Bennett, C., J. M. Gilchrist, E. Pitoni, R. C. Burton, R. M. Hodge, J. Troncoso, S. A. Ali, R. Dickerson, C. Price-Smith, and M. Parlar. "Design Methodology for Selection of Horizontal Open-Hole Sand Control Completions Supported by Field Case Histories." *SPE-65140-MS*. Presented at the SPE European Petroleum Conference, 24-25 October 2000, Paris, France

Biezen, E., and K. Ravi. "Designing Effective Zonal Isolation for High-Pressure/High-Temperature and Low Temperature Wells." *SPE-57583-MS*. Presentation at the SPE/IADC Middle East Drilling Technology Conference, 8-10 November 1999, Abu Dhabi, United Arab Emirates

Bois, A. P., A. Garnier, F. Rodot, J. Sain-Marc, and N. Aimard. "How To Prevent Loss of Zonal Isolation Through a Comprehensive Analysis of Microannulus Formation." *SPE Drilling & Completion* (2011): 13-31. *SPE-124719-PA*.

Bosma, M.G. R., E. K. Cornelissen, and A. Schwing. "Improved Experimental Characterization of Cement/Rubber Zonal Isolation Materials." *SPE-64395-MS*. Presented at the SPE Asia Pacific Oil and Gas Conference and Exhibition, 16-18 October 2000, Brisbane, Australia

Bour, D., and Rickard, B. Application of Foamed Cement on Hawaiian Geothermal Well.

Bourgoyne, A. T., S. L. Scott, and J. B. Regg. "Sustained Casing Pressure in Offshore Producing Wells." *OTC-11029-MS*. Presented at the Offshore Technology Conference, 3 May 1999, Houston, Texas

Bowersock, J., and C. A. Stokley. "Advanced Cementing Tools Enhance Well Integrity." *Tam International World Oil* 234 66.

Brooks, R., J. D. Newberry, P. Cook, and F. Wendlinger. "Preventing Annular Gas Flow In Conjunction With 2 Stage Cementing." *SPE-116447-MS*. Presented at the SPE Asia Pacific Oil and Gas Conference and Exhibition, 20-22 October, 2008 Perth, Australia

Burman, J., K. D. Renfro, and M. A. Conrad. "Marco Polo Deepwater TLP: Completion Implementation and Performance." *SPE-95331-MS*. Presented at the SPE Annual Technical Conference and Exhibition, 9-12 October 2005, Dallas, Texas

Byrom, T. G. "CHAPTER 8 - Casing Design Performance, In Casing and Liners for Drilling and Completion." *Gulf Publishing Company* (2007): 261-311.

Byrom, Ted G. ", 6 - Casing Performance, In Gulf Drilling Guides." *Casing and Liners for Drilling and Completion 2* (n.d.): 145-201.

Carter, T. S. "Improving Completion Viability in HPHT Completions." *SPE-97592-MS*. N.p., n.d. Web. Presented at the SPE High Pressure/High Temperature Sour Well Design Applied Technology Workshop, 17-19 May 2005, The Woodlands, Texas

Ceccarelli, T. U., E. H. Albino, G. M. Watson, and Deffieux D. "Deepwater Completion Designs: A Review of Current Best Practices." *SPE-122518-MS*. Presented at the Asia Pacific Oil and Gas Conference & Exhibition, 4-6 August 2009, Jakarta, Indonesia

Chita, L. C., and A. L. Cordeiro. "Deepwater Drilling." *OTC-5808-MS*. Presented at the Offshore Technology Conference, 2 May 1988, Houston, Texas

Chitwood, J. E., and W. A. Hunter. "Well Drilling, Completion, and Maintenance Technology Gaps." *OTC-13090-MS*. Presented at the Offshore Technology Conference, 30 April 2001, Houston, Texas

Complak, R., and W. Beecroft. "Studies of Annular Gas Flow Following Primary Cementing." *Journal of Canadian Petroleum Technology* 40.04 (1980): n. pag.

Copeland, D. "Completion Challenges for Ultra HPHT Completions." *SPE-97561-PT*. Presented at the SPE High Pressure/High Temperature Sour Well Design Applied Technology Workshop, 17-19 May 2005, The Woodlands, Texas

Cordeiro, A. L., L. A. S Rocha, and I. M. Martins. "Marlim Field: The Evolution of Deepwater Drilling/Completion/Workover." *OTC-10717-MS*. Presented at the Offshore Technology Conference, 3 May 1999, Houston, Texas

Darbe, R., C. Gordon, and R. Morgan. "Slurry Design Considerations For Mechanically Enhanced Cement Systems." *AADE-08-DF-HO-06*. Presented at the Association of Drilling Engineers Houston Chapter Fluids Technical Conference, 4 - 8 September 2008

De La Roji, R., C. Egyed, and J. P. Lips. "Nano-engineered Oil Well Cement Improves Flexibility and Increases Compressive Strength: A Laboratory Study." *SPE-156501-MS*. Presented at SPE International Oilfield Nanotechnology Conference and Exhibition, 12-14 June 2012, Noordwijk, The Netherlands

De Souza Nunes, M. J., P. G. Bedrikovetsky, B. Newbury, C. J. A Furtado, A. L. S De Souza, and R. Paiva. "). Formation Damage Zone Radius and Its Applications to Well Stimulation." *SPE-122843-MS*. Presented at the 8th European Formation Damage Conference, 27-29 May 2009, Scheveningen, The Netherlands

Doherty, D. "Factors Key to Deepwater Cementing." *The American Oil & Gas Reporter* 54 (2011): 84+.

Dooply, M., N. Flamant, A. Kanahuati, N. Iza, and T. Pringuey. "Foam Cement Job Simulations: Learning From Field Measurements." *SPE-166094-MS*. Presented at the SPE Annual Technical Conference and Exhibition, 30 September-2 October 2013, New Orleans, Louisiana, USA

Eaton, F. L., W. R. Reinhardt, and J. S. Bennett. "Liner Hanger Trapped Annulus Pressure Issues at the Magnolia Deepwater Development." *SPE-99188-MS*. Presented at the IADC/SPE Drilling Conference, 21-23 February 2006, Miami, Florida, USA

Elphick, J. J., R. P. Marcinew, and Barry Brady. "Effective Fracture Stimulation in High-Permeability Formations." *SPE-25380-MS*. Presented at the SPE Asia Pacific Oil and Gas Conference, 8-10 February 1993, Singapore

Foianini, I., G. A. Frisch, and P. Jones. "Successful Identification and Bond Assessment of Epoxy-Based Resin Cement Behind Production Casing: Integrating Cementing Technology With New Log Interpretation Methodology to Provide an Innovative Well Integrity Solution." *SPWLA-2014-HHH*. Presented at the SPWLA 55th Annual Logging Symposium, 18-22 May, 2014 Abu Dhabi, United Arab Emirates

Foster, J., T. Grigsby, and J. LaFontaine. "). The Evolution of Horizontal Completion Techniques for the Gulf of Mexico: Where Have We Been and Where Are We Going?" *SPE-53926-MS*. Presented at the Latin American and Caribbean Petroleum Engineering Conference, 21-23 April 1999, Caracas, Venezuela

Garcia, J. A., and C. R. Clark. "An Investigation of Annular Gas Flow Following Cementing Operations." *SPE-5701-MS*. Presented at the SPE Symposium on Formation Damage Control, 29-30 January, 1976 Houston, Texas

Gomez, J. R. "Developing Environmentally Compliant Materials for Cementing and Stimulation Operations." *SPE-127196-MS*. Presented at the SPE International Conference on Health, Safety and Environment in Oil and Gas Exploration and Production, 12-14 April 2010, Rio de Janeiro, Brazil

Goodson, J. E. "Selecting Seal Materials for Deepwater Completions." *OTC-19297-MS*. Presented at the Offshore Technology Conference, 5-8 May 2008, Houston, Texas, USA

Gottschling, J. C. "Openhole vs. Cased-Hole Hydraulic Fracturing." *SPE 97172*

Griffith, J. E., G. Lende, K. Ravi, A. Saasen, N. E. Nodland, and O. H. Jordal. "Foam Cement Engineering and Implementation for Cement Sheath Integrity at High Temperature and High Pressure." *SPE-87194-MS*. Presented at the IADC/SPE Drilling Conference, 2-4 March 2004, Dallas, Texas

Hadda, Z., M. B. Smith, F. D. De Moraes, and O. M. M. Moreira. "The Design and Execution of Frac Jobs in the Ultra Deepwater Lower Tertiary Wilcox Formation." *SPE-147237-MS*. Presented at the SPE Annual Technical Conference and Exhibition, 30 October-2 November 2011, Denver, Colorado, USA

Haddad, Z. A., M. B. Smith, and F. D. De Moraes. "Challenges of Designing Multi-Stage Frac Packs in the Lower Tertiary Formation - Cascade and Chinook Fields." *SPE-140498-MS*. Presented at the SPE Hydraulic Fracturing Technology Conference, 24-26 January 2011, The Woodlands, Texas, USA

Heathman, J. F., and F. E. Beck. "Finite Element Analysis Couples Casing and Cement Designs for HPHT Wells in East Texas." *SPE-98869-MS*. Presented at the IADC/SPE Drilling Conference, 21-23 February 2006, Miami, Florida, USA

Hamid, S., A. Khojastefar, and G. Ali Sobhi. "A New Cement Additive To Improve The Physical Properties Of Oil Well Cement And To Enhance Zonal Isolation" *Journal of Petroleum Science and Technology*, 2013

Han, G., J. Revay, L. J. Kalfayan, J. Perez, A. A. Walters, and R. C. Bachman. "Production and Rock Stability around a FracPacked GOM Well." *SPE-146419-MS*. Presented at the SPE Annual Technical Conference and Exhibition, 30 October-2 November 2011, Denver, Colorado, USA

Heathman, J. F., and F. E. Beck. "Finite Element Analysis Couples Casing and Cement Designs for HPHT Wells in East Texas." *SPE-98869-MS*. Presented at the IADC/SPE Drilling Conference, 21-23 February 2006, Miami, Florida, USA

Hunter, B., K. Ravi, and D. Kulakofsky. "Three Key Mechanisms Deliver Zonal Isolation." *www.iadc.org*. Presented at the IADC Drilling Gulf of Mexico Conference, Galveston, TX. 5-6 Dec. 2007

Ispas, I., R. A. Bray, I. D. Palmer, and N. G. Higgs. "). Prediction and Evaluation of Sanding and Casing Deformation in a GOM-Shelf Well." *SPE-78236-MS*. Presented at the SPE/ISRM Rock Mechanics Conference, 20-23 October 2002, Irving, Texas

Javora, P. H., R. F. Stevens, C. S. De Vine, S. J. Jeu, M. H. Simmons, G. T. Firmin, G. L. Poole, B. M. Franklin, and Q. Qu. "Deepwater Completion Challenges Redefine Best Practices for Completion and Packer Fluid Selection." *SPE-103209-MS*. Presented at the SPE Annual Technical Conference and Exhibition, 24-27 September 2006, San Antonio, Texas, USA

Jiang, L., D. Guillot, M. Meraji, P. Kumari, B. Vidick, B. Duncan, and S. B. Sansudin. "Measuring Isolation Integrity In Depleted Reservoirs." *SPWLA-2012-078*. Presented at the SPWLA 53rd Annual Logging Symposium, 16-20 June, Cartagena, Colombia 2012

Kadry, E. K. "Blow out Occurrence Caused by Annular Gas Flow after Cementing." *SPE-57578-MS*. Presented at the SPE/IADC Middle East Drilling Technology Conference, 8-10 November 1999, Abu Dhabi, United Arab Emirates

Kellingray, D. "Cementing - Planning for Success to Ensure Isolation for the Life of the Well." *SPE-112808-DL*. 2007

King, G. E., and D. E. King. "Differences Between Barrier Failure and Well Failure, and Estimates of Failure Frequency Across Common Well Types, Locations and Well Age." *SPE-166142-MS*. Presented at the SPE Annual Technical Conference and Exhibition, 30 September-2 October 2013, New Orleans, Louisiana, USA

Kinzel, H. (September 1993). "Proper centralizers can improve horizontal well cementing" *Oil and Gas Journal*. <http://www.ogj.com/articles/print/volume-91/issue-38/in-this-issue/exploration/proper-centralizers-can-improve-horizontal-well-cementing.html>

Krishana, R., and R. P. Darbe. "Overcoming the Cementing Challenges in Deep Gas Environment." *SPE-132090-MS*. Presented at the SPE Deep Gas Conference and Exhibition, 24-26 January 2010, Manama, Bahrain

Laws, M., A. M. Al-Riyami, H. Soek, J. E. Edwards, Y. A. ., Elmarsafawi, A. Sidhoumi, and A. Hassan. "Special Cement System And Cementing Techniques Improve Zonal Isolation In SouthOman Fields." *SPE-102414-MS*. Presented at SPE Annual Technical Conference and Exhibition, 24-27 September 2006, San Antonio, Texas, USA

Lecampion, B., A. Bungler, J. Kear, and D. Quesada. "Interface Debonding Driven by Fluid Injection in a Cased and Cemented Wellbore: Modeling and Experiments." *International Journal of Greenhouse Gas* 18 (2013): 208-23.

Lecampion, B., D. Quesada, M. Loizzo, A. Bungler, J. Kear, L. Deremble, and Jean Desroches. "Interface Debonding as a Controlling Mechanism for Loss of Well Integrity: Importance for CO2 Injector Wells." 4 (2011): 5219-226.

Levine, D. C., E. W. Thomas, and H. P. Bezner. "Annular Gas Flow After Cementing: A Look At Practical Solutions." *SPE-8255-MS*. Presented at the SPE Annual Technical Conference and Exhibition, 23-26 September 1979, Las Vegas, Nevada

Li, X., S. J. Tinker, M. B. Terralog, and S. M. Willson. "Compaction Considerations for the Gulf of Mexico Deepwater King West Field Completion Design." *SPE-92652-MS*. Presented at the SPE/IADC Drilling Conference, 23-25 February 2005, Amsterdam, Netherlands

Liu, B., J. Yang, B. Zhou, D. Yan, R. Tian, Z. Liu, and X. Huang. "Study of Casing Annulus Pressure for Deepwater Drilling and Completions." *SPE-170318-MS*. Presented at the SPE Deepwater Drilling and Completions Conference, 10-11 September, 2014 Galveston, Texas, USA

Lizak, K. F., and C. Hinnant. "Deepwater Frac-Pack Maximum Treating Pressure Limits, An Examination Using Bottom-Hole Pressure Gauges." *OTC-20434-MS*. Presented at the Offshore Technology Conference, 3-6 May 2010, Houston, Texas, USA

Marquez, M., M. M. Knobles, Wm. D. Norman, C. Oudtshoorn, and S. Naha. "Frac Pack Completion Scorecard: The Importance of Scoring High." *SPE-166253-MS*. Presented at the SPE Annual Technical Conference and Exhibition, 30 September-2 October 2013, New Orleans, Louisiana, USA

Mazero, K. (2011) "HPHT completions: always a moving target" www.drillingcontractor.org/hpht-completions-always-a-moving-target-9344

Maldonado, B. (September 2005). "Special design strategies vital as HTHP completions edge towards 500°F, 30,000 psi. Drilling Contractor. <http://iadc.org/dcpi/dc-septoct05/Sept05-hpht.pdf>

McAndrews, K. L. "Consequences of Macondo: A Summary of Recently Proposed and Enacted Changes to U.S Offshore Drilling Safety and Environmental Regulation." *SPE-143718-PP*. Presented at the SPE Americas E&P Health, Safety, Security, and Environmental Conference, 21-23 March, Houston, Texas

McDaniel, J., L. Watters, and N. K. Combs. "). Zonal Isolation Assurance: Relating Cement Mechanical Properties to Mechanical Durability." *SPE-2014-1913405-MS*. Presented at the SPE/AAPG/SEG Unconventional Resources Technology Conference, 25-27 August 2014, Denver, Colorado, USA

Miller, R. A., M. L. Payne, and P. Erpelding. "Designer Casing for Deepwater HPHT Wells. Society of Petroleum Engineers." *SPE-97565-MS*. Presented at the SPE High Pressure/High Temperature Sour Well Design Applied Technology Workshop, 17-19 May 2005, The Woodlands, Texas

Morgenthaler, L., and L. A. Fry. "A Decade of Deepwater Gulf of Mexico Stimulation Experience." *SPE-159660-MS*. Presented at the SPE Annual Technical Conference and Exhibition, 8-10 October 2012, San Antonio, Texas, USA

Morgenthaler, L. N., S. B. Malochee, and C. D. Smith. "Real Time Stimulation Evaluation in Deepwater Well Completions." *SPE-30460-MS*. Presented at the SPE Annual Technical Conference and Exhibition, 22-25 October 1995, Dallas, Texas

Morris, K., P. J. Deville, and P. Jones. "Resin-Based Cement Alternatives for Deepwater Well Construction." *SPE-155613-MS*. Presented at the SPE Deepwater Drilling and Completions Conference, 20-21 June 2012, Galveston, Texas, USA

Mueller, D. T. "Deepwater Cementing Standards: Applicability and Regulatory Impact of Best Practices." *OTC23664*. Web. Presented at the Offshore Technology Conference, Houston, TX 30 April 2013

Murtaza, M., M. K. Rahman, A. A. Al-Majed, and A. Samad. "Mechanical, Rheological and Microstructural Properties of Saudi Type G Cement Slurry with Silica Flour Used in Saudi Oil Field under HPHT

Conditions." *SPE-168101-MS*. Presented at the SPE Saudi Arabia Section Technical Symposium and Exhibition, 19-22 May 2013, Al-Khobar, Saudi Arabia

Nasvi, M.C. M., P. G. Ranjith, and J. Sanjayan. "Comparison of Mechanical Behaviors of Geopolymer And Class G Cement As Well Cement At Different Curing Temperatures For Geological Sequestration of Carbon Dioxide." *ARMA-2012-232*. Presented at the 46th U.S. Rock Mechanics/Geomechanics Symposium, 24-27 June 2012, Chicago, Illinois

Nelson, Erik B., and Dominique Guillot. *Well Cementing*. Second ed. Sugar Land: Schlumberger, 2006. Print.

Ozyurtkan, M. H., G. Altun, and I. M. Serpen. "An Experimental Study on Mitigation of Oil Well Cement Gas Permeability." *IPTC-16577-MS*. Presented at the International Petroleum Technology Conference, 26 March 2013.

Parcevaux, P., P. Rae, and P. Drecq. "8 Prevention of Annular Gas Migration." *Developments in Petroleum Science* 28 (1990): 8 -1+.

Patterson, D. E., Waters, J. W., and Larpenter, M. L. "Unconventional Multi-Zone Frac Pack Design With Significant Cost Savings." *SPE 147095*

Patterson, R., T. J. Willms, K. Foley, and J. Edwards. "High-Pressure, High-Temperature Consolidated Completion in the Continental Shelf Environment of the Gulf of Mexico: Case History." *OTC-18976-MS*. Presented at the Offshore Technology Conference, 30 April-3 May, Houston, Texas, U.S.A.

Procyk, A. D., D. P. Jamieson, J. A. Miller, Robert C. Burton, R. M. Hodge, and Nobuo Morita. "Completion Design for a Highly Compacting Deepwater Field." *SPE Drilling & Completion* 24.04 (2009): 642-58.

Proehl, T., and F. Sabins. "Deepstar CTR 7501 - "Drilling and Completion Gaps for HPHT Wells in Deep Water [//www.bsee.gov/Research-and-Training/Technology-Assessment-and-Research/tarprojects/500-599/519AA/](http://www.bsee.gov/Research-and-Training/Technology-Assessment-and-Research/tarprojects/500-599/519AA/)>.

Ravi, K., M. Bosma, and O. Gastebled. "Safe and Economic Gas Wells through Cement Design for Life of the Well." *SPE-75700-MS*. Presented at the SPE Gas Technology Symposium, 30 April-2 May 2002, Calgary, Alberta, Canada

Ravi, K., N. Moroni, E. Barbieri, A. Mesmacque, and A. Zanchi. "Intelligent and Intervention less Zonal Isolation for Well Integrity in Italy." *SPE-119869-MS*. Presented at the SPE Middle East Oil and Gas Show and Conference, 15-18 March 2009, Bahrain, Bahrain

Ravi, K., Y. R. Barhate, Siva Rama, K. Janshyala, C. E. Fonseca, and J. Anjos. "Cement Sheath Integrity in Fast Creeping Salts: Effect of Well Operations." *SPE-166622-MS*. Presented at the SPE Offshore Europe Oil and Gas Conference and Exhibition, 3-6 September 2013, Aberdeen, UK

Reddy, B. R., A. K. Santra, D. E. McMechan, D. W. Gray, C. Brenneis, and R. Dunn. "Cement Mechanical Property Measurements Under Wellbore Conditions." *SPE Drilling & Completion* 22.01 (2007): 33-38. *SPE-95921-PA*.

Reddy, B. R., R. Vargo, B. Sepulvado, and D. Weisinger. "Value Created Through Versatile Additive Technology and Innovation for Zonal Isolation in Deepwater Environments." *SPE-77757-MS*. Presented at the SPE Annual Technical Conference and Exhibition, 29 September-2 October 2002, San Antonio, Texas

Reddy, R. B., P. Vijn, J. Chatterji, D. Bach, and J. M. Wilson. "Trends in the Development of Environmentally Acceptable Additives for Zonal Isolation Applications." *SPE-65393-MS*. Presented at the SPE International Symposium on Oilfield Chemistry, 13-16 February 2001, Houston, Texas

Reveth, V., R. G. Rojas, and Gupta. "Achieving Long Term Integrity: An Engineered Solution For Production Casings In Deepwater Environments. Society of Petroleum Engineers." *SPE-169910-MS*. Presented at the SPE Energy Resources Conference, 9-11 June 2014, Port of Spain, Trinidad and Tobago

Ribeiro, O.J. S., and L.A G. Costa. "Deepwater Subsea Completion: State Of The Art And Future Trends." *OTC-7240-MS*. Presented at the Offshore Technology Conference, 3 May 1993, Houston, Texas

Rivas, L. F., J. Sanclemente, and W. K. Ricketts. "Tahiti Subsurface - Technology Challenges and Accomplishments." *OTC-19861-MS*. Presented at the Offshore Technology Conference, 4-7 May 2009, Houston, Texas

Sabins, F., "MMS Project: Long-Term Integrity of Deepwater Cement Systems Under Stress/Compaction Conditions." 31 July, 2002

Sabins, F., & Proehl, T. "DeepStar CTR 7501 Drilling and Completion Gaps for HPHT Wells in Deep Water." 21 June, 2006

Saldungaray, P. M., Troncoso, J., Sofyan, M., Santoso, B. T., Parlar, M., Price-Smith, C., Bailey, W. "Frac-Packing Openhole Completions: An Industry Milestone." *SPE 73757*

Sanders, W., W. Baumann, H. A. R. Williams, F. D. De Moraes, J. Shipley, M. E. Bethke, and S. Ogier. "Efficient Perforation Of High-Pressure Deepwater Wells." *OTC-21758-MS*. Presented at the Offshore Technology Conference, 2-5 May, 2011 Houston, Texas, USA

Scorpio, L., P. Nice, G. Mortali, L. Intiso, E. I. Piccolo, H. Nasvik, and H. Amaya. "Testing of Stimulation Acidizing Packages on High Strength Corrosion Resistant Tubing Alloys for High Pressure Deep Water Wells." *NACE-2014-3945*. Presented at CORROSION 2014, 9-13 March 2014, San Antonio, Texas, USA

Shaughnessy, J. M., W. K. Armagost, R. P. Herrmann, and M. A. Cleaver. "Problems of Ultra-Deepwater Drilling." *SPE-52782-MS*. Presented at the SPE/IADC Drilling Conference, 9-11 March 1999, Amsterdam, Netherlands

Sinha, B. K., T. R. Bhatton, J. V. Cryer, S. Nieting, G. A. Ugueto, A. Bakulin, and M. R. Hauser. "Estimation of Near-Wellbore Alteration and Formation Stress Parameters From Borehole Sonic Data." *SPE Reservoir Evaluation & Engineering* 11.03 (2008): 478-86. *SPE-95841-PA*.

Slay, J. B., and K. Ferrell. "Proper Performance Testing to Maintain Seal Integrity in Deepwater Completions." *OTC-19626-MS*. Presented at the Offshore Technology Conference, 5-8 May 2008, Houston, Texas, USA

Snyder, L. J. "Deepwater Drilling And Production Technology." *API-77-E001*. Presented at the Annual Meeting Papers, Division of Production, 3-6 April 1977, Houston, Texas

Stiles, D. "Effects of Long-Term Exposure to Ultrahigh Temperature on the Mechanical Parameters of Cement." *SPE-98896-MS*. Presented at the IADC/SPE Drilling Conference, 21-23 February 2006, Miami, Florida, USA

Stuart, C., and S. Foo. "Application of an Intelligent System To Ensure Integrity Throughout The Entire Well Life Cycle." *SPE/IADE 135907*. Presented at the Asia Pacific Drilling Technology Conference, Ho Chi Minh City Vietnam 1-3 November 2010

Talabani, S., G. A. Chukwu, and D. G. Hatzignatiou. "Gas Channeling and Micro-Fractures in Cemented Annulus." *SPE-26068-MS*. Presented at the SPE Western Regional Meeting, 26-28 May 1993, Anchorage, Alaska

Tellisi, M., Kris Ravi, and P. Pattillo. "Characterizing Cement Sheath Properties For Zonal Isolation." *WPC-18-0865*. Presented at the 18th World Petroleum Congress, 25-29 September 2005, Johannesburg, South Africa

Teodoriu, C., I. O. Ugwu, and J. J. Schubert. "Estimation of Casing-Cement-Formation Interaction Using a New Analytical Model." *SPE-131335-MS*. Presented at the SPE EUROPEC/EAGE Annual Conference and Exhibition, 14-17 June 2010, Barcelona, Spain

Thomas, J. J., S. James, J. A. Ortega, S. Musso, F. Auzerais, K. J. Krakowiak, A. T. Akono, F. J. Ulm, and R. J. M. Pellenq. "Fundamental Investigation of the Chemical and Mechanical Properties of High-Temperature-Cure Oilwell Cements." *OTC-23668*. Presented at the Offshore Technology Conference, Houston TX, 30 April 2012

Thompson, G., R. Patterson and J. Sloan. (December 2012). "Design and development considerations for HTHP subsurface safety valves" *World Oil*, 233 (12). <http://www.worldoil.com/December-2012-Design-and-development-considerations-for-HPHT-subsurface-safety-valves.html>

Tinsley, J. M., E. C. Miller, and F. L. Sabins. "Study of Factors Causing Annular Gas Flow Following Primary Cementing." *Journal of Petroleum Technology* (1980): 1427-437.

Vilela, A., C. Hightower, R. Montanha, R. Luiz, R. Queiroz, and A. Pereira. "Deepwater Four Zones Selective Washpipeless Frac-Pack Completion Inside a Bad Cemented Liner: A Case History." *SPE-90510-MS*. Presented at the SPE Annual Technical Conference and Exhibition, 26-29 September 2004, Houston, Texas

Weirich, J., Jeff Li, T. Abdelfattah, and C. A. Pedroso. "Frac Packing: Best Practices and Lessons Learned From More Than 600 Operations." *SPE Drilling & Completion* 28.02 (2013): 119-34. *SPE-147419-PA*.

Wendler, C., M. F. Schoener-Scott, and C. Wendler. "Testing and Perforating in the HPHT Deep and Ultradeep Water Environment." *SPE-158857-MS*. Presented at the SPETT 2012 Energy Conference and Exhibition, 11-13 June 2012, Port-of-Spain, Trinidad

Williams, R. H., D. K. Khatri, M. L. Vaughan, G. Landry, L. Janner, B. Mutize, and M. Herrera. "Particle Size Distribution-Engineered Cementing Approach Reduces Need for Polymeric Extenders in Haynesville Shale Horizontal Reach Wells." *2118/147330-MS*. Presented at the SPE Annual Technical Conference and Exhibition, 30 October-2 November 2011, Denver, Colorado, USA

Wu, B., B. Wu, X. Zhang, and R. G. Jeffery. "Wellbore Stability Analyses for HPHT Wells Using a Fully Coupled Thermo-Poroelastic Model." *SPE-144978-MS*. Presented at the SPE Asia Pacific Oil and Gas Conference and Exhibition, 20-22 September 2011, Jakarta, Indonesia

Zeiler, C., D. Alleman, and Q. Qi. "Use of Viscoelastic Surfactant-Based Diverting Agents for Acid Stimulation: Case Histories in GOM." *SPE-90062-MS*. Presented at the SPE Annual Technical Conference and Exhibition, 26-29 September 2004, Houston, Texas

APPENDIX B PHYSICAL MODELING

APPENDIX B.1 TESTING METHODS AND MECHANICAL PROPERTIES

Rheology: Slurry surface rheology is measured at ambient temperature with a rotational viscometer. Downhole slurry rheology is measured after conditioning in an atmospheric consistometer if the BHCT is 190°F or less. If the BHCT is greater than 190°F the slurry is conditioned under temperature and pressure in a pressurized consistometer.

API Thickening Time: Slurry thickening time is tested using a pressurized consistometer to simulate downhole pressure and temperature to determine how long the slurry can be pumped before setting.

API Static Fluid Loss: The slurry is conditioned to temperature in an atmospheric consistometer and placed in a fluid loss cell. A 1000 psi differential pressure is applied across the slurry and the amount of fluid released in 30 minutes is recorded. The fluid loss test is a representation of fluid loss from the slurry into the formation during placement.

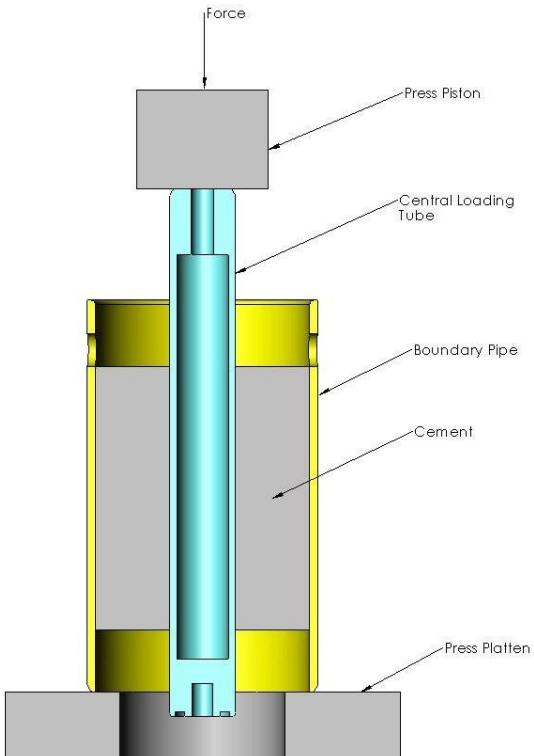
API Stirred Fluid Loss: The slurry is conditioned at 190°F or above in the fluid loss cell. After conditioning, the cell is rotated and a 1000 psi differential pressure is applied and the amount of fluid released in 30 minutes is recorded.

Free Fluid: A column of slurry is left static at downhole temperature and the volume of free fluid collected at the top of the sample is measured. This is an indication of static slurry stability.

UCA: Compressive strength and time to initial set is measured non-destructively with an Ultrasonic Cement Analyzer (UCA) for 24 hours or 48 hours.

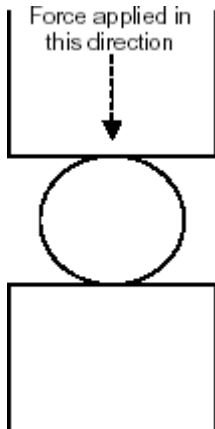
Shearbond was conducted to measure how tightly the cement is bonded to the central pipe, and was measured by mechanically forcing the inner pipe from a small-scale wellbore model. The simulated formation / cement sheath / central loading tube assembly was placed in a press. The cement and simulated formation was supported while axial load was placed on the central loading tube until movement was detected between the pipe and cement. The load at which this movement occurred was divided by the inner pipe area in contact with the cement to calculate the mechanical shear bond. Figure 13 shows the test schematically.

FIGURE 13: SHEAR BOND TEST



Tensile testing was performed using a splitting tensile strength method. For this test, the slurry is cured in a 1.5x5-in mold to make three specimens. After curing, each specimen was prepared by cutting $\frac{1}{4}$ " section from each end. Those pieces were discarded, and the specimen was split into three 1 inch segments specified as top, middle or bottom. Density is then calculated for each segment using Archimedes principle. Each sample is then crushed in the testing apparatus as shown in Figure 14. The maximum reading is noted and used to calculate the tensile strength as per the equation below.

FIGURE 14: DIAGRAM OF TENSILE TEST



Tensile strength is calculated by the following equation:

Equation 7: Tensile strength equation

$$T (\text{psi}) = (2 * F) / (\text{Pi} * L * D)$$

Where:

T = Tensile Strength (psi)

F = Maximum Force Recorded (lbf)

Pi = 3.14

L = Sample Length (in.)

D = Sample diameter (in.)

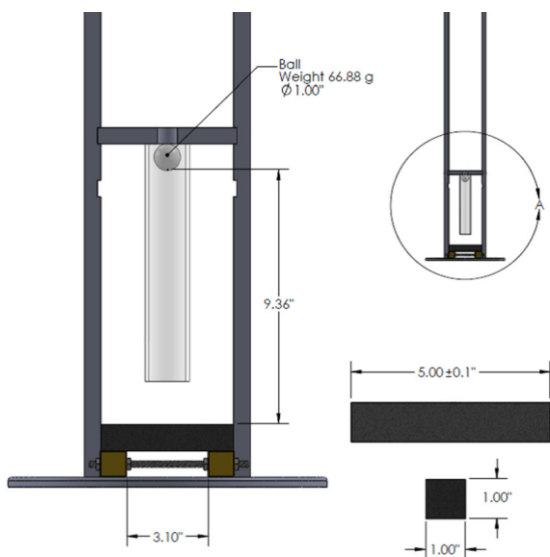
Impact Resistance

This test consists of repeatedly dropping a steel ball on a cement bar until it breaks.

Cement slurry is poured in 5"x1"x1" bar molds and cured at BHST in a water bath for 48 hours. After curing, the slurry bar is placed in the impact test apparatus shown below. A 1" ball (66.88 g) is dropped from a constant height on the cement bar. To ensure a consistent point of impact, the ball is dropped

through a 1.25" PVC guide pipe placed above the slurry bar. The ball is dropped until the bar breaks, the number of impacts is recorded and used to calculate the energy required to break the bar; this energy is defined as impact resistance of the slurry.

FIGURE 15: IMPACT SETUP



Heat capacity: When heat is transferred to an object, it will cause the temperature of the object to increase. Likewise, when heat is removed, the temperature of the object will decrease. The ratio of heat change to the resulting temperature change is defined as heat capacity. The relationship among the heat (Q) that is transferred, heat capacity (C) and the change in temperature (ΔT) can be summarized as:

$$Q = C \cdot \Delta T$$

Thermal conductivity: When heat is transferred to an object, the rate of transfer across the material varies. The property of material to conduct heat is defined as thermal conductivity. It can be measured by the quantity of heat that passes a certain amount of time through a geographically defined object.

Coefficient of thermal expansion: During a heat transfer, the volume of the object will change in response of temperature change. Coefficient of thermal expansion is defined by the degree of expansion divided by the change of temperature.

Mechanical Properties of Ultimate compressive strength (UCS), Young's Modulus, Poisson's Ratio, and anelastic strain tests were performed using a standard load frame equipped with LVDT's. Loading for UCS was at a rate of 35psi/sec until failure. To determine Young's Modulus and Poisson's Ratio, the sample was first loaded to 5% of the UCS, then cycled from 5% to 50% of the UCS for three cycles before ending the test. The sample was fitted with LVDTs to determine radial and axial deformations during loading.

APPENDIX B.2 ANELASTIC STRAIN

Anelastic strain is a measure of the tendency of cement to permanently deform under less-than-ultimate stress loading. When combined with other mechanical properties, this behavior may explain loss of annular seal in low-intensity loading scenarios. The anelastic strain behavior of oilfield cements mean that the strain response of cement under stress is very non-linear, and that any discussion of Young's (Elastic) Modulus must be tempered with the knowledge that the strict definitions of Elastic Modulus do not apply to oilfield cements.

APPENDIX B.3 ANNULAR SEAL

Pressure and Temperature Annular Seal

The Annular Seal Tests were developed in order to measure the ability of cement to maintain an annular seal in a simulated small-scale wellbore. Apparatus was designed to allow the cement to be stressed by either internal pipe pressure application-and-release cycles, or by alternately heating and cooling the inner pipe. Various methods were developed to simulate the formation at the outer periphery of the cement sheath. Steel was used to simulate hard formations, and PVC pipe for intermediate to soft-strength formations. These represent the methodology used in the annular seal testing in this project.

Two test apparatus and protocols were developed, one for the pressure loading condition, and one for the thermal loading condition. The apparatus are designed to allow for the application of substantial pressures and temperatures, and are similar in design.

FIGURE 16: PRESSURE ANNULAR SEAL APPARATUS

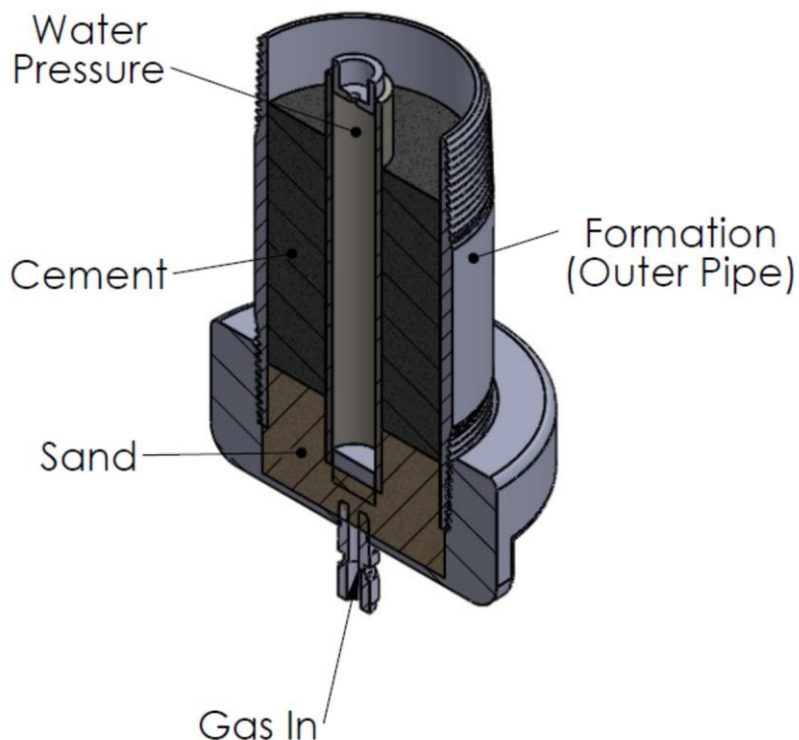
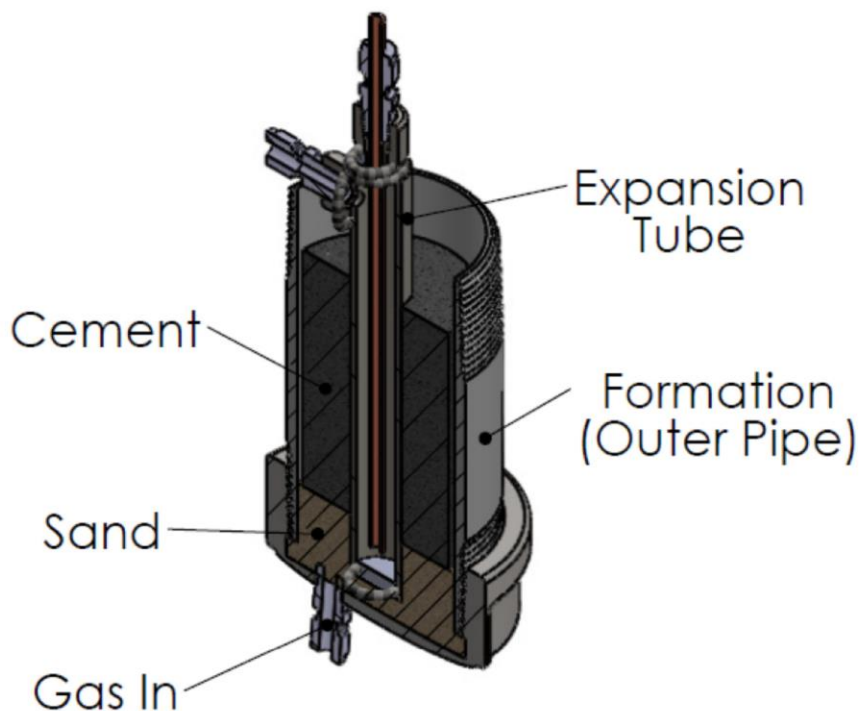
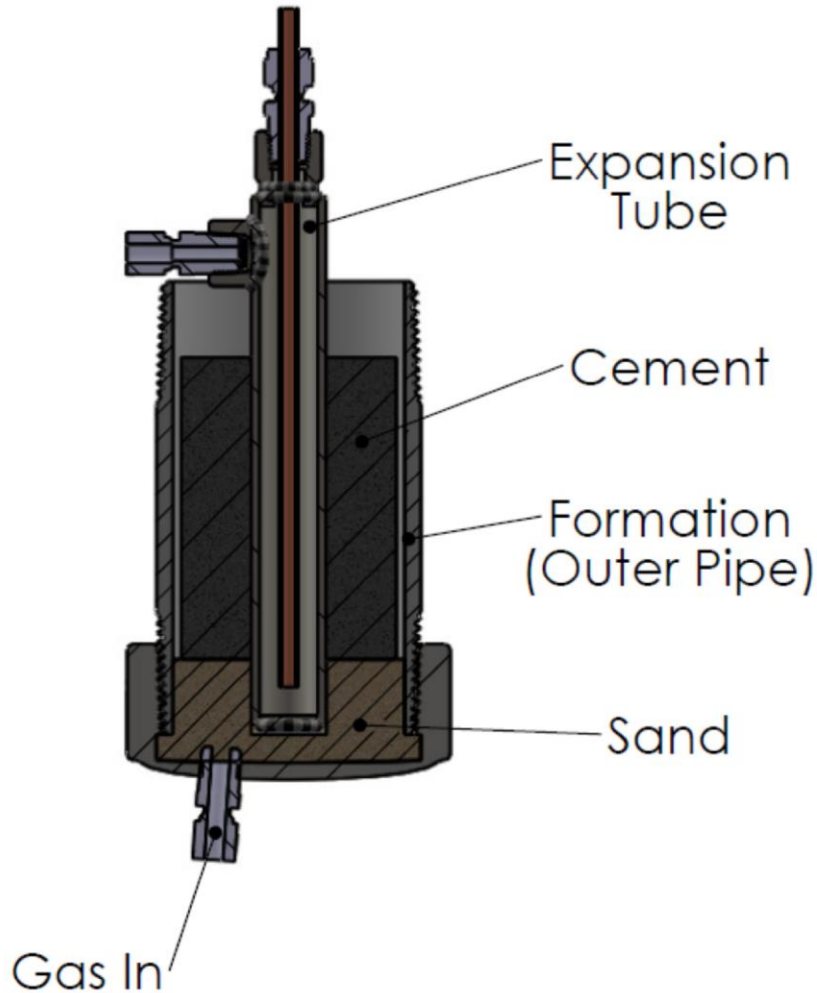


FIGURE 17: THERMAL ANNULAR SEAL APPARATUS



THIS REPORT WAS INADVERTENTLY DISSEMINATED IN THE PUBLIC DOMAIN/ONLINE SINCE 09/2015 WITHOUT A DISCLAIMER. DISCLAIMER HAS BEEN ADDED – “THIS INFORMATION IS DISTRIBUTED SOLELY FOR THE PURPOSE OF PEER REVIEW UNDER APPLICABLE INFORMATION QUALITY GUIDELINES. IT HAS NOT BEEN FORMALLY DISSEMINATED BY BSEE. IT DOES NOT REPRESENT AND SHOULD NOT BE CONSTRUED TO REPRESENT ANY AGENCY DETERMINATION OR POLICY

FIGURE 18: THERMAL ANNULAR SEAL APPARATUS



THIS REPORT WAS INADVERTENTLY DISSEMINATED IN THE PUBLIC DOMAIN/ONLINE SINCE 09/2015 WITHOUT A DISCLAIMER. DISCLAIMER HAS BEEN ADDED – “THIS INFORMATION IS DISTRIBUTED SOLELY FOR THE PURPOSE OF PEER REVIEW UNDER APPLICABLE INFORMATION QUALITY GUIDELINES. IT HAS NOT BEEN FORMALLY DISSEMINATED BY BSEE. IT DOES NOT REPRESENT AND SHOULD NOT BE CONSTRUED TO REPRESENT ANY AGENCY DETERMINATION OR POLICY

APPENDIX B.4 LARGE-SCALE LABORATORY SEAL PERFORMANCE TESTING

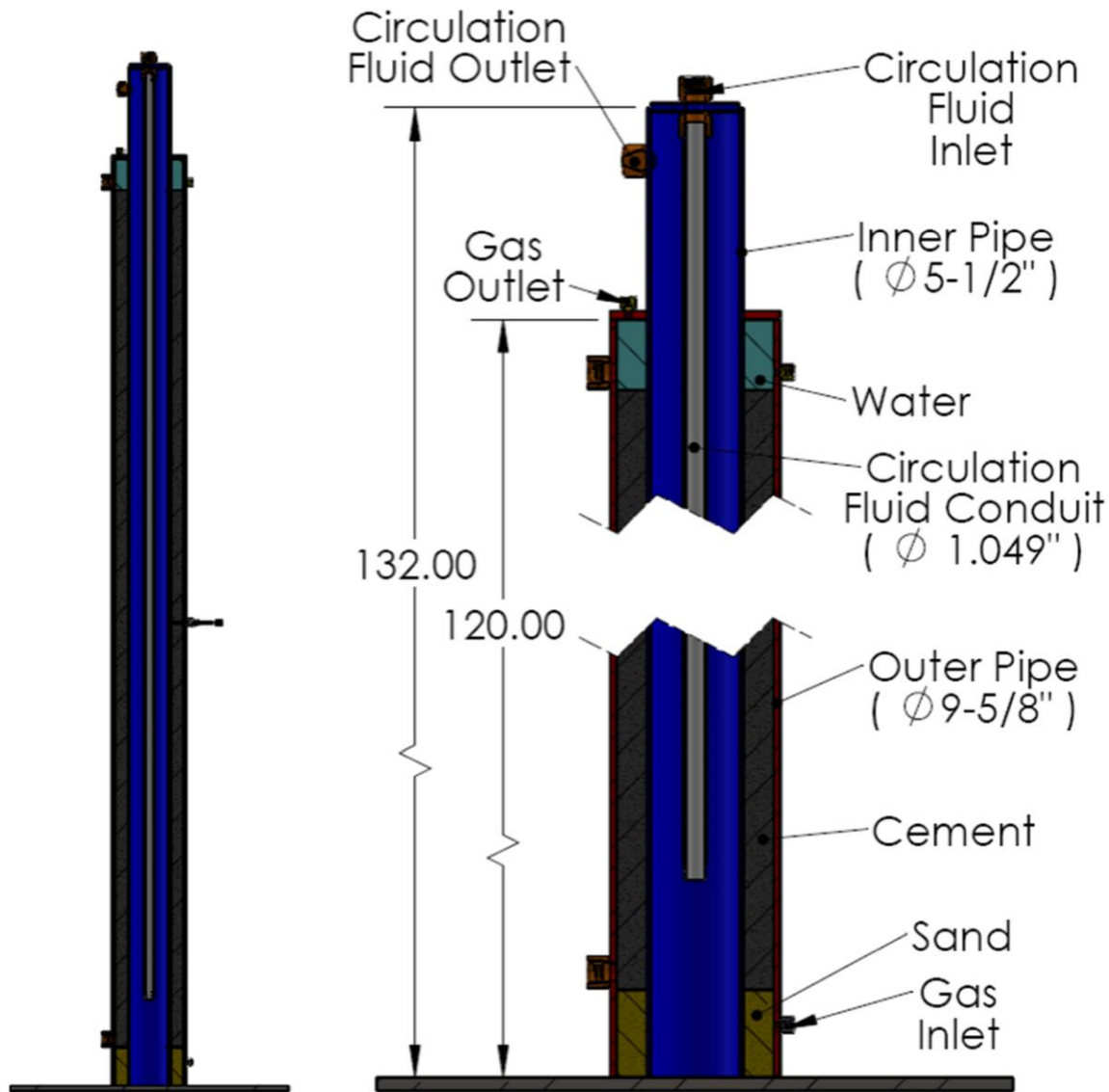
Schematics of the large-scale tests fixtures for thermal and pressure testing are presented in Figures 19 and 20 below. For thermal testing, chilled water is circulated through the center pipe for 30 minutes followed by 30 minutes of circulating heated fluid. Thus a thermal differential of around 100°F can be applied to the inner casing-cement interface. The pressure cycling test is performed by repeatedly increasing the pressure of the inner pipe to 2000 psi and then bleeding the pressure back to around ambient pressure.

To begin the pressure cycling test, sufficient cement, dry additives, and water to prepare approximately 10 gallons of cement were weighed. Dry components were blended into the cement and the dry blend was mixed with the water using a high-shear paddle mixer. The cement was then stirred 20 minutes to ensure complete mixing. Next, the slurry was pumped into place in the fixture annulus. This cement was cured for 7 days at which time UCA tests indicated the composition developed compressive strength similar to that developed by the small-scale cement compositions cured 2 days at 140°F. Thus, mechanical properties of the cement systems in small and large scale tests were determined to be comparable.

After curing, the annular seal competence was confirmed by application of 20 psi gas pressure at the bottom of the annulus with no pressure increase occurring at the top of the annulus during the 1-hour test duration. Then, the inner pipe was filled with water and pressure cycling started. Cycling schedule was pressurize from 0 to 2000 psi in 30 seconds, hold for 30 seconds, and release pressure allowing 1 minute for the pressure in the pipe to return to ambient conditions. This cycle was controlled automatically and repeated continuously throughout the time each day that CSI's laboratory was manned. The data acquisition system logged pressure in the inner pipe as well as pressure at both top and bottom of the annulus.

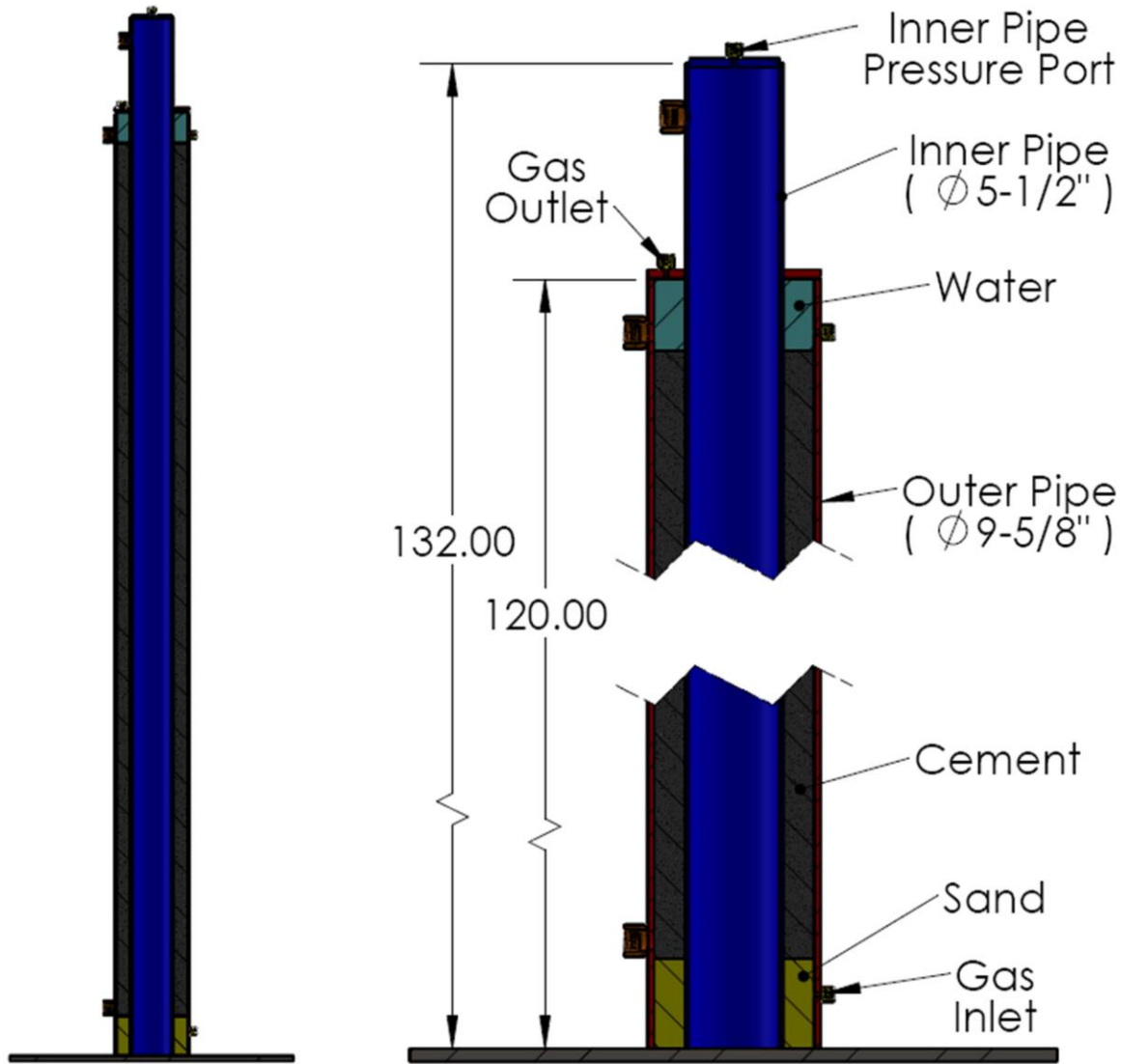
After failure, the top plate on the fixture was cut off and the annulus was re-pressurized. Leak location was noted.

FIGURE 19: LARGE SCALE ANNULAR SEAL TEST (TEMPERATURE)



THIS REPORT WAS INADVERTENTLY DISSEMINATED IN THE PUBLIC DOMAIN/ONLINE SINCE 09/2015 WITHOUT A DISCLAIMER. DISCLAIMER HAS BEEN ADDED – “THIS INFORMATION IS DISTRIBUTED SOLELY FOR THE PURPOSE OF PEER REVIEW UNDER APPLICABLE INFORMATION QUALITY GUIDELINES. IT HAS NOT BEEN FORMALLY DISSEMINATED BY BSEE. IT DOES NOT REPRESENT AND SHOULD NOT BE CONSTRUED TO REPRESENT ANY AGENCY DETERMINATION OR POLICY

FIGURE 20: LARGE SCALE ANNULAR SEAL TEST (PRESSURE)



THIS REPORT WAS INADVERTENTLY DISSEMINATED IN THE PUBLIC DOMAIN/ONLINE SINCE 09/2015 WITHOUT A DISCLAIMER. DISCLAIMER HAS BEEN ADDED – “THIS INFORMATION IS DISTRIBUTED SOLELY FOR THE PURPOSE OF PEER REVIEW UNDER APPLICABLE INFORMATION QUALITY GUIDELINES. IT HAS NOT BEEN FORMALLY DISSEMINATED BY BSEE. IT DOES NOT REPRESENT AND SHOULD NOT BE CONSTRUED TO REPRESENT ANY AGENCY DETERMINATION OR POLICY

Appendix B.5 Energy and Resistance Calculations

Calculation Methods and Assumptions

Correlations describing behavior of a complex system can produce misleading results. Relationships developed in the laboratory do not always hold for systems of different scale (size, flow rate, material, etc.). Thus, engineers spend significant effort to design scale models in the lab so that results can be applied in operations. Choice of scaling parameter is never straight forward and seldom produces results that can be widely extrapolated. Additionally, testing of complex physical systems can become overwhelming if exact replication of full-scale environment is attempted. Pressure and temperature duplication often produce assembly and plumbing nightmares with complex operating procedures that increase testing cost, create safety issues, and compromise meaningful data collection.

One approach to avoiding this scaling dilemma is to analyze the test system and resulting data in terms of Dimensionless Scaling Analysis. With this approach, functional relationships can be expressed in terms of dimensionless numbers even without explicit knowledge of equations governing the fundamental process. A relationship for an oilfield system developed via this process will be applicable regardless of scale from small scale in the laboratory to full scale field operations.

Dimensionless Scaling Analysis was applied in analysis of the annular seal tests conducted for this project. The assumptions, evaluation process, and resulting dimensionless scaling variable descriptions are presented below.

The general concept of evaluating cement seal performance in terms of stress introduced into a well relies on several initial assumptions:

- The well represents a system comprised of casing, cement, and formation. The system internal interfaces and variations in properties of the system components produce complex interactions that make specific analysis difficult and hard to scale.
- Holistic approach and dimensionless scaling analysis produce useful prediction techniques for evaluating seal effectiveness.
- Energy analysis assumes 100% transfer of energy into the system.
- All energy affects the entire system as governed by intrinsic properties of the system components.
- Multiple physical properties, mechanical properties, and thermal properties of the cement and the other materials in the system as well as physical dimensions of the system govern cement's resistance to failure under stress.

This analytical approach of developing scalable relationships among a group of variables describing a complex system has been employed successfully in several studies performed by the investigators. Most recently this method was employed in the cited work by McDaniel et al (2014) that appears

below. This most recent relationship developed described only impact effects from drill pipe whip on seal durability. This narrow focus led to inclusion of a limited series of variables. For this current investigation, the range of properties affecting durability had to include thermal as well as mechanical. Annular volume terms were added to account for system dimension factors driving heat transfer and mechanical stress induced by pressure. Therefore, the relationship finally chosen to correlate the data from this project is significantly more broad and complex than starting point.

Relationship development and variable description for this project are presented below. It must be emphasized that development of Dimensionless Scaling Analysis relationships is not an exact science. Numerous variables and relationships are explored to discover a viable correlation. Thus, the process is continuous and, there is always room for improvement. The variable relationships presented here are not specifically based on scientific equations and engineering facts. Instead, they are based on iterative testing of variable arrangements based on general engineering analysis and intuitive system analysis. The correlation described here is a snapshot based on results amassed by the investigators thus far. Continued incorporation of the analytical tool in future projects will refine the results. The results of this study (both Dimensionless Scaling Analysis and Finite Element Analysis) are being introduced into an ongoing RPSEA funded study of cement seal integrity for wells drilled with OBM or SBM (RPSEA 12121-6503).

Energy Applied

For the purposes of this study, energy inputs come in two forms: mechanical and thermal. The two forms are isolated for lab testing but occur in concert in field application.

Pressure cycling produces energy input into the Mechanical Annular Seal laboratory test. Energy is calculated by:

$$E = \sum (\text{Pressure}_{\text{high}} - \text{Pressure}_{\text{low}}) \times \text{Fluid Volume}$$

Thus, if an inner pipe with fluid volume of 100 in³ is pressurized to 10,000 psi, $E = 10,000 \text{ psi} \times 100 \text{ in}^3$
 $= 1,000,000 \text{ in-lb}_f$.

Cyclic pressurization is cumulative. Thus 10 cycles from 0 to 10,000 psi in the example above yields

$$E = 10 \times 10,000 \text{ psi} \times 100 \text{ in}_3 = 10,000,000 \text{ in-lb}_f.$$

The same method applies for field systems but volume is greater.

Thermal energy transfer when flowing fluid of one temperature through a conduit of another temperature occurs via forced convection and is governed by the general equation:

$$Q = U \times A \times \Delta T \times t$$

in which U is the overall heat transfer coefficient and A is the surface area of the conduit. Estimation of U requires substantial evaluation of the system and significant error in U can be introduced by fluid parameters (film coefficients). For this initial estimation of thermal energy applied to an OCS well during hydraulic fracturing, an engineering approximation relating U to fluid properties with application in high turbulent flow was applied. Even though the flow rate was lower than applicable for the shelf configuration, this shortcut was used as a good approximation for thermal energy. This relationship is:

$$U = k/d \times 0.23 (jd/\mu)^{0.8} \times (\mu \times c_p/k)^{0.4}$$

where

k = thermal conductivity of the fluid

d = pipe diameter

j = mass flow rate

μ = fluid viscosity

c_p = heat capacity of the fluid.

More general form of this turbulent flow heat transfer relationship (first presented by Dittus) in terms of 3 dimensionless scaling variables, Reynolds Number, Nusselt Number and Prandtl Number is:

$$Ud/k = Nu = 0.023 Re^{0.8} Pr^{0.4}.$$

For laminar flow conditions encountered in laboratory and large scale thermal stress testing, the calculation of U is in terms of Nusselt number ($Nu = UD/k$). Nu becomes a constant of 3.66 at the lab-scale test conditions.

Thermal effects of flowing fluid of different temperature through the system center pipe for small-scale, large-scale, and field scale systems are not steady state. Temperature in the pipe is changing continuously throughout the thermal cycle. In order to calculate Q for this unsteady state condition, time-weighted averages of fluid temperature were calculated for each injection configuration. Inlet and discharge temperatures were recorder over time for lab testing. Thermal simulations of BHT vs time were run on field applications. These simulations were then averaged over time to provide average temperature differences for each energy input.

Calculation of field energy imparted by a stimulation treatment was previously approached by combining the thermal and mechanical energies imparted by the flowing fluid into a single dimensionless energy variable. The system's resistance to applied energy was expressed as a single variable also. This approach failed to produce any meaningful relationship. In this study, the different

forms of energy and the system's resistance were analyzed and compared separately and combined at the end to produce the correlation.

This relationship was developed iteratively by a 4-step process:

1. Postulate variable combinations that are dimensionless and relate to magnitude of energy applied to the system or to the system's ability to resist failure due to energy application
2. Apply correlation using lab-generated, small-scale data. Assess the correlation's accuracy to describe the lab results.
3. Repeat steps 1 and 2 adjusting the dimensionless variables until a reasonable trend of system composition and associated seal performance is described by the correlation.
4. Apply the correlation to large-scale laboratory data and to field data in order to assess the correlation's scalability and sensitivity.

E_a

This dimensionless variable is used to magnitude of energy applied to various systems with different dimensions or components. The equation for this relationship is:

$$E_a = E_{am} + E_{ah}$$

Separate relationships for mechanically and thermally applied E_a were developed.

$$E_{am} = \frac{Q_m}{E_s} \times \frac{E_f}{S_{T_t} \times p_f} \times \frac{1}{V_{annulus}}$$

$$E_{ah} = \frac{Q_h}{E_s} \times \frac{p_{steel}}{p_f} \times \frac{C_f}{C_{steel}} \times \frac{k'_f}{C'_t} \times \frac{E_f}{S_{T_t} \times p_f} \times \frac{1}{V_{hole}}$$

R_e

Similar treatments of effective cement resistance, R_e produced the following relationships:

$$R_e = R_{em} + R_{eh}$$

$$R_{em} = \frac{L}{D_{hole}} \times \frac{S_{T_t}}{S_{T_c}} \times \frac{S_{I_c}}{E_c} \times \frac{1}{E_c \times W/C} \times \frac{p_c}{p_f}$$

$$R_{eh} = \frac{C_{steel}}{C_c} \times \frac{C'_c}{k'_c} \times \frac{L}{50 \times D_{hole}} \times \frac{S_{T_t}}{S_{T_c}} \times \frac{S_{I_c}}{E_c} \times \frac{1}{E_c \times W/C} \times \frac{p_c}{p_f}$$

Variable descriptions, units, and reasoning behind inclusion in the correlation appear below. Each component of E_a and R_e is discussed along with parameters and performance properties comprising each component. Several parameters or properties appear multiple times but are described here only the first time they appear. The reasoning for their subsequent inclusions is covered in the initial description.

E_a – Applied Energy (dimensionless): This dimensionless variable describes the energy applied to the casing-cement-formation system in terms of the actual energy, mechanical physical, and thermal properties of the system, and system dimensions. The term accounts for all energy applied.

E_{am} –Applied Energy from Mechanical Actions (dimensionless): Dimensionless Scaling Variable to correlate actual energy applied to a system to the dimensions and materials comprising the system.

Q_m -Mechanical Energy (in-lb_f): Energy applied to the system from mechanical actions such as pressure cycling or impact.

E_s -Young’s Modulus (psi): Energy applied to the system always initiates through the steel pipe. Energy transmission or dissipation by the steel alters the effective energy. Mechanical and thermal energy inputs are divided by Young’s Modulus of the steel to account for this.

E_f , S_{Tf} , and ρ_f -Young’s Modulus of formation (psi), formation tensile strength (psi), and formation specific gravity (dimensionless): These two mechanical properties and one physical property of the formation are included in all E_a calculations to account for the integrity of the outermost system component. Higher strength, more ductile formation acts to improve seal integrity thus lowering the apparent E_a .

$V_{annulus}$ -Volume of the annulus (in³): Larger volumes of cement result in more durable seal; e.g. longer cemented length improves seal durability as does thicker cement sheath. Thus, larger volumes reduce apparent energy application.

E_{ah} – Thermal Applied Energy: Applied Energy from heating or cooling (dimensionless): Dimensionless Scaling Variable to correlate actual thermal energy applied to a system to the dimensions and materials comprising the system. While, thermal energy applied to the system due production intervention is long-term and reaches steady state, thermal energy from well treatment injections is relatively short term. This unsteady state energy application appears to be overestimated by steady state energy calculations. Several scaling factors are added to account for this.

Q_h - Thermal Energy (in-lb_f): Energy applied to the system from heating or cooling.

ρ_{steel}/ρ_f - Specific gravity ratio of casing and formation (dimensionless): This ratio was added as a scaling factor to account for unsteady state conditions. Fundamental reasoning for adding the ratio is that higher relative density of the formation dampens thermal energy effect.

C-Coefficient of Thermal Expansion ($1/^\circ\text{F}$): The contrast of these values for casing and formation relate to thermally induced mechanical stress placed on the cement.

k' -time-adjusted thermal conductivity (in $\text{lb}_f/\text{in } ^\circ\text{F}$) = $k \times \Delta t$: Thermal conductivity of a material denotes the rate at which thermal energy will transit through it. Since system stresses are caused thermal gradients created by unsteady-state heat transfer across the system, the duration of the thermal gradient affects the apparent energy applied also. Heat removed by flowing fracturing fluids through the casing will drive heat flow from the formation through the cement. Duration of gradient as well as magnitude of thermal gradient are accounted for with this adjusted formation variable.

C_p' -area- and density-adjusted heat capacity (in $\text{lb}_f/\text{in } ^\circ\text{F}$) = $C_p \times \rho \times A_{\text{hole wall}}$: Heat capacity of a material denotes the magnitude of thermal energy contained in the material. For this application, system configuration is always a casing-annulus while system area varies with diameter and length. The adjusted heat capacity allows easier dimensional analysis when accounting for thermal energy residing in the system. The formation heat capacity term in the E_{ah} equation drives apparent energy application lower as more thermal energy is stored directly adjacent to the cemented annulus.

V_{hole} -volume of drilled hole (in^3): As discussed above for annular volume, larger volumes produce more durable seal. Hole volume replaced annular volume in the E_{ah} correlation as a scalar making thermal and mechanical data fit the correlation more closely.

R_e – Effective Resistance (dimensionless): This dimensionless variable describes the casing-cement-formation system's ability to withstand energy application without failure. The term does not automatically account for all resistance of a system. The operator must determine which types of energy are applied to a subject system and include only those R_e variables to match the energy inputs.

R_{em} – Mechanical Effective Resistance (dimensionless): This variable describes resistance in terms of mechanical properties, physical properties, and dimensions of the system.

L/D_{hole} -Length of system (in) over hole diameter (in): This dimensionless ratio accounts for dimensional resistance effects form increasing aspect ratio.

$S_{\text{Tf}}/S_{\text{Tc}}$ - Ratio of tensile strengths of formation and cement (psi/psi): This dimensionless ratio accounts for increased system resistance to hoop stress by increasing tensile strength of the formation supporting the system.

$S_{\text{ic}}/E_{\text{c}}$ -Ratio of impact strength of cement to Young's modulus of cement (psi/psi): this dimensionless variable modifies mechanical resistance in terms of cement impact strength and brittleness.

ϵ_{c} -Anelastic Strain ($1/\text{psi}$): This variable accounts for effects of plastic deformation of cement and its effect on seal durability.

w/c-water to cement ratio (dimensionless): This term relates the porosity and resulting strength of a cement composition to system resistance.

R_{eh} – Thermal Effective Resistance (dimensionless): This dimensionless variable describes system resistance in terms of mechanical properties, physical properties, thermal properties, and dimensions of the system. All variables comprising the term have been previously described. Note that thermal properties of cement (C'_{pc} , k_c , C_c) are included to account for thermal property effects on the system's resistance to thermal stress. A scalar of 50 was incorporated into L/D term to improve agreement between mechanical and thermal components of the correlation.

WORKS CITED FOR FAILURE MODE AND PHYSICAL MODELING

Bui, B. T., and Tutuncu, A. N. "Modeling the Failure of Cement Sheath in Anisotropic Stress Field" *SPE 167178*. Presented at the SPE Unconventional Resources Conference, 5-7 November 2013, Alberta, Canada.

De Andrade, J., Torsaeter, M., Todorovic, J., Opedal, N., Stroisz, A., and Vralstad, T. "Influence of Casing Centralization on Cement Sheath Integrity During Thermal Cycling" *SPE-168012*. Presented at the SPE Drilling Conference and Exhibition, 4-6 March 2014, Fort Worth, Texas.

Dusseault, M. B., Gray, M. N., and Nawrocki, P. A. "Why Oilwells Leak: Cement Behavior and Long-Term Consequences". *SPE 64733*. Presented at the SPE International Oil and Gas Conference and Exhibition 7-10 November 2000 Beijing, China.

Goodwin, K. J., and Crook, R. J. "Cement Sheath Stress Failure" *SPE 20453*, 1 December 1992.

Heathman, J. F., and Beck, F. E. "Finite Element Analysis Couples Casing and Cement Designs for HTHP Wells in East Texas" *SPE 98869*. Presented at the SPE Drilling Conference 21-23 February 2006, Miami, Florida, USA

Li, Y., Liu, S., Wang, Z., Yuan, J., and Qi, F. "Analysis of Cement Sheath Coupling Effects of Temperature and Pressure in Non-Uniform in-Situ Stress Field" *SPE 131878*. Presented at the SPE International Oil & Gas Conference and Exhibition 8-10 June 2010, Beijing, China.

Mueller, D. T., GoBoncan, V., Dillenbeck, R. L., and Heinold, T. "Characterizing Casing-Cement-Formation Interactions Under Stress Conditions: Impact on Long-Term Zonal Isolation" *SPE 90450*. Presented at the SPE Annual Technical Conference and Exhibition 26-29 September 2004, Houston, Texas, USA.

Sabins, F., "MMS Project: Long-Term Integrity of Deepwater Cement Systems Under Stress/Compaction Conditions." 31 July, 2002

Stiles, D. "Effects of Long-Term Exposure to Ultrahigh Temperature on the Mechanical Parameters of Cement" *SPE 98896*. Presented at the SPE Drilling Conference 21-23 February 2006, Miami, Florida, USA.

Wang, W., and Dahi T. A. "Cement Sheath Integrity During Hydraulic Fracturing; An Integrated Modeling Approach" *SPE 168642* Presented at the SPE Hydraulic Fracturing Technology Conference 4-6 February 2014, The Woodlands, Texas, USA.

Yuan, Z., Al-yami A. S, Schubert, J. J., and Teodoriu, C. "Cement Failure Probability under HPHT Conditions Supported By Long Term Laboratory Studies and Field Cases" *SPE 154746* Presented at the SPE Annual Technical Conference and Exhibition 8-10 October 2012, San Antonio, Texas, USA.

APPENDIX C FINITE ELEMENT ANALYSIS

FIGURE 21: GENERAL VIEW OF SMALL SCALE FEA MODEL

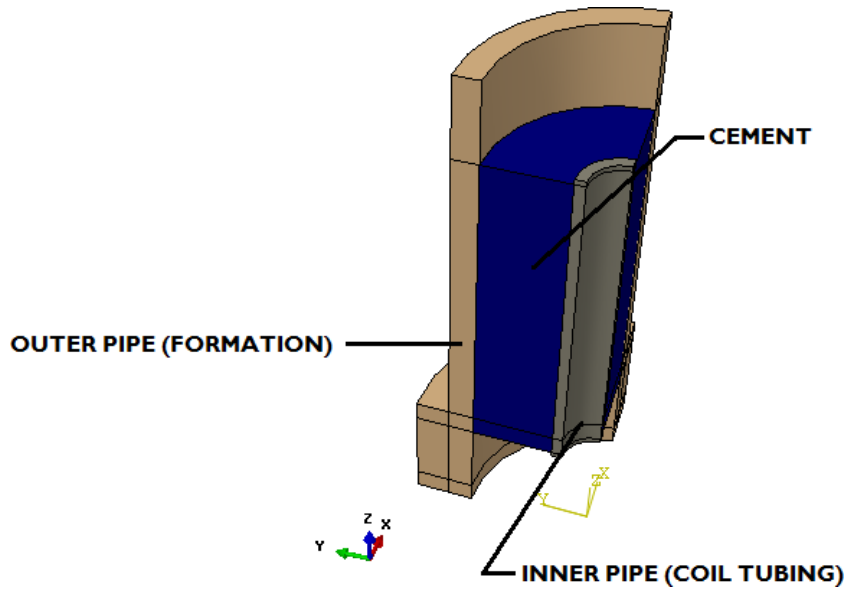


FIGURE 22: VIEW OF MESHING OF SMALL SCALE MODEL

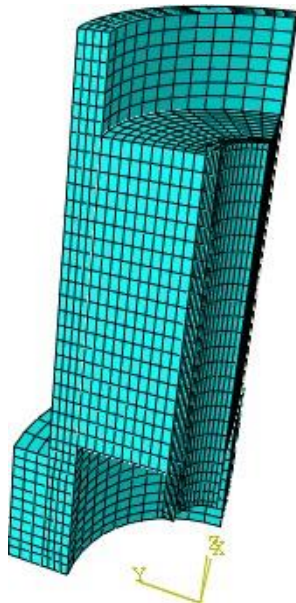
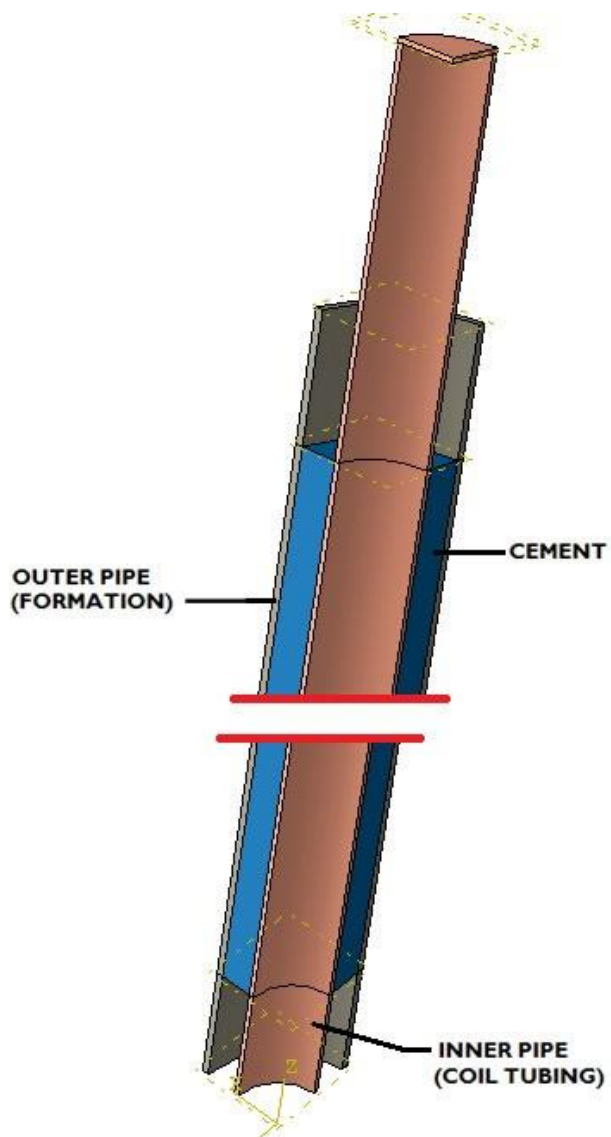


FIGURE 23: GENERAL VIEW OF LARGE SCALE FEA MODEL



THIS REPORT WAS INADVERTENTLY DISSEMINATED IN THE PUBLIC DOMAIN/ONLINE SINCE 09/2015 WITHOUT A DISCLAIMER. DISCLAIMER HAS BEEN ADDED – “THIS INFORMATION IS DISTRIBUTED SOLELY FOR THE PURPOSE OF PEER REVIEW UNDER APPLICABLE INFORMATION QUALITY GUIDELINES. IT HAS NOT BEEN FORMALLY DISSEMINATED BY BSEE. IT DOES NOT REPRESENT AND SHOULD NOT BE CONSTRUED TO REPRESENT ANY AGENCY DETERMINATION OR POLICY

FIGURE 24: VIEW OF MESHING OF LARGE SCALE MODEL

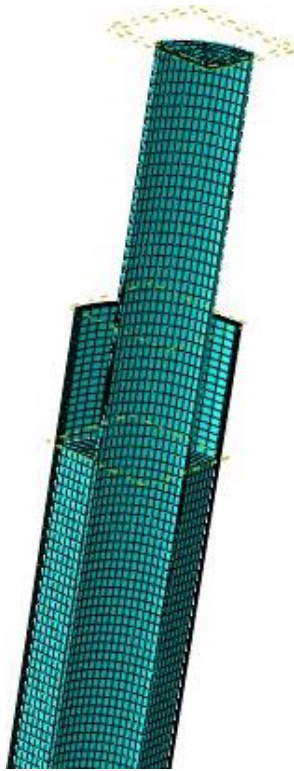
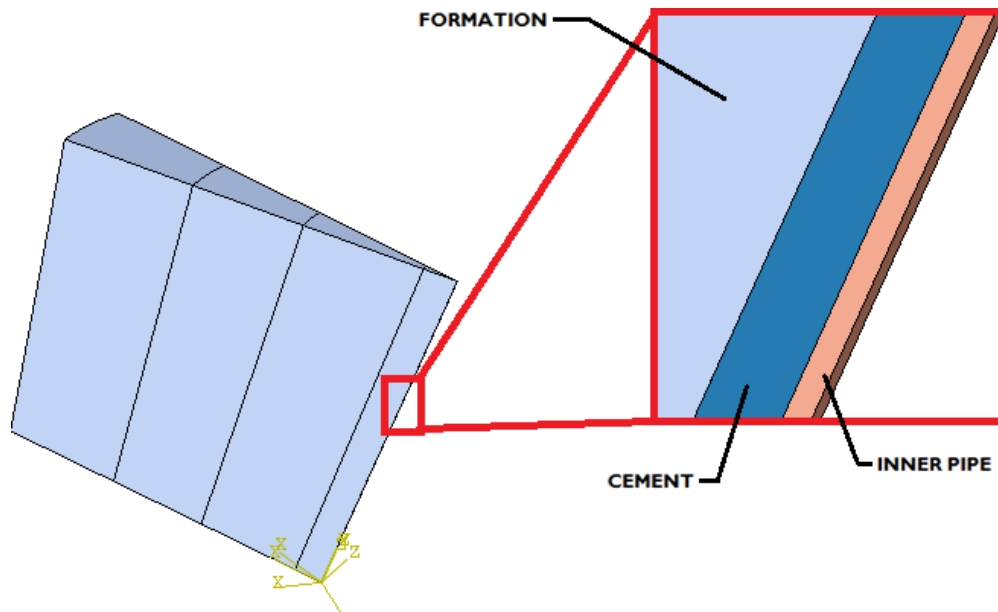


FIGURE 25: GENERAL VIEW OF DOWN-HOLE SYSTEM FEA MODEL



THIS REPORT WAS INADVERTENTLY DISSEMINATED IN THE PUBLIC DOMAIN/ONLINE SINCE 09/2015 WITHOUT A DISCLAIMER. DISCLAIMER HAS BEEN ADDED – “THIS INFORMATION IS DISTRIBUTED SOLELY FOR THE PURPOSE OF PEER REVIEW UNDER APPLICABLE INFORMATION QUALITY GUIDELINES. IT HAS NOT BEEN FORMALLY DISSEMINATED BY BSEE. IT DOES NOT REPRESENT AND SHOULD NOT BE CONSTRUED TO REPRESENT ANY AGENCY DETERMINATION OR POLICY

FIGURE 26: VIEW OF MESHING OF DOWN-HOLE SYSTEM FEA MODEL

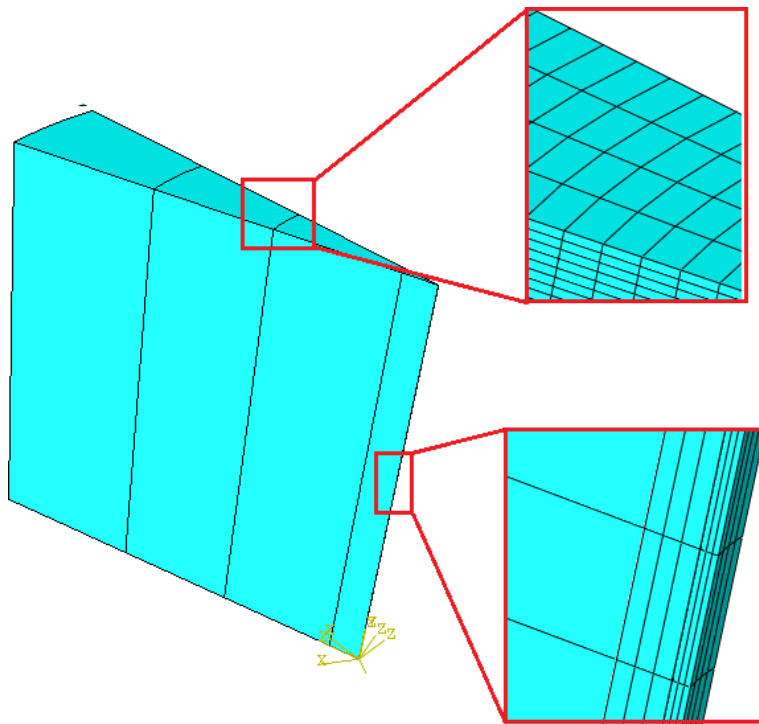


FIGURE 27: SMALL SCALE MODEL BOUNDARY CONDITIONS

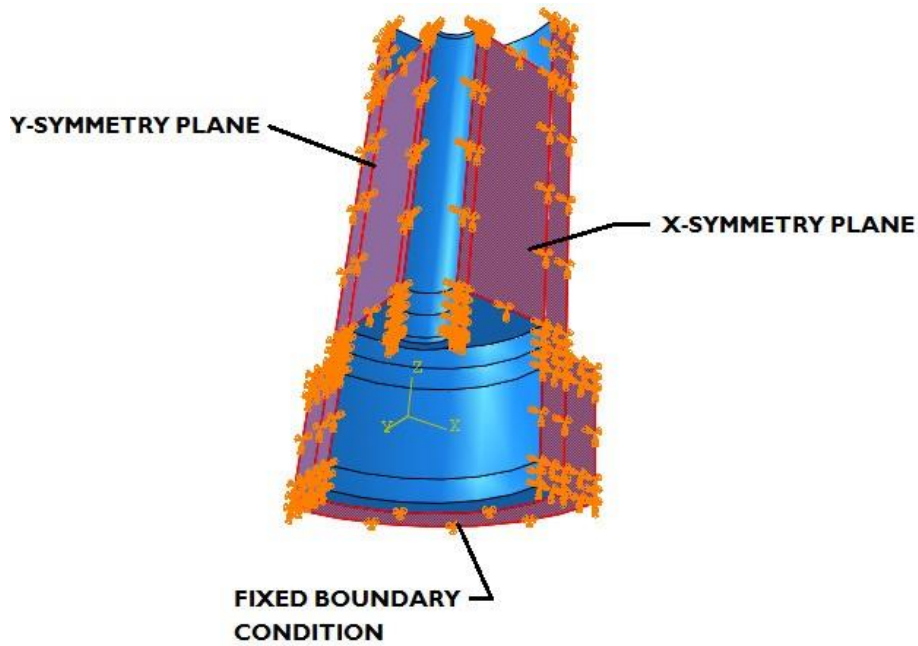


FIGURE 28: LARGE SCALE MODEL BOUNDARY CONDITIONS

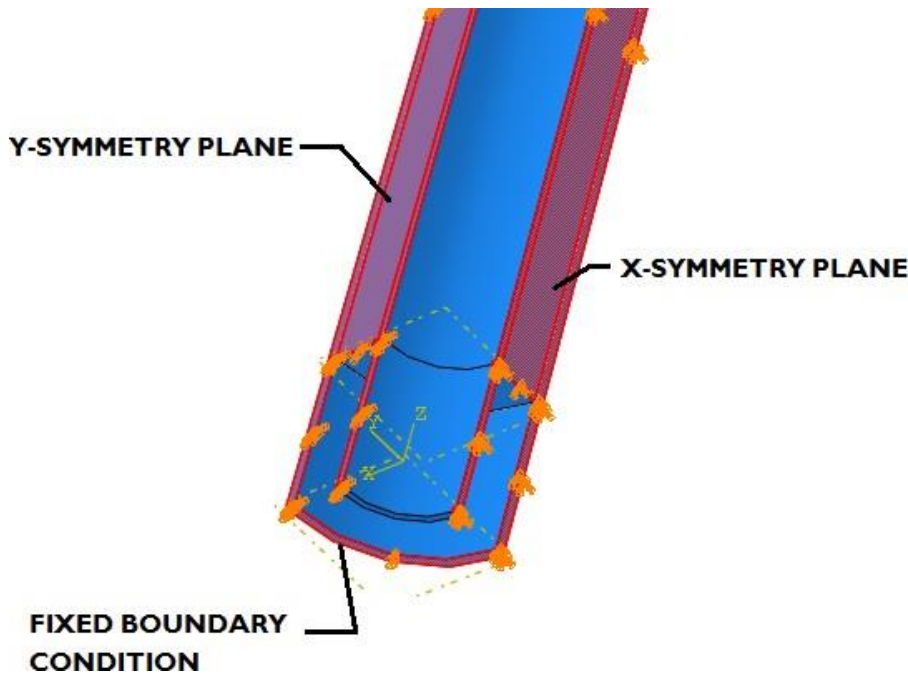


FIGURE 29: DOWN-HOLE SYSTEM MODEL BOUNDARY CONDITIONS

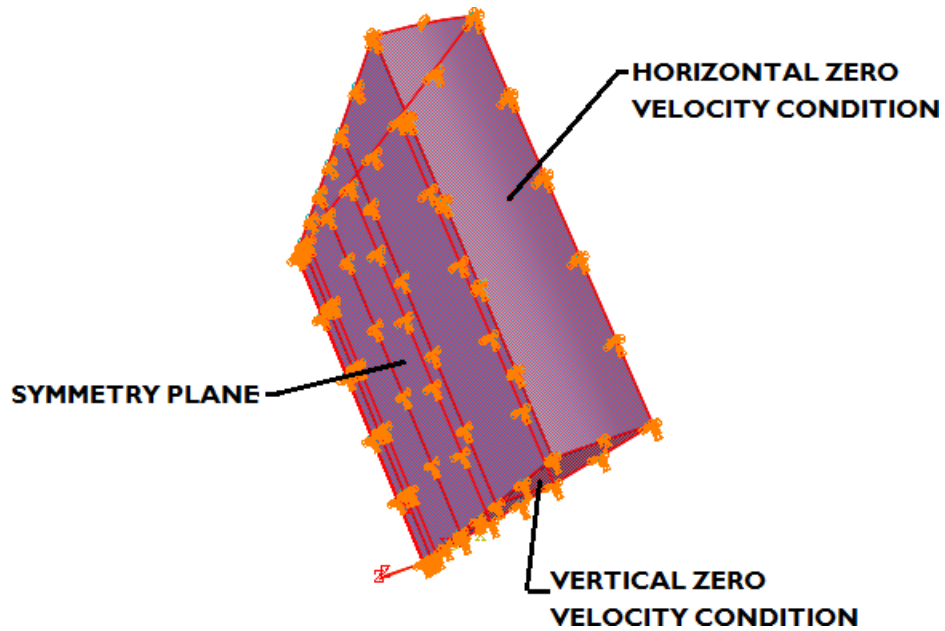
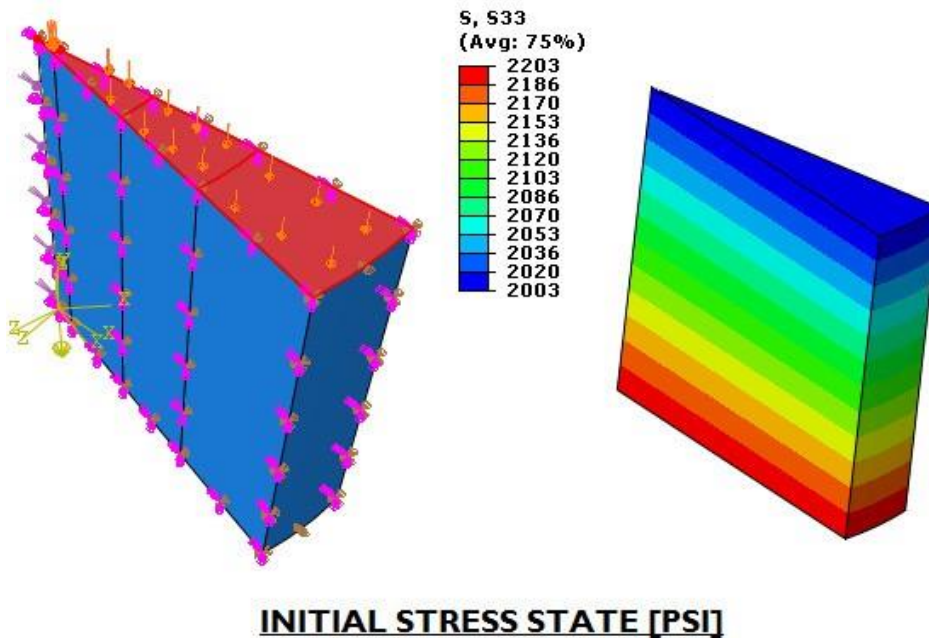


FIGURE 30: INITIAL VERTICAL STRESS STATE FOR DOWN-HOLE SYSTEM



THIS REPORT WAS INADVERTENTLY DISSEMINATED IN THE PUBLIC DOMAIN/ONLINE SINCE 09/2015 WITHOUT A DISCLAIMER. DISCLAIMER HAS BEEN ADDED – “THIS INFORMATION IS DISTRIBUTED SOLELY FOR THE PURPOSE OF PEER REVIEW UNDER APPLICABLE INFORMATION QUALITY GUIDELINES. IT HAS NOT BEEN FORMALLY DISSEMINATED BY BSEE. IT DOES NOT REPRESENT AND SHOULD NOT BE CONSTRUED TO REPRESENT ANY AGENCY DETERMINATION OR POLICY

FIGURE 31: TYPICAL CONTACT INTERACTION LOCATIONS

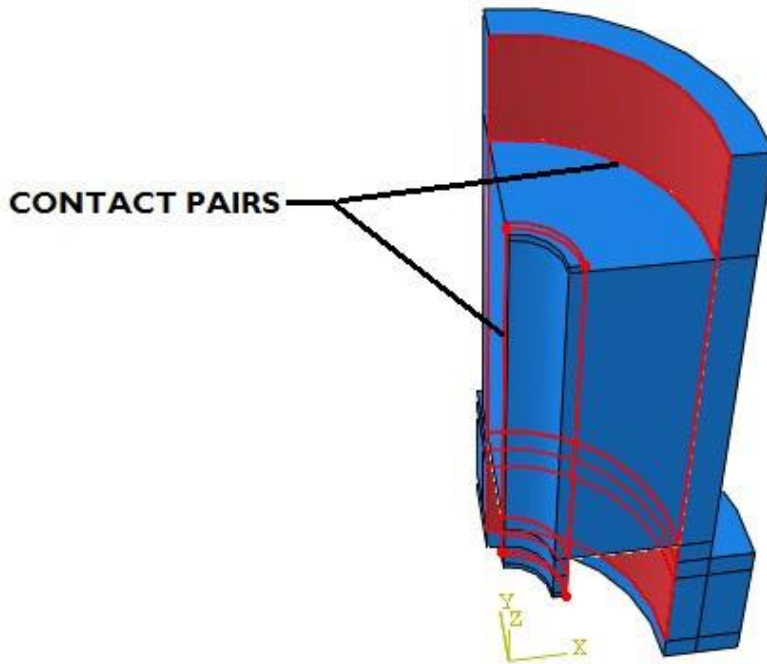


FIGURE 32: SMALL SCALE THERMAL BOUNDARIES

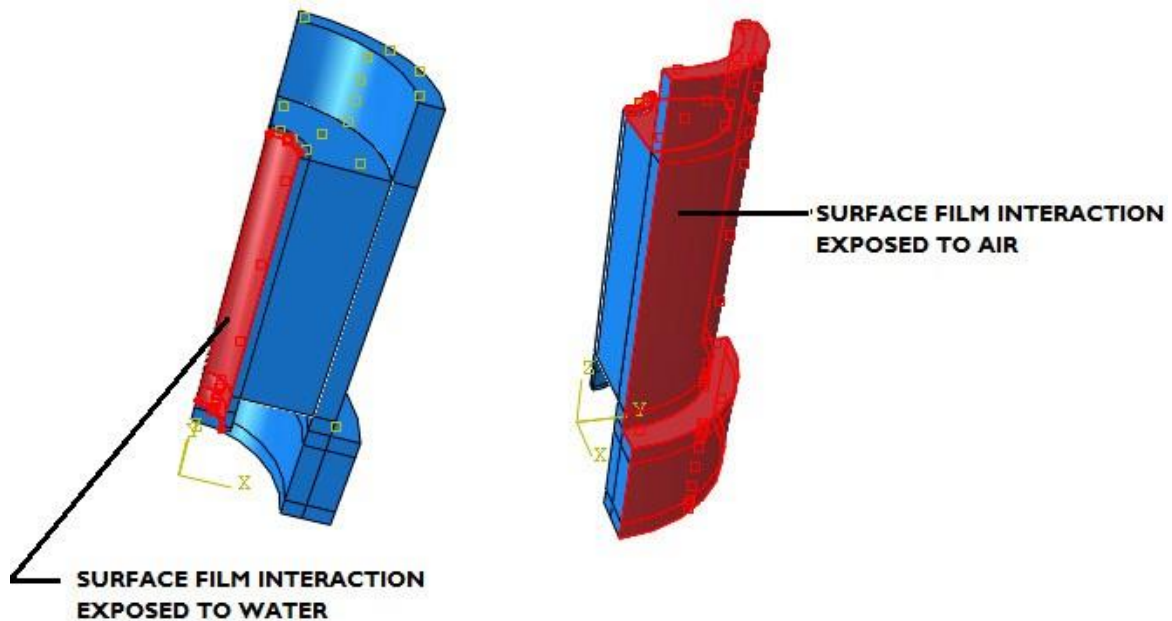


FIGURE 33: LARGE SCALE THERMAL BOUNDARIES

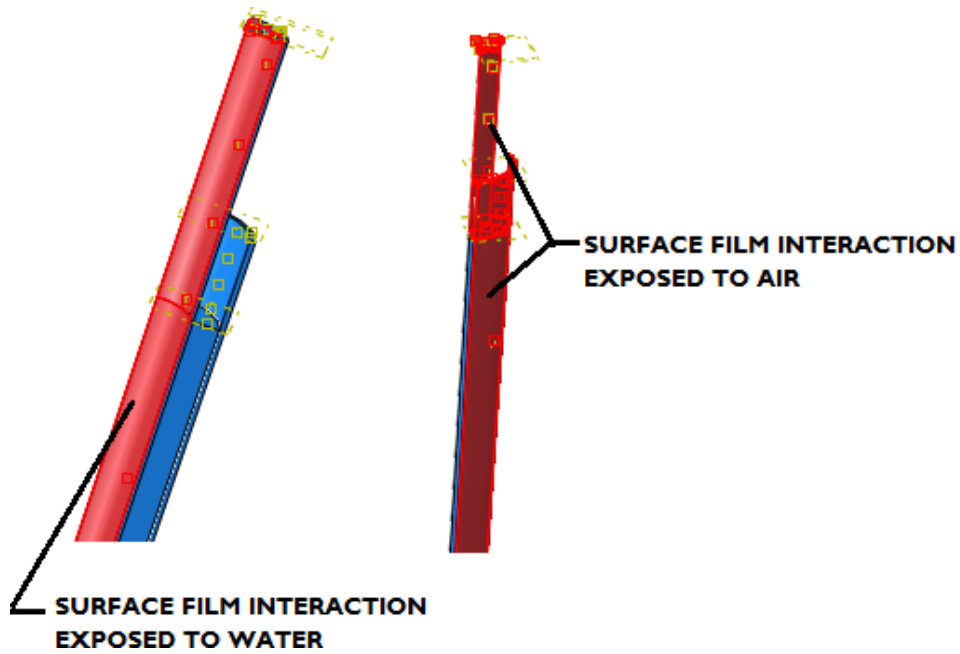


FIGURE 34: DOWN-HOLE SYSTEM THERMAL BOUNDARIES

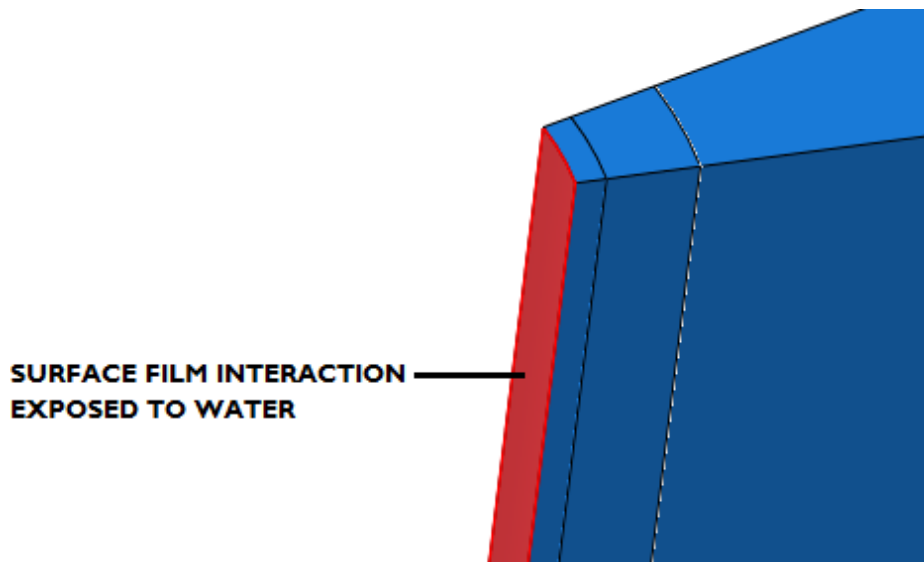


FIGURE 35: SMALL SCALE TEMPERATURE DISTRIBUTIONS (CPVC OUTER PIPE)

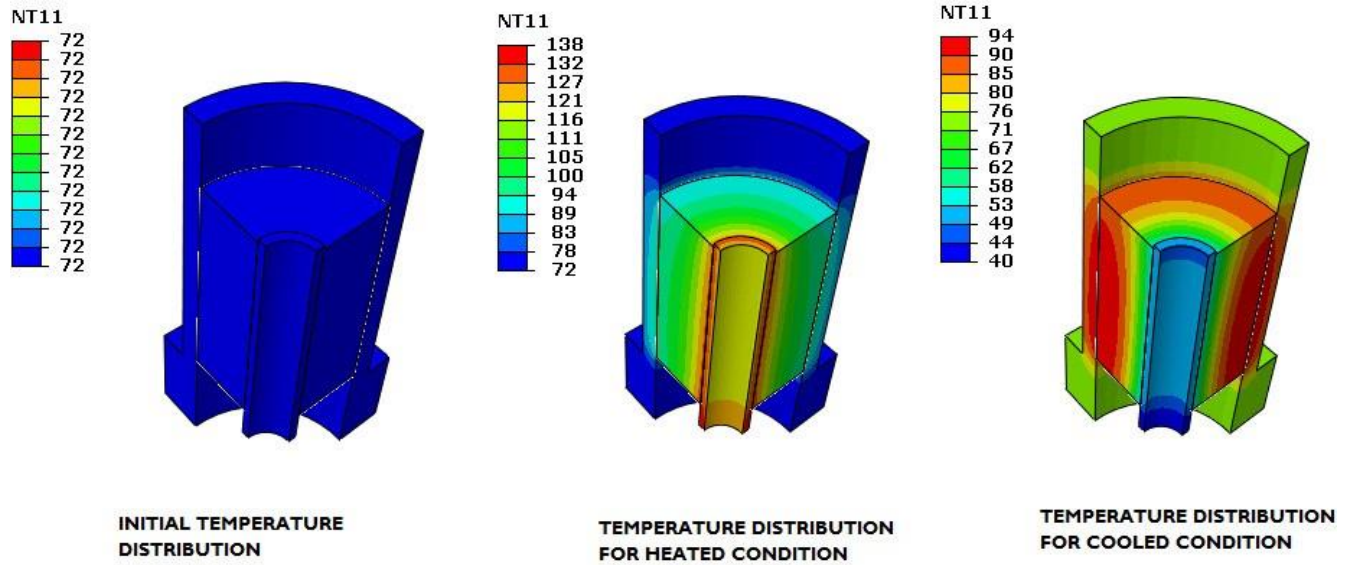


FIGURE 36: SMALL SCALE TEMPERATURE DISTRIBUTIONS (STEEL OUTER PIPE)

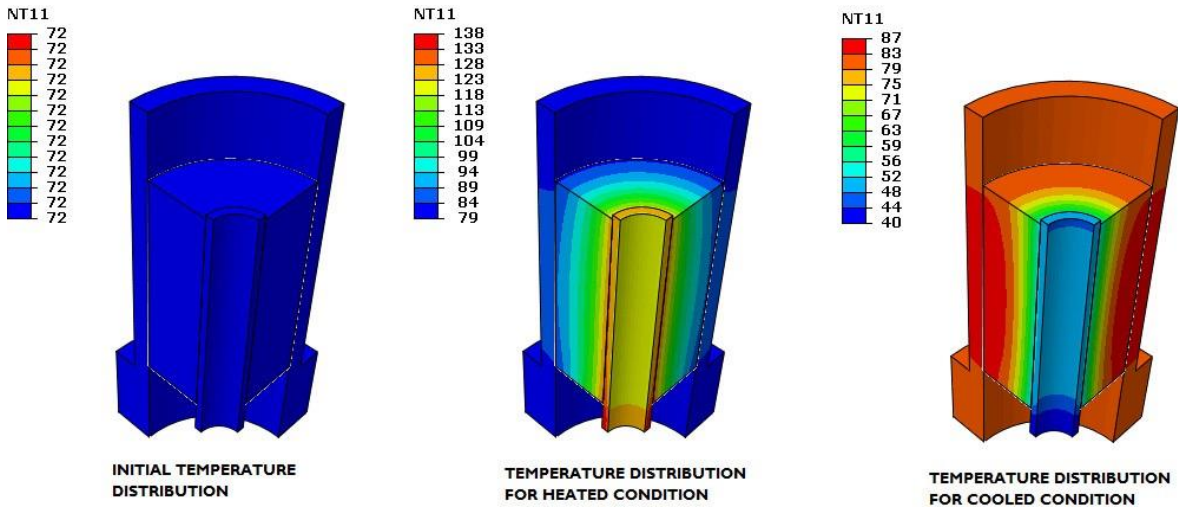


FIGURE 37: LARGE SCALE TEMPERATURE DISTRIBUTIONS

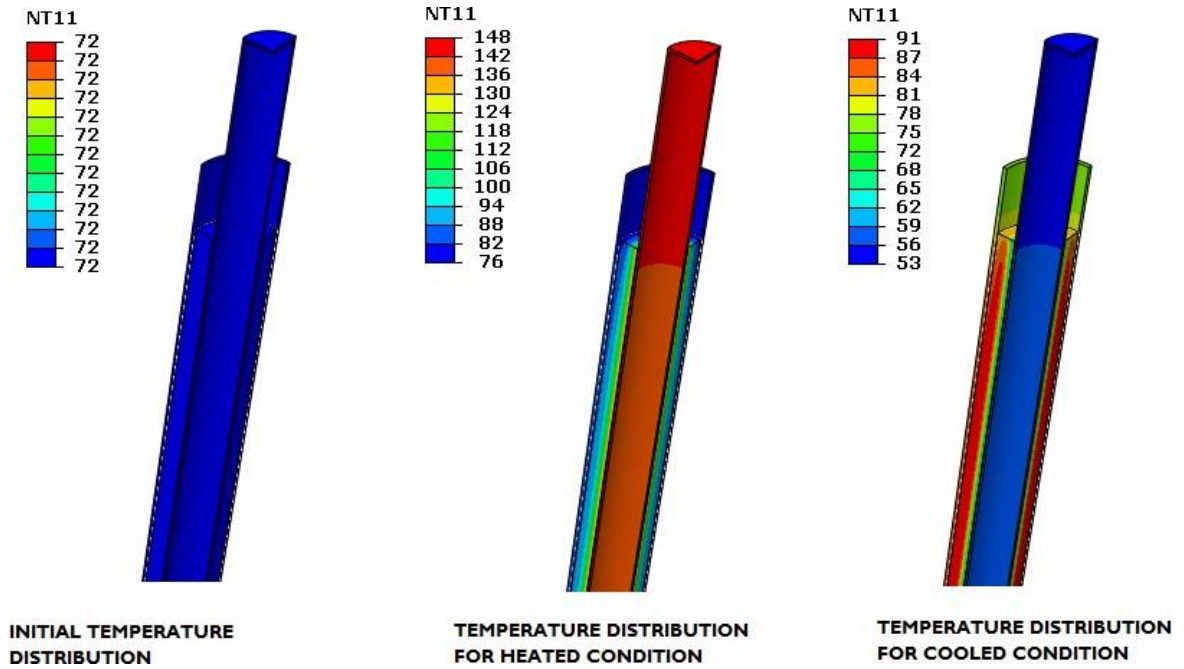


FIGURE 38: DOWN-HOLE SYSTEM TEMPERATURE DISTRIBUTION

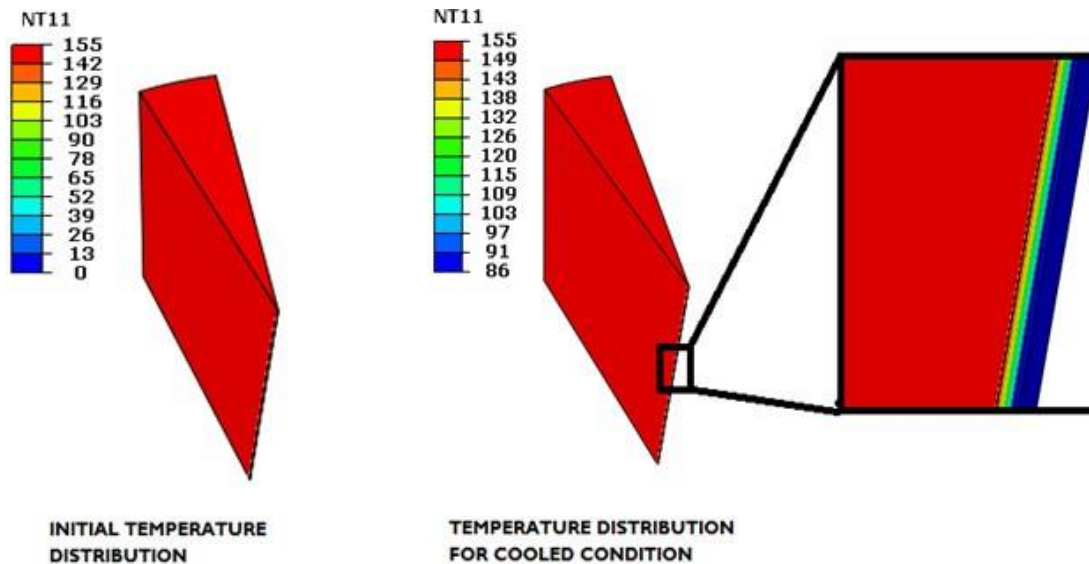


FIGURE 39: SMALL SCALE PRESSURE LOADING

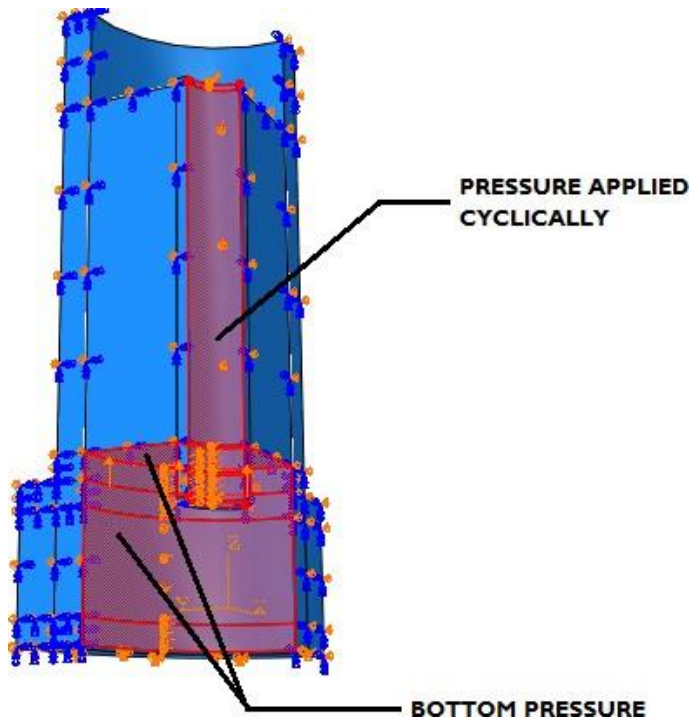


FIGURE 40: LARGE SCALE PRESSURE LOADING

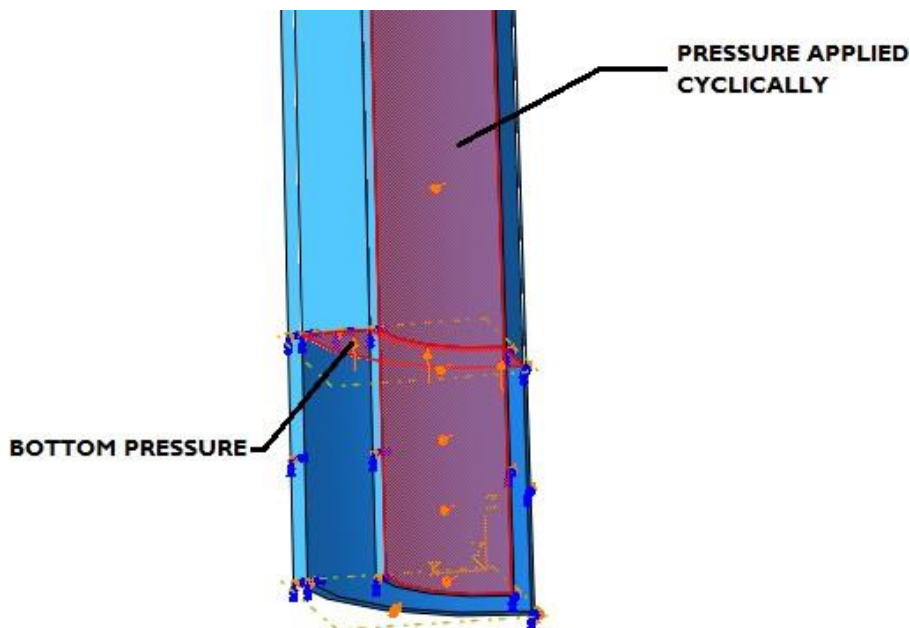


FIGURE 41: DOWN-HOLE SYSTEM PRESSURE LOADING

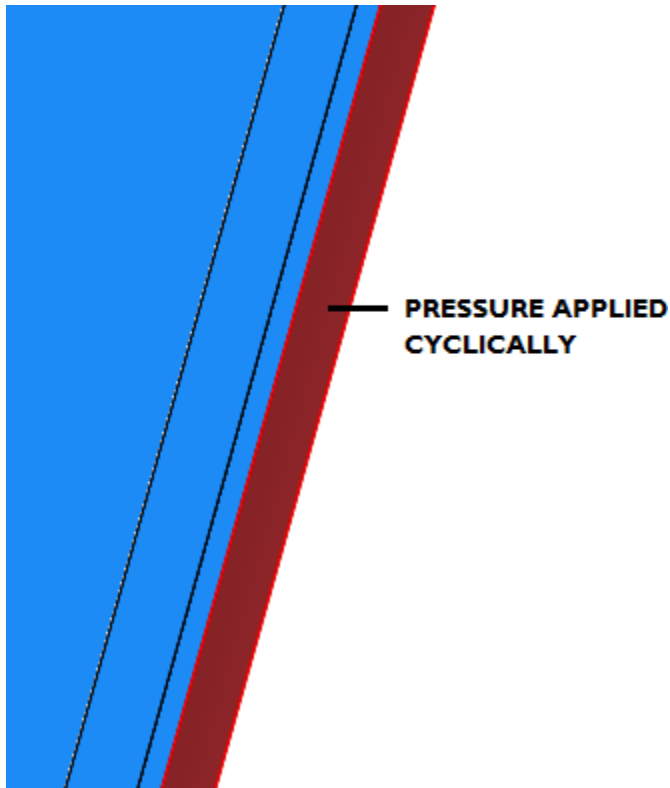
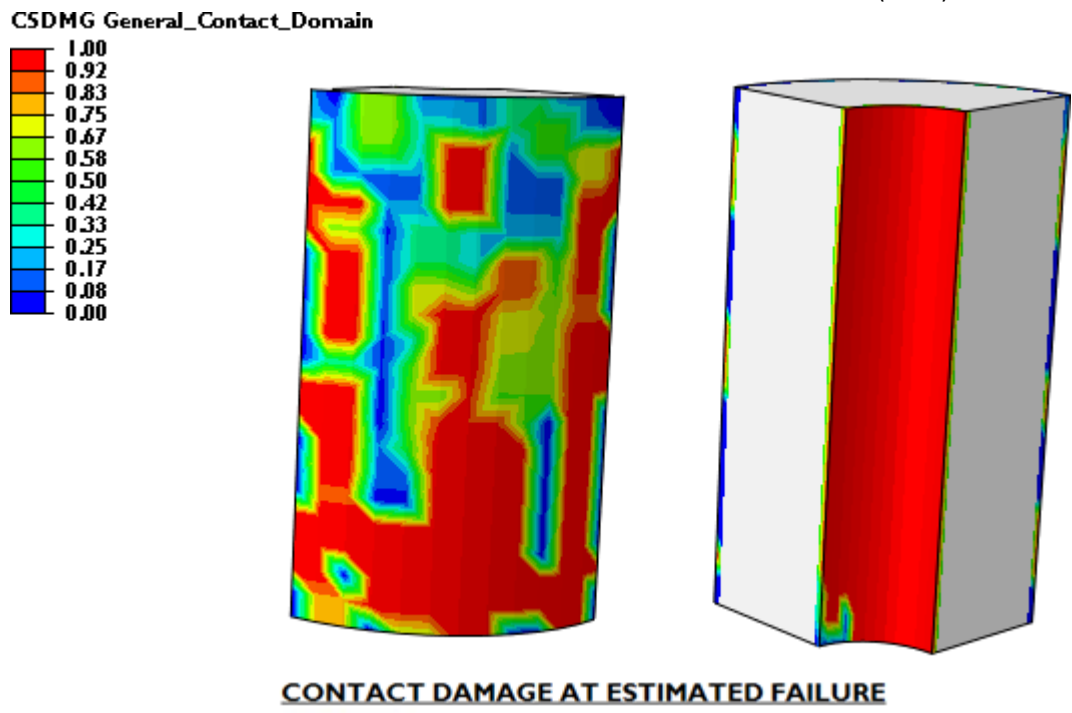


FIGURE 42: DAMAGE OF ELEMENTS IN SMALL SCALE PRESSURE TESTS (CPVC)

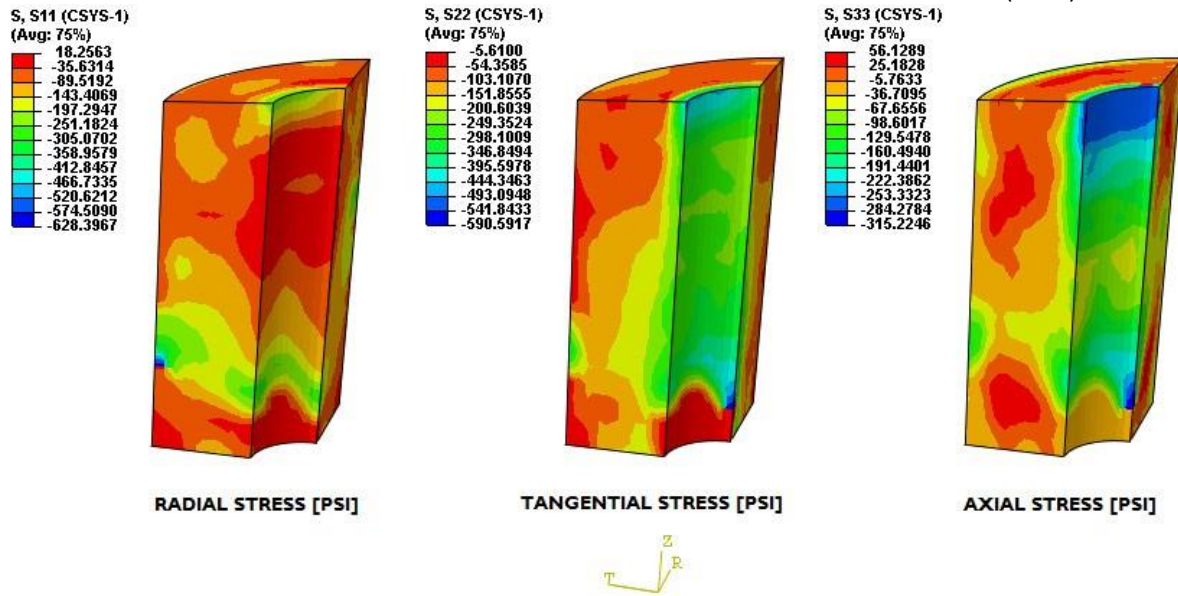


FIGURE 43: CONTACT DAMAGE OF SURFACES IN SMALL SCALE PRESSURE TESTS (CPVC)



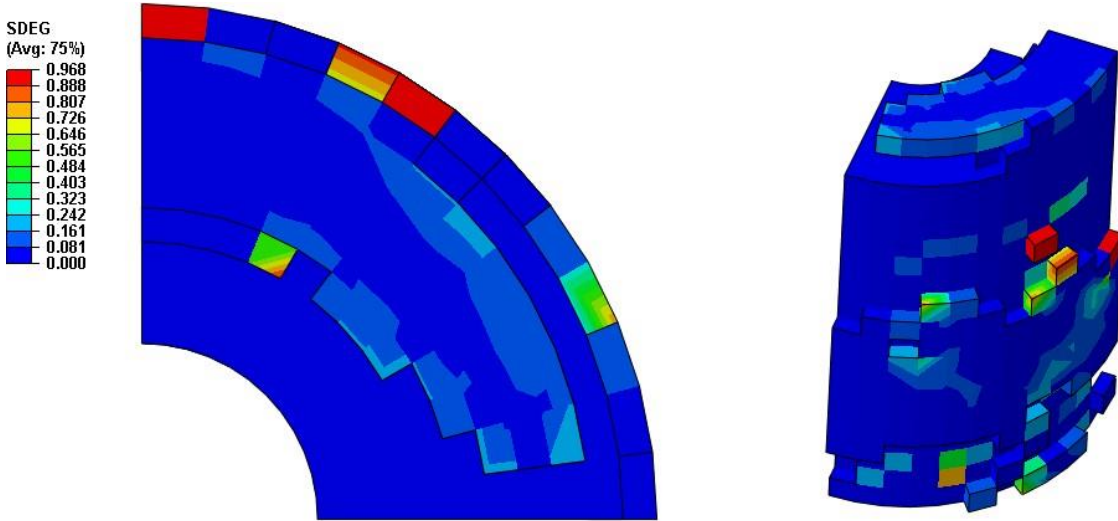
THIS REPORT WAS INADVERTENTLY DISSEMINATED IN THE PUBLIC DOMAIN/ONLINE SINCE 09/2015 WITHOUT A DISCLAIMER. DISCLAIMER HAS BEEN ADDED – “THIS INFORMATION IS DISTRIBUTED SOLELY FOR THE PURPOSE OF PEER REVIEW UNDER APPLICABLE INFORMATION QUALITY GUIDELINES. IT HAS NOT BEEN FORMALLY DISSEMINATED BY BSEE. IT DOES NOT REPRESENT AND SHOULD NOT BE CONSTRUED TO REPRESENT ANY AGENCY DETERMINATION OR POLICY

FIGURE 44: SMALL SCALE STRESS CONTOURS AT ESTIMATED FAILURE FOR PRESSURE TESTS (CPVC)



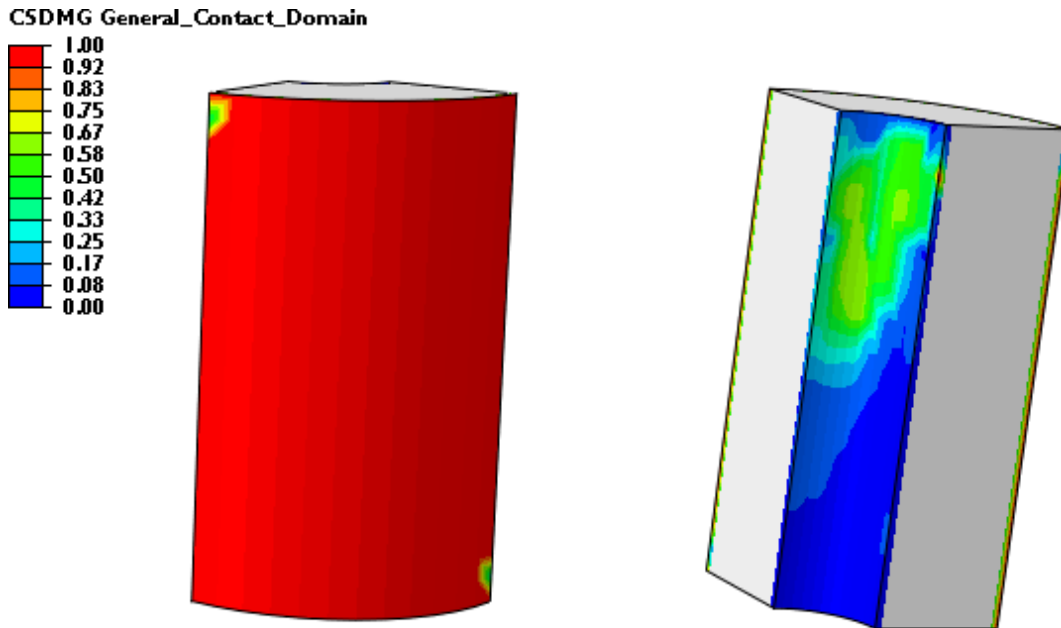
THIS REPORT WAS INADVERTENTLY DISSEMINATED IN THE PUBLIC DOMAIN/ONLINE SINCE 09/2015 WITHOUT A DISCLAIMER. DISCLAIMER HAS BEEN ADDED – “THIS INFORMATION IS DISTRIBUTED SOLELY FOR THE PURPOSE OF PEER REVIEW UNDER APPLICABLE INFORMATION QUALITY GUIDELINES. IT HAS NOT BEEN FORMALLY DISSEMINATED BY BSEE. IT DOES NOT REPRESENT AND SHOULD NOT BE CONSTRUED TO REPRESENT ANY AGENCY DETERMINATION OR POLICY

FIGURE 45: DAMAGE OF ELEMENTS IN SMALL SCALE PRESSURE TESTS (STEEL)



ELEMENT DAMAGE AT ESTIMATED FAILURE

FIGURE 46: CONTACT DAMAGE OF SURFACES IN SMALL SCALE PRESSURE TESTS (STEEL)



CONTACT DAMAGE AT ESTIMATED FAILURE

THIS REPORT WAS INADVERTENTLY DISSEMINATED IN THE PUBLIC DOMAIN/ONLINE SINCE 09/2015 WITHOUT A DISCLAIMER. DISCLAIMER HAS BEEN ADDED – “THIS INFORMATION IS DISTRIBUTED SOLELY FOR THE PURPOSE OF PEER REVIEW UNDER APPLICABLE INFORMATION QUALITY GUIDELINES. IT HAS NOT BEEN FORMALLY DISSEMINATED BY BSEE. IT DOES NOT REPRESENT AND SHOULD NOT BE CONSTRUED TO REPRESENT ANY AGENCY DETERMINATION OR POLICY

FIGURE 47: SMALL SCALE STRESS CONTOURS AT ESTIMATED FAILURE FOR PRESSURE TESTS (STEEL)

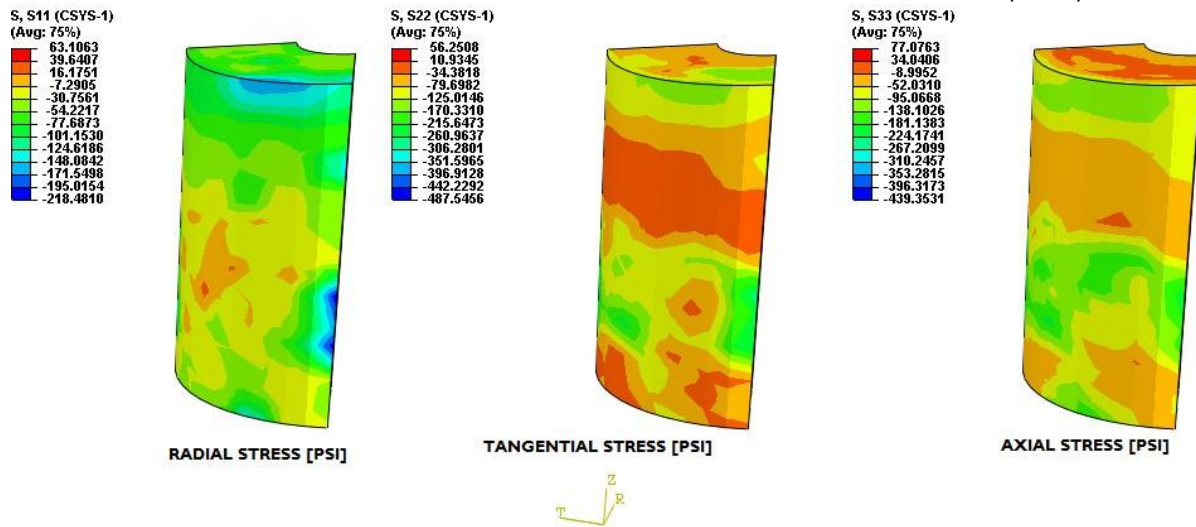
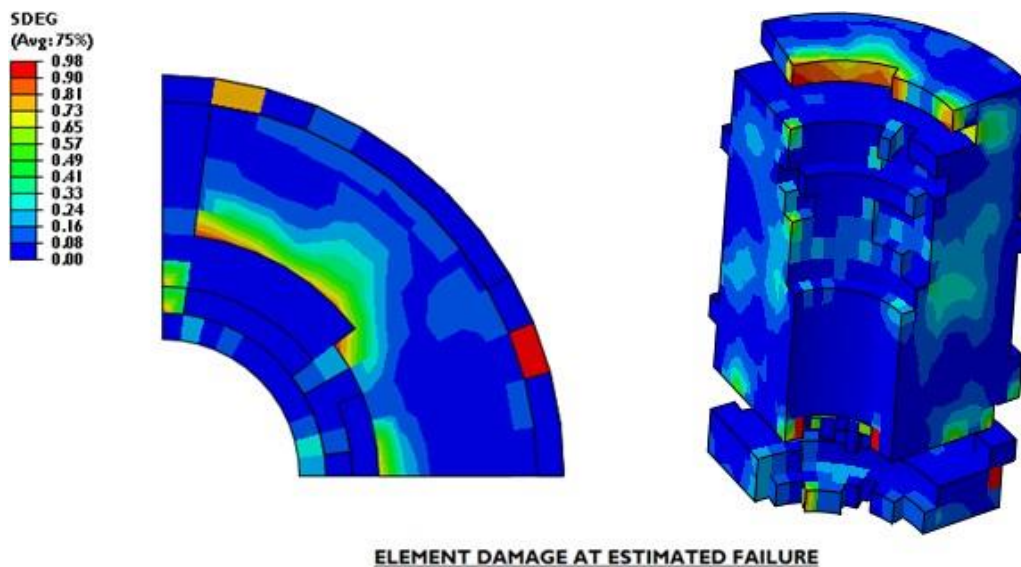


FIGURE 48: DAMAGE OF ELEMENTS IN SMALL SCALE THERMAL TESTS (CPVC)



THIS REPORT WAS INADVERTENTLY DISSEMINATED IN THE PUBLIC DOMAIN/ONLINE SINCE 09/2015 WITHOUT A DISCLAIMER. DISCLAIMER HAS BEEN ADDED – “THIS INFORMATION IS DISTRIBUTED SOLELY FOR THE PURPOSE OF PEER REVIEW UNDER APPLICABLE INFORMATION QUALITY GUIDELINES. IT HAS NOT BEEN FORMALLY DISSEMINATED BY BSEE. IT DOES NOT REPRESENT AND SHOULD NOT BE CONSTRUED TO REPRESENT ANY AGENCY DETERMINATION OR POLICY

FIGURE 49: CONTACT DAMAGE OF SURFACES IN SMALL SCALE THERMAL TESTS (CPVC)

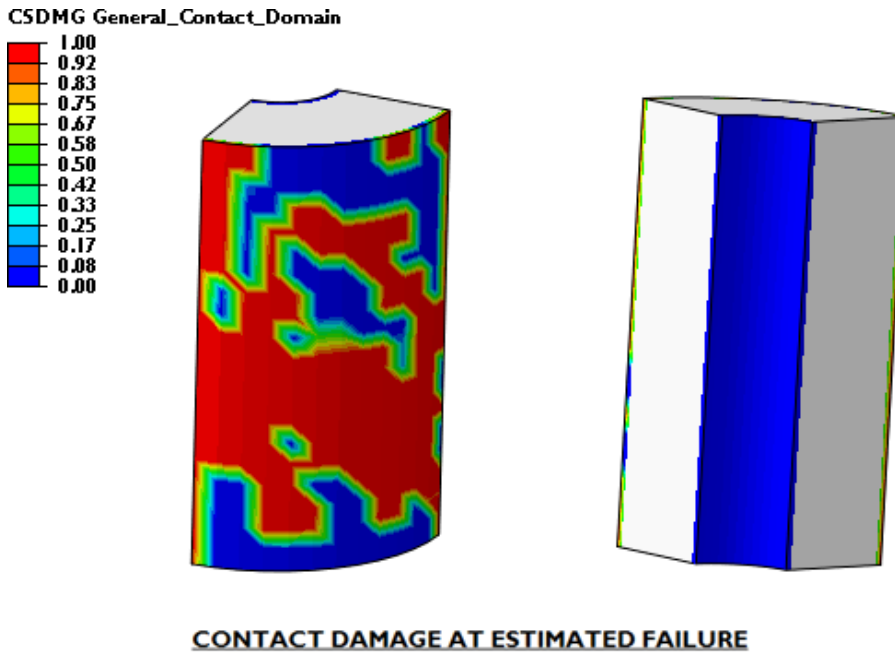


FIGURE 50: SMALL SCALE STRESS CONTOURS AT FAILURE FOR THERMAL TESTS (CPVC)

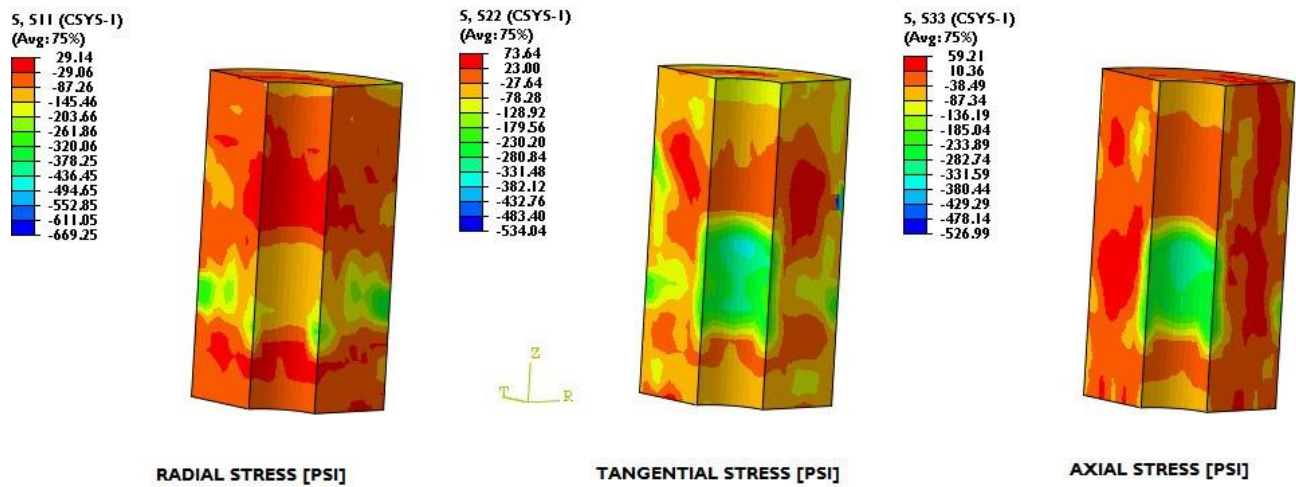


FIGURE 51: DAMAGE OF ELEMENTS IN SMALL SCALE THERMAL TESTS (STEEL)

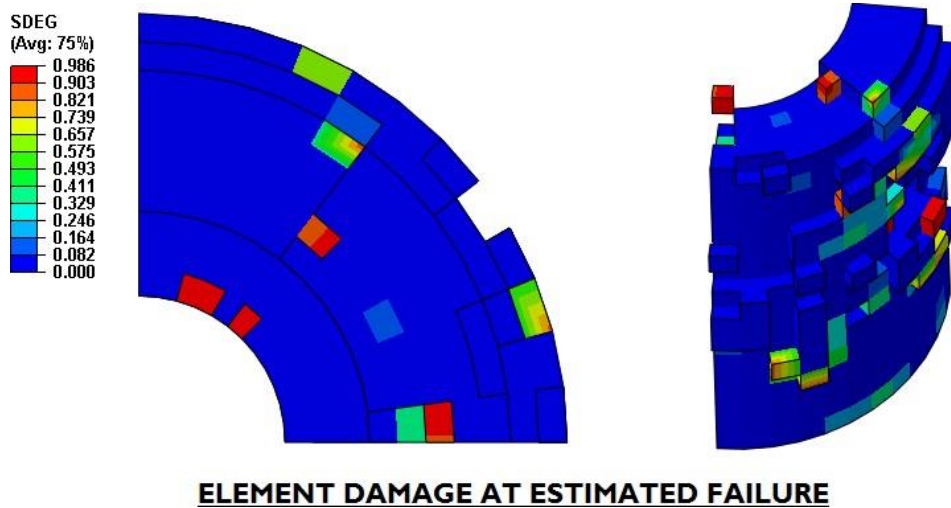


FIGURE 52: CONTACT DAMAGE OF SURFACES IN SMALL SCALE THERMAL TESTS (STEEL)

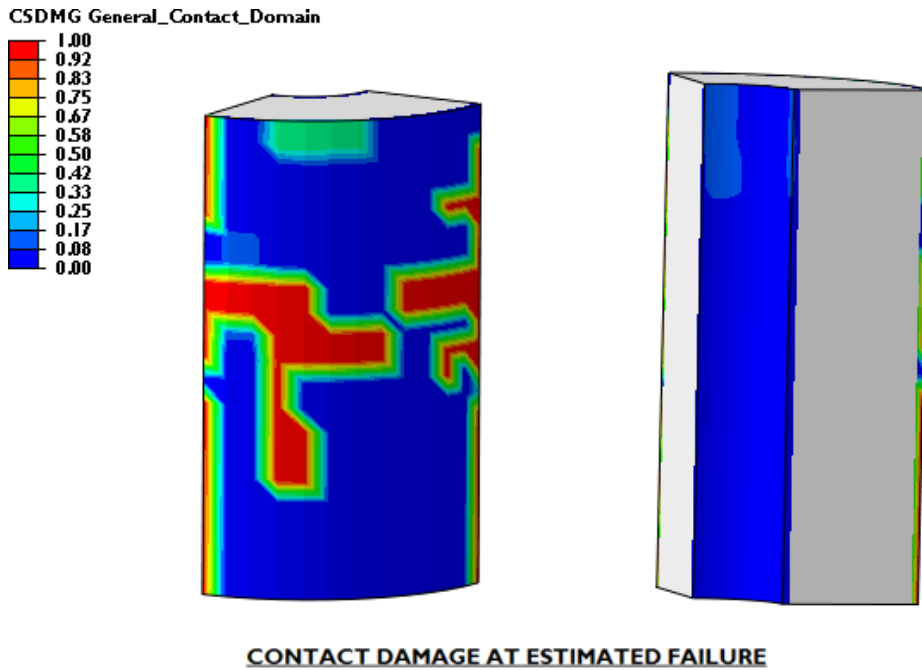


FIGURE 53: SMALL SCALE STRESS CONTOURS AT FAILURE FOR THERMAL TESTS (STEEL)

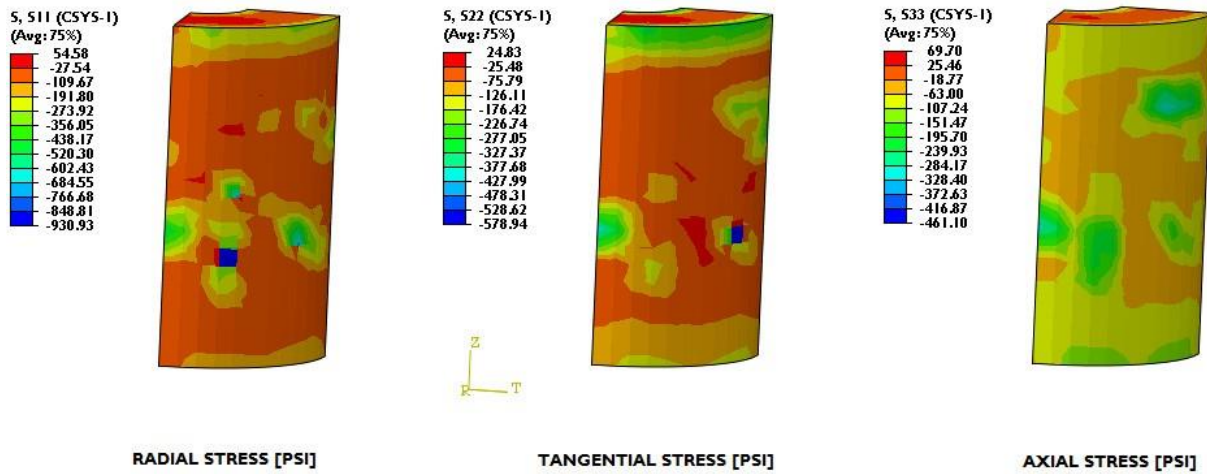
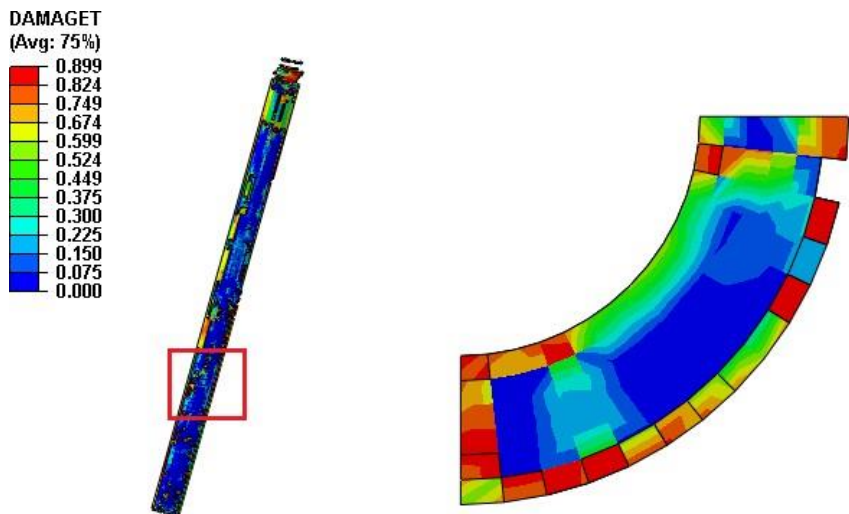


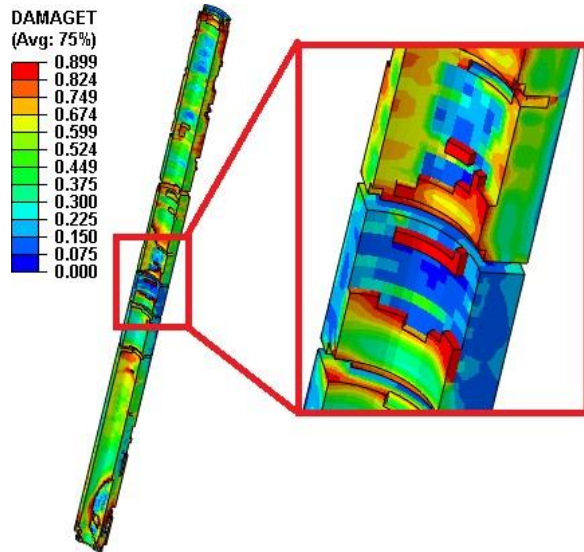
FIGURE 54: LARGE SCALE ELEMENT DAMAGE AT ESTIMATED FAILURE UNDER PRESSURE LOADING



ELEMENT TENSILE DAMAGE AT ESTIMATED FAILURE

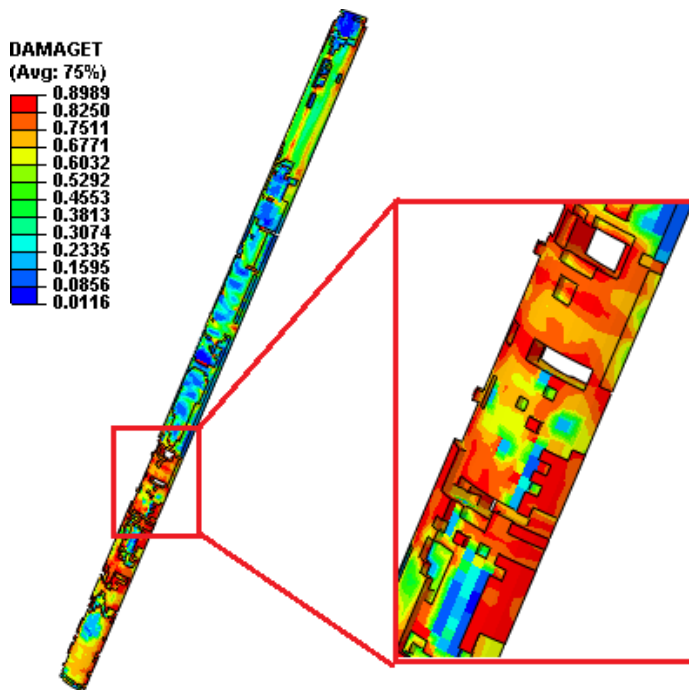
THIS REPORT WAS INADVERTENTLY DISSEMINATED IN THE PUBLIC DOMAIN/ONLINE SINCE 09/2015 WITHOUT A DISCLAIMER. DISCLAIMER HAS BEEN ADDED – “THIS INFORMATION IS DISTRIBUTED SOLELY FOR THE PURPOSE OF PEER REVIEW UNDER APPLICABLE INFORMATION QUALITY GUIDELINES. IT HAS NOT BEEN FORMALLY DISSEMINATED BY BSEE. IT DOES NOT REPRESENT AND SHOULD NOT BE CONSTRUED TO REPRESENT ANY AGENCY DETERMINATION OR POLICY

FIGURE 55: LARGE SCALE ELEMENT DAMAGE AT ESTIMATED FAILURE UNDER THERMAL LOADING



ELEMENT TENSILE DAMAGE AT ESTIMATED FAILURE

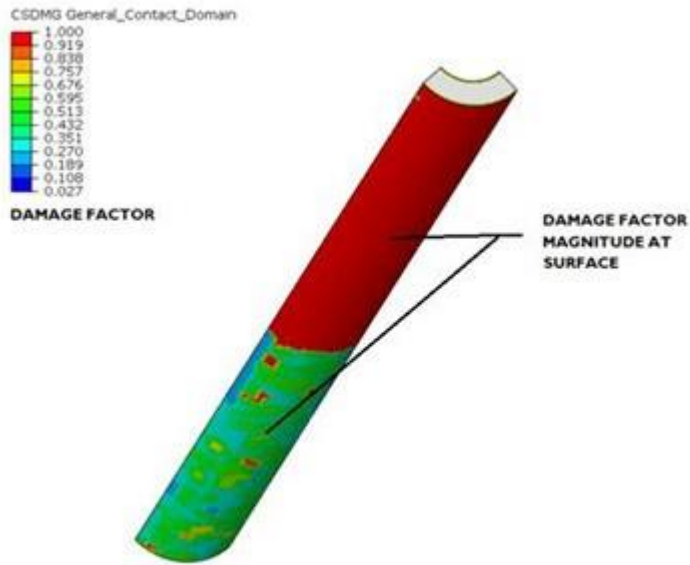
FIGURE 56: LARGE SCALE ELEMENT DAMAGE AT ESTIMATED FAILURE UNDER COMBINED LOADING



ELEMENT TENSILE DAMAGE AT ESTIMATED FAILURE

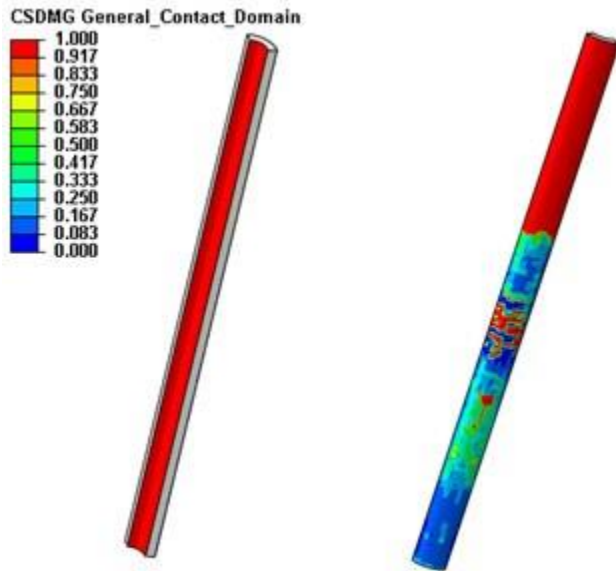
THIS REPORT WAS INADVERTENTLY DISSEMINATED IN THE PUBLIC DOMAIN/ONLINE SINCE 09/2015 WITHOUT A DISCLAIMER. DISCLAIMER HAS BEEN ADDED – “THIS INFORMATION IS DISTRIBUTED SOLELY FOR THE PURPOSE OF PEER REVIEW UNDER APPLICABLE INFORMATION QUALITY GUIDELINES. IT HAS NOT BEEN FORMALLY DISSEMINATED BY BSEE. IT DOES NOT REPRESENT AND SHOULD NOT BE CONSTRUED TO REPRESENT ANY AGENCY DETERMINATION OR POLICY

FIGURE 57: LARGE SCALE CONTACT DAMAGE AT ESTIMATED FAILURE UNDER PRESSURE LOADING



CONTACT DAMAGE AT ESTIMATED FAILURE

FIGURE 58: LARGE SCALE CONTACT DAMAGE AT ESTIMATED FAILURE UNDER THERMAL LOADING



CONTACT DAMAGE AT ESTIMATED FAILURE

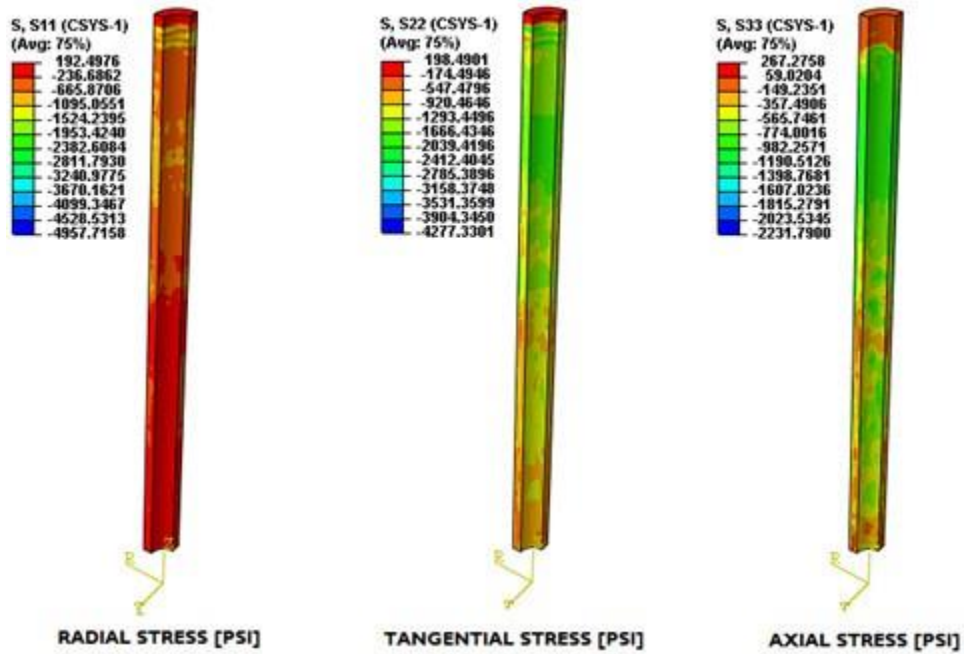
THIS REPORT WAS INADVERTENTLY DISSEMINATED IN THE PUBLIC DOMAIN/ONLINE SINCE 09/2015 WITHOUT A DISCLAIMER. DISCLAIMER HAS BEEN ADDED – “THIS INFORMATION IS DISTRIBUTED SOLELY FOR THE PURPOSE OF PEER REVIEW UNDER APPLICABLE INFORMATION QUALITY GUIDELINES. IT HAS NOT BEEN FORMALLY DISSEMINATED BY BSEE. IT DOES NOT REPRESENT AND SHOULD NOT BE CONSTRUED TO REPRESENT ANY AGENCY DETERMINATION OR POLICY

FIGURE 59: LARGE SCALE CONTACT DAMAGE AT ESTIMATED FAILURE UNDER COMBINED LOADING



THIS REPORT WAS INADVERTENTLY DISSEMINATED IN THE PUBLIC DOMAIN/ONLINE SINCE 09/2015 WITHOUT A DISCLAIMER. DISCLAIMER HAS BEEN ADDED – “THIS INFORMATION IS DISTRIBUTED SOLELY FOR THE PURPOSE OF PEER REVIEW UNDER APPLICABLE INFORMATION QUALITY GUIDELINES. IT HAS NOT BEEN FORMALLY DISSEMINATED BY BSEE. IT DOES NOT REPRESENT AND SHOULD NOT BE CONSTRUED TO REPRESENT ANY AGENCY DETERMINATION OR POLICY

FIGURE 60: LARGE SCALE STRESS DISTRIBUTION AT ESTIMATED FAILURE UNDER PRESSURE LOADING



THIS REPORT WAS INADVERTENTLY DISSEMINATED IN THE PUBLIC DOMAIN/ONLINE SINCE 09/2015 WITHOUT A DISCLAIMER. DISCLAIMER HAS BEEN ADDED – “THIS INFORMATION IS DISTRIBUTED SOLELY FOR THE PURPOSE OF PEER REVIEW UNDER APPLICABLE INFORMATION QUALITY GUIDELINES. IT HAS NOT BEEN FORMALLY DISSEMINATED BY BSEE. IT DOES NOT REPRESENT AND SHOULD NOT BE CONSTRUED TO REPRESENT ANY AGENCY DETERMINATION OR POLICY

FIGURE 61: LARGE SCALE STRESS DISTRIBUTION AT ESTIMATED FAILURE UNDER THERMAL LOADING

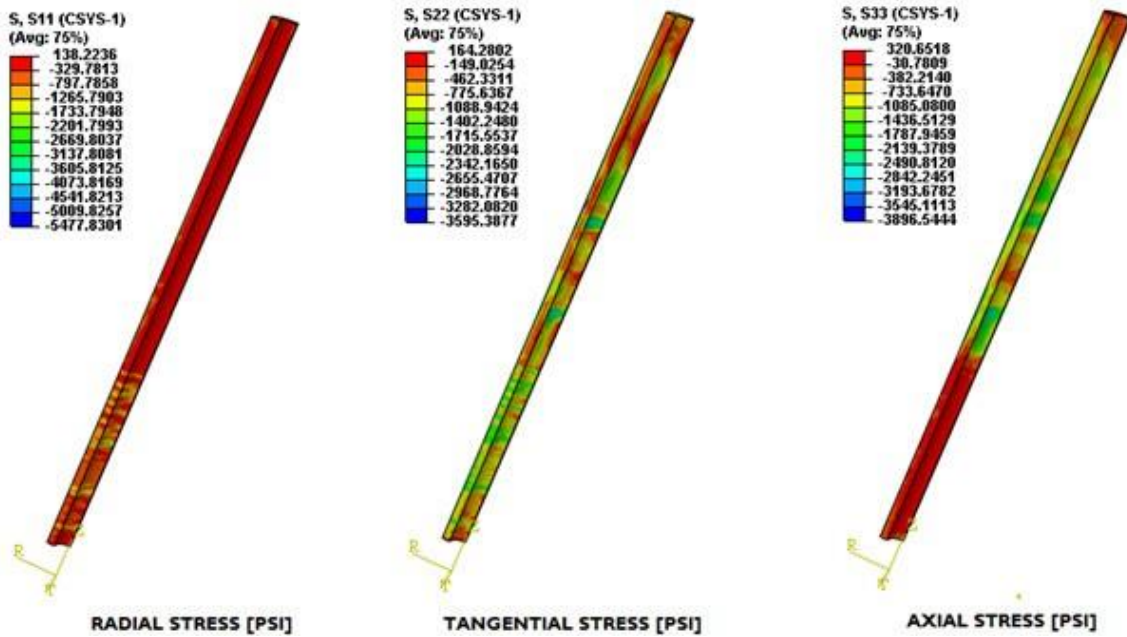
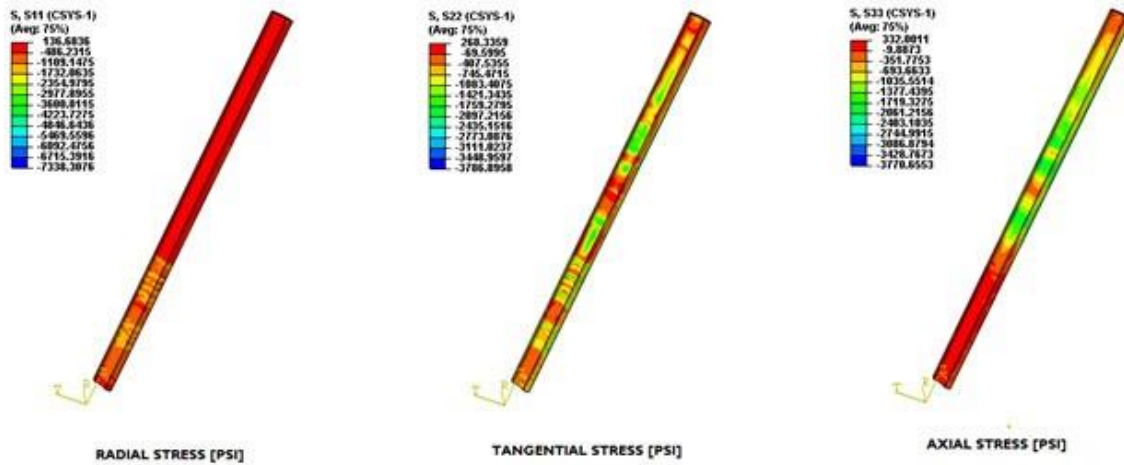
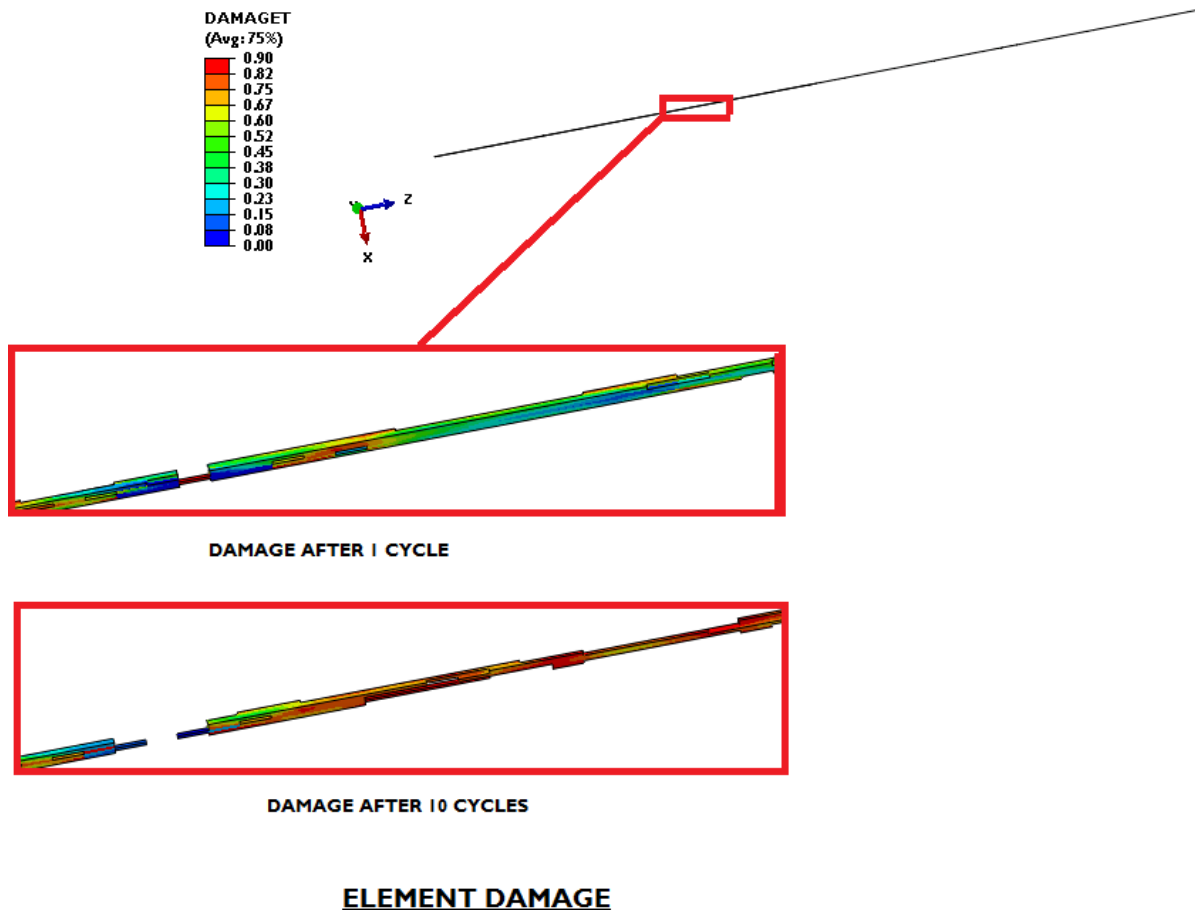


FIGURE 62: LARGE SCALE STRESS DISTRIBUTION AT ESTIMATED FAILURE UNDER COMBINED LOADING



THIS REPORT WAS INADVERTENTLY DISSEMINATED IN THE PUBLIC DOMAIN/ONLINE SINCE 09/2015 WITHOUT A DISCLAIMER. DISCLAIMER HAS BEEN ADDED – “THIS INFORMATION IS DISTRIBUTED SOLELY FOR THE PURPOSE OF PEER REVIEW UNDER APPLICABLE INFORMATION QUALITY GUIDELINES. IT HAS NOT BEEN FORMALLY DISSEMINATED BY BSEE. IT DOES NOT REPRESENT AND SHOULD NOT BE CONSTRUED TO REPRESENT ANY AGENCY DETERMINATION OR POLICY

FIGURE 63: DOWN-HOLE SYSTEM ELEMENT DAMAGE



THIS REPORT WAS INADVERTENTLY DISSEMINATED IN THE PUBLIC DOMAIN/ONLINE SINCE 09/2015 WITHOUT A DISCLAIMER. DISCLAIMER HAS BEEN ADDED – “THIS INFORMATION IS DISTRIBUTED SOLELY FOR THE PURPOSE OF PEER REVIEW UNDER APPLICABLE INFORMATION QUALITY GUIDELINES. IT HAS NOT BEEN FORMALLY DISSEMINATED BY BSEE. IT DOES NOT REPRESENT AND SHOULD NOT BE CONSTRUED TO REPRESENT ANY AGENCY DETERMINATION OR POLICY

APPENDIX D PAPER ON ZONAL ISOLATION

URTeC: 1913405

Zonal Isolation Assurance: Relating Cement Mechanical Properties to Mechanical Durability

Jessica McDaniel, SPE, Larry Watters, SPE, N. Kyle Combs, SPE, CSI Technologies LLC.

Copyright 2014, Unconventional Resources Technology Conference (URTeC)

This paper was prepared for presentation at the Unconventional Resources Technology Conference held in Denver, Colorado, USA, 25-27 August 2014.

The URTeC Technical Program Committee accepted this presentation on the basis of information contained in an abstract submitted by the author(s). The contents of this paper have not been reviewed by URTeC and URTeC does not warrant the accuracy, reliability, or timeliness of any information herein. All information is the responsibility of, and, is subject to corrections by the author(s). Any person or entity that relies on any information obtained from this paper does so at their own risk. The information herein does not necessarily reflect any position of URTeC. Any reproduction, distribution, or storage of any part of this paper without the written consent of URTeC is prohibited.

Abstract

Sustained casing pressure (SCP) is a common problem in US shale reservoirs. Wells drilled in US shale plays present many issues that can affect complete zonal isolation, such as long horizontal sections and complicated post cementing operations like continued drilling or hydraulic fracturing. Incomplete zonal isolation can create a path for gas migration. Short term gas migration occurs when the cement slurry is in transition from liquid to solid while long term gas migration, the focus of this paper, occurs after the cement has set. Cementing methods to alleviate gas flow via one flow path initiation mechanism will not solve gas flow resulting via the other mechanism. A previous investigation was performed in response to field data showing a significant difference in SCP incidence with one cement system compared to another, specifically on the intermediate by surface annulus. This first investigation identified the flow initiation mechanism as long-term gas migration and linked the improved seal performance to improved mechanical properties and overall durability. This paper reports continued investigation of mechanical properties of different cement compositions and their effects on long term seal durability.

Testing methods developed for this project are designed to determine the cumulative energy applied by cyclic stresses that cement can withstand as well as to correlate this to the intrinsic properties of cement systems. This method determines the amount of cyclic stress cement can withstand in a field situation before compromising the annular seal.

THIS REPORT WAS INADVERTENTLY DISSEMINATED IN THE PUBLIC DOMAIN/ONLINE SINCE 09/2015 WITHOUT A DISCLAIMER. DISCLAIMER HAS BEEN ADDED – “THIS INFORMATION IS DISTRIBUTED SOLELY FOR THE PURPOSE OF PEER REVIEW UNDER APPLICABLE INFORMATION QUALITY GUIDELINES. IT HAS NOT BEEN FORMALLY DISSEMINATED BY BSEE. IT DOES NOT REPRESENT AND SHOULD NOT BE CONSTRUED TO REPRESENT ANY AGENCY DETERMINATION OR POLICY

This paper describes development of the method to evaluate the ability of cement systems to withstand energy applied laboratory scale. Cement systems evaluated include differing API classes, gypsum concentrations, and fluid loss additives as well as two systems used in the Marcellus field. A preliminary quantitative relationship between laboratory-measured cement seal failure and a dimensionless ratio of cement mechanical properties and well geometry has been developed. This relationship applied to field data from the previous study corroborates the relationship's potential as a cement system screening tool for prevention of gas leakage and SCP.

Successful outcome of this ongoing investigation provides a laboratory design method to improve annular seal durability thereby alleviating SCP in the Marcellus shale. By reducing SCP, the costs and risks associated with gas migration will be reduced drastically. Other potential improvement areas include improvement in hydraulic fracturing efficiency and ultimately in production efficiency.

Introduction and Theory

Commercial success of U. S. shale production depends on drilling a large number of wells efficiently and economically. Environmental and safety success depends on establishing long-term integrity of the flow conduit from the reservoir to the surface. However, because shale well construction is complicated, it can be difficult to achieve both. Significant engineering is necessary at every step of the construction process to ensure optimized performance. The study described here illustrates the effectiveness of identifying performance issues in the shale well construction process in the Marcellus shale and developing an engineering basis for the issue along with a possible solution.

Sustained casing pressure, or SCP, occurrence in Marcellus wells has been the subject of two previous long-term investigations covered in SPE168650 and SPE168874. Early on, one investigation discovered that the majority of SCP experienced occurred on the intermediate casing annulus. Interestingly, it was discovered that cements for this string were designed to prevent gas migration and met all regulatory strength development criteria. The operating and cement companies in the area had devoted significant effort to engineer cement systems to meet the intermediate string cementing challenges. Cements were designed with fluid loss control and short gel strength transition times to prevent short-term gas migration. Density, set control, and strength development were balanced to produce cost effective cement systems that possessed adequate compressive strength development to allow drilling ahead after the minimum required WOC. The previous study focused on mechanical property differences between two intermediate cement systems. Although both systems were designed in accordance with the performance criteria, wells with one system exhibited SCP much more often than those cemented with the other. In this case, short term gas flow potential for the intermediate casing string was low and should have been controlled by either of the cement systems. Considering that operational activity on the intermediate string included an extended period of drilling the production section, the most likely cause of SCP was identified as the mechanical stresses applied to the new cement sheath during drilling ahead. The mechanical integrity of each cement system was evaluated under cyclic stress. Results confirmed that the system which allowed most SCP developed lower mechanical properties.

Based on that initial assessment presented by McDaniel et al. (2014), an evaluation process of failure mechanisms and causes of annular seal breach leading to SCP appearing behind these intermediate casing strings has been developed and tested in the laboratory. The results presented herein are from preliminary stages of the investigation, testing an array of cement systems with suitable design properties and varying mechanical property development. This initial investigation resulted in refinement of a dimensionless scaling relationship quantifying a cement system's ability to endure cyclic stress application. Significant development work will follow to confirm the SCP theory and test methods to alleviate it.

The initial results presented here reveal the importance of complete understanding of seal failure mechanism and the associated drivers. This understanding of the complexity of seal failure as a function of the whole well structure (casing, cement, and formation) dictates proper technology to prevent the problem. This basic study emphasizes the necessity of conducting routine engineering analysis as an integral step in the manufacturing drilling process embraced in today's shale gas drilling and completion methodology to identify technical issues, to develop solutions for the issues, to implement the procedural changes effectively, and to measure success. It has been demonstrated that this attention to drilling and completion engineering in the background of a shale field development process can yield improved operational success (Bassett et al 2012).

Long term gas flow describes gas flow that often begins weeks or months after cement placement, and is caused by very different mechanisms than short term gas migration. It can be referred to as gas leakage as opposed to gas migration and is typically a response to a weakness in the mechanical properties of the cement, poor mud removal before cement placement, shrinkage of the set cement, damage of the cement sheath due to subsequent well operations, or some other type of long-term degradation. Long term gas leakage is usually much less severe than short term gas migration, but is still a problem that must be resolved.

Jones and Berdine (1940) describe how drilling fluid, either as a fluid or dehydrated loosely packed filter cake that was not removed before a cement job, leaves easily accessible flow channels for gas to migrate through. In addition, Wilkins and Free (1989) describe how cements with high water content or low strengths may possess either high permeability or large volumetric shrinkage over time, also creating flow paths for gas. When post-set shrinkage occurs, the cement sheath will de-bond from the casing wall or formation, creating a micro annulus for gas to flow through.

Of particular interest to the project described in this paper is the third option listed above: damage of the cement sheath due to well operations. Goodwin and Crook (1990) describe in detail how cement integrity can be damaged or completely destroyed by thermally or hydraulically induced pressure extremes or pressure cycles during the well operations after cement has been placed and allowed to set. During post-cementing operations such as drill out and hydraulic fracturing extreme forces can be exerted along the cement sheath. Should the force exerted exceed the mechanical properties of the set cement, fracturing could be induced along the casing to cement interface, allowing

gas to flow. Stress cycling can also cause failure along the cement to casing interface even if the maximum stress magnitude exerted is less than the mechanical property limit of the cement. Another study addresses properties of cement used in a well prior to a hydraulic fracturing operation (SPE169574). The study shows the change in hydraulic isolation performance between the regular cement and the improved cement. In the improved cement, the percentage of wells with communication decreases, showing that cement properties can have significant impact on the hydraulic isolation of fracturing stages.

Long term gas leakage is prevented by cement mechanical property optimization or well operations optimization. Mechanical properties of the set cement can be increased to prevent fracturing during post-cementing operations. In addition, operations to place the cement can be optimized by enhancing mud removal capabilities of the fluids pumped before the cement. If slurry optimization cannot be performed, post-cementing operations must be optimized to exert less force, but still perform the task they are required.

This investigation began with examination of energy resistance correlations reported by Sabins (2004). The generalized stress resistance correlations, originally developed for deep water application, were previously evaluated by McDaniel et al (2014) with unsatisfactory correlation to the shale well data. The energy resistance variables were modified to place more emphasis on additional mechanical properties of the cement systems (e.g. impact strength). This revised correlation demonstrated good correlation to laboratory seal failure results.

Field confirmation of the energy resistance relationship required estimation of stresses applied to the well seal during drill out. No previously reported value was discovered, so the stress magnitude was estimated through analysis of the previous field data using the revised correlation and estimated stress magnitude yielded acceptable results indicating that the initial stress-resistance correlation is a good starting point.

At this point in the long-term investigation, the necessity of analyzing cement seal performance via a multi-variable, systems approach is undeniable. Keying on one mechanical property such as compressive strength to indicate seal durability is not sufficient. Thorough evaluation of cement system performance, well construction layout, and stresses imposed by continued well operations must be included in the design process. This engineering design process can be integrated into manufacturing-style drilling.

Testing

This project is an extension of the study performed by McDaniel et al (2014), Cement Sheath Durability: Increasing Cement Sheath Integrity to Reduce Gas Migration in the Marcellus Shale Play. The intention of this study is to further investigate the trends seen in the previous paper and to create dimensionless ratios to identify energy

resistance of a cement sheath and compare it to the energy applied to the cement sheath. Ultimately, this will be useful when the field energy is quantified and compared to the energy resistance.

The testing for this study included:

- Compressive strength
- Young’s Modulus
- Poisson’s Ratio
- Impact strength
- Tensile Strength
- Anelastic Strain
- Annular Seal Durability

Each of these tests is described in detail in the previous study (McDaniel et al 2014). Prior to testing, cement samples were cured 24-48 hours in a curing chamber under bottom hole pressure and static temperature if the sample mold allowed, or in a water bath under bottom hole static temperature if the curing chamber was not an option.

The cement systems chosen for this study were selected based on results seen in the previous project. That study brought up questions about class of cement, gypsum content, and fluid loss additive used. The list of cement systems is shown in Table 1.

Sample	API Cement Class	Additives	Concentration %bwoc
1	Class H	CaCl ₂	2.00
2	Class A	CaCl ₂	2.00
3	Class H	CaCl ₂	2.00
		Gypsum	3.00
4	Class A	CaCl ₂	2.00
		Gypsum	3.00



5	Class H	CaCl ₂	2.00
		Gypsum	5.00
6	Class A	CaCl ₂	2.00
		Gypsum	5.00
7	Class H	CaCl ₂	2.00
		FL 1	0.30
8	Class H	CaCl ₂	2.00
		FL 2	0.30
9	Class A	CaCl ₂	2.00
		FL 1	0.30
10	Class A	CaCl ₂	2.00
		FL 2	0.30
11*	Class H	CaCl ₂	2.00
		Gypsum	3.00
		FL 1	0.20
		Suspension	0.50
		Antifoam	0.40
12*	50/50 Class A/Gypsum	FL 2	0.85
		Retarder	0.30
		Dispersant	0.50
		Anti-foam	0.30
		Anti-static	0.02
		CaCl ₂	2.00
13*	Class H	Gypsum	5.00
		FL 2	0.60
		Anti-foam	0.30

TABLE 1: CEMENT SYSTEM COMPOSITIONS. FL 1 AND FL 2 ARE TWO FLUID LOSS AGENTS. SYSTEMS MARKED * WERE FROM THE PREVIOUS STUDY (SPE 168650)

► CSI Technologies makes no representations or warranties, either expressed or implied, and specifically provides the results of this report "as is" based upon the provided information.

Results and Discussion

Results from each test are listed in the chart below.

Sample	Ultimate Compressive Strength (psi)	Young's Modulus (psi)	Poisson's Ratio	Tensile Strength (psi)	Anelastic Strain Potential	Annular Seal Durability (in-lb)	Impact Strength (in-lb/in ²)	Density (lb/gal)	Water to Cement Ratio
1	1520	8.79E+05	0.32	99.00	2.33E-05	1.27E+04	3.41	15.6	0.46
2	2922.00	1.13E+06	0.28	206.00	2.14E-05	3.71E+05	4.77	15.6	0.47
3	2829.00	1.18E+06	0.29	143.00	2.60E-05	2.05E+05	4.77	15.6	0.48
4	1692.00	7.57E+05	0.19	199.00	3.56E-05	3.58E+05	6.13	15.6	0.48
5	1732.00	7.59E+05	0.23	62.00	1.51E-05	3.36E+05	3.41	15.6	0.48
6	2058.00	8.46E+05	0.25	148.00	1.39E-05	4.34E+05	3.41	15.6	0.49
7	2545.00	1.34E+06	0.29	327.00	1.31E-05	8.35E+05	4.77	15.6	0.46
8	2080.00	1.64E+06	0.26	253.00	1.90E-05	6.76E+05	5.45	15.6	0.46
9	2008.00	9.54E+05	0.32	229.00	1.46E-05	6.12E+05	3.41	15.6	0.47
10	1555.50	1.63E+06	0.26	191.00	1.40E-05	3.20E+05	2.73	15.6	0.47
11	1885.00	1.24E+06	0.23	161.00	1.10E-05	6.49E+05	4.20	15.6	0.48
12	1685.00	6.51E+05	0.16	114.60	8.49E-05	3.20E+05	1.96	15.8	0.84
13	1760.00	9.21E+05	0.25	143.50	2.71E-05	-	4.77	15.6	0.48

TABLE 2: RESULTS FROM TESTING

When comparing the results of each test, the authors found trends indicating improved performance associated with specific cement properties. However, these trends showed weak correlations between individual cement properties and performance on energy tests.

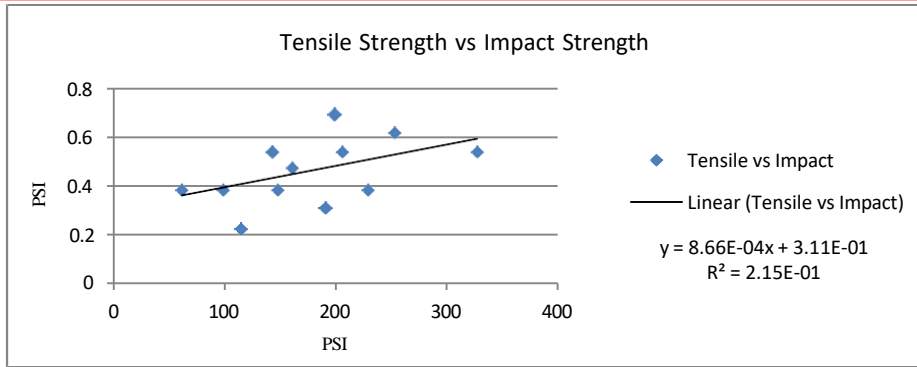


FIGURE 1: TENSILE STRENGTH VS ANNULAR SEAL DURABILITY

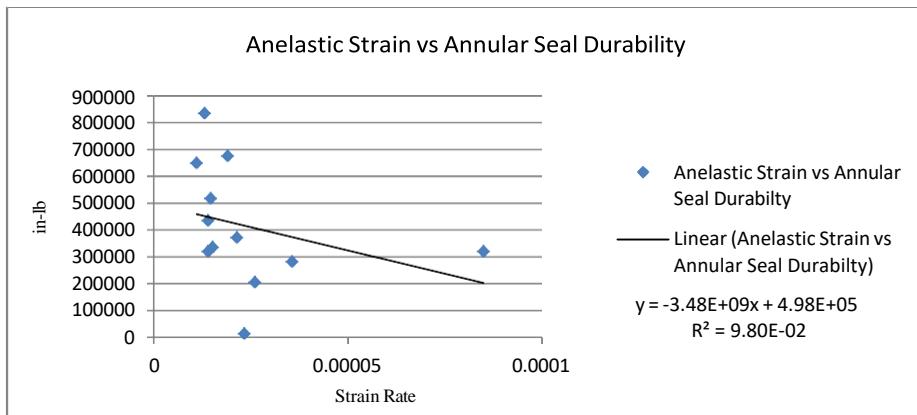


FIGURE 2: ANELASTIC STRAIN VS ANNULAR SEAL DURABILITY

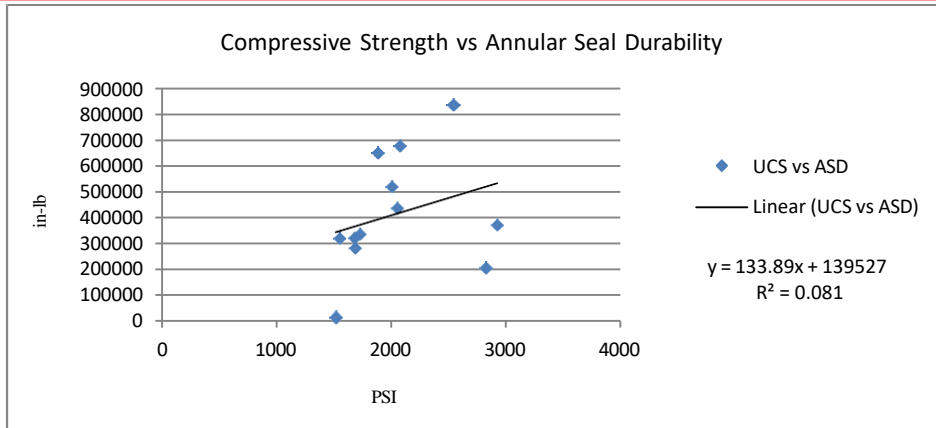


FIGURE 3: COMPRESSIVE STRENGTH VS ANNULAR SEAL DURABILITY

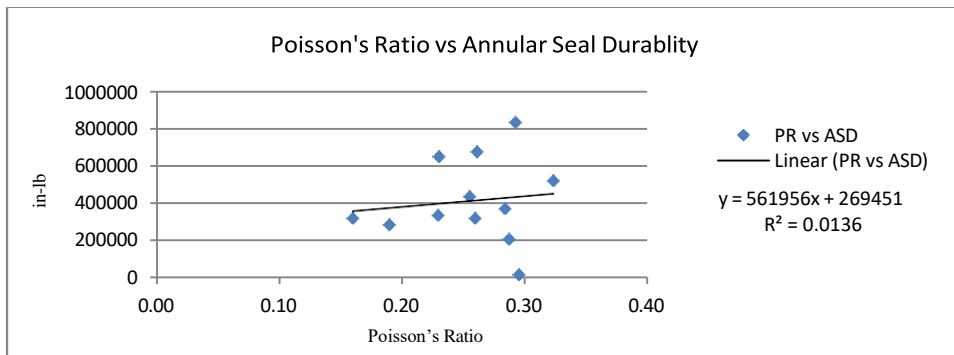


FIGURE 4: POISSON'S RATIO VS ANNULAR SEAL DURABILITY

These weak, single-variable correlations suggested that this problem may be more complicated than the authors had first considered. A look back to Sabins' work for MMS, showed that cement properties can be correlated into dimensionless variables and plotted against energy applied to failure. The utility of this approach lies in scalability of the results. Laboratory-measured performance measurements can be applied to varying field conditions or dimensions making the method a widely applicable tool for cement property design and comparison.

Using the original correlations from Sabins 2004, the authors found the correlation did not fit the current data set. However, by using the theories from this study, new correlations were created.

Energy applied was determined using the borehole geometry and the energy applied during the annular seal durability test. The revised dimensionless variable is:

$$Ea = \frac{\text{Energy from stressor} * \text{Pipe ID}}{\text{Pipe Cross sectional area} * \text{Formation Young's Modulus} * \text{Annular Area}}$$

Variable	Definition	Units	Lab Data	Field Data
Energy from stressor	Energy calculated from annular seal durability test or from well operations	in-Lb	From data set results	From data set
Pipe ID	Casing ID	Inches	0.75	8.835
Pipe Cross sectional area	Cross sectional area of casing	In ²	0.34	11.45
Formation Young's Modulus	Young's modulus of the surrounding formation	psi	500,000	10,000,000
Annular Area	Cross-sectional area of where cemented annulus	in ²	6.28	180

TABLE 3: DEFINITIONS OF VARIABLES FOR EA

In this relationship, the applied energy can be from the annular seal durability test or the well operations in the field. The other factors in this ratio are how the applied energy affects the cement sheath.

- Energy from stressor: energy imparted on the cement sheath from either the annular seal durability test or estimated field stress
- Pipe ID: a larger diameter on the pipe will decrease the amount of force applied to the cement, therefore decreasing the amount of energy applied to the cement sheath.
- Pipe cross sectional area: a thicker casing will expand less when pressure is applied, therefore applying less force to the cement sheath, decreasing the amount of energy applied to the cement sheath.

- Formation Young’s modulus: A higher formation Young’s modulus will provide a better confining force on the cement, decreasing the effects of the force on the cement, by preventing excess deformation of the cement.
- Annular area: A larger annular area allows for a thicker cement sheath, which can help reduce the effects of a cyclic stress event on the cement sheath.

Energy resistance is determined using set cement properties that relate to mechanical durability.

$$Re = \frac{\text{Poisson's Ratio} * \text{Tensile Strength} * \text{Impact Strength}}{\text{Pipe OR} * \text{W: C Ratio} * \text{Cement Young's modulus} * \text{Anelastic Strain} * \text{Compressive Strength}}$$

Poisson’s Ratio	Poisson’s ratio of the cement	unitless
Tensile Strength	Tensile strength of the cement	psi
Impact Strength	Impact strength of the cement	in-lb/in ²
Pipe OR	Outer radius of the inner pipe	Inches
W:C ratio	Water to cement ratio of the cement slurry	Unitless
Cement Young’s Modulus	Young’s modulus of the cement	psi
Anelastic Strain	Anelastic strain of the cement	unitless
Compressive Strength	Compressive strength of the cement as determined by destructive crush testing	psi

TABLE 4: DEFINITIONS OF VARIABLES FOR RE

The dimensionless ratio for Energy Resistance was determined by observing the effect a mechanical property has on the cement system when tested to failure. Each mechanical property has an effect on the cement during a cyclic stress event.

- Young’s Modulus: A high Young’s modulus is associated with increased stiffness and brittleness. However, if the value is too low, the cement may not be strong enough. This property must be optimized in a cement system, and for the relationship in this study, it is negatively correlated with energy resistance.

- Poisson’s Ratio: An increase in Poisson’s ratio is associated with an increase in a cement system’s durability during a cyclic stress event.
- Anelastic strain potential: This is a measure of how much a cement deforms plastically over time when exposed to a cyclic load. The more the cement sample deforms, the higher the anelastic strain potential is, so ideally, this number is low for more durable cement.
- Ultimate compressive strength: This is another property that must be optimized. Very high compressive strengths correspond to more brittle materials. With cement, it is easy to get very high compressive strengths.
- Impact strength: the more impact strength a cement system has, the better it will perform when exposed to a cyclic stressing event. This property is positively correlated with energy resistance
- Tensile strength: Generally, cement has a very low tensile strength, so a high tensile strength would improve cement’s durability. This is positively correlated with energy resistance.

By plotting the revised Energy Applied (Ea) variable on the X axis, against the revised Energy Resistance (Re) variable on the Y axis, a more meaningful correlation was found and is seen in Figure 5.

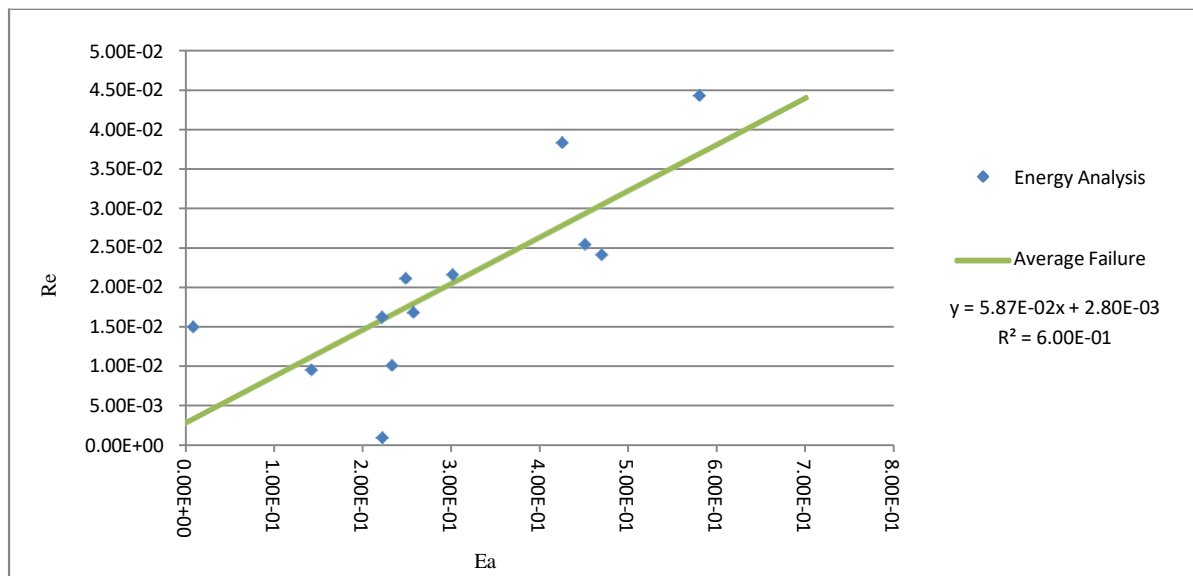


FIGURE 5: CHART SHOWING EA VS RE FOR LABORATORY TESTING

The trendline in this case represents where each of these samples should fail on average. With a predicted energy applied on the specimen, if the Ea/Re point falls below the line, failure of the annular seal is predicted. If the point falls above the line, that particular specimen should survive the energy applied. With the variables being dimensionless, this relationship is scalable to field applications.

Field Data Application

To test the validity of this relationship, another set of data from McDaniel (2014) was introduced. The authors measured the additional cement properties and estimated field energy to determine E_a and R_e . The two systems studied in the field showed a significant difference in performance (McDaniel 2014), with System 1 showing a nearly 90% success rate and System 2’s success rate under 50%. In this study, System 1 corresponds to sample 11, and System 2 is sample 12. The estimated energy magnitude resulting from drillout is 2×10^6 in-lb. Using this energy estimate, E_a was calculated for predicted forces.

$$E_a = \frac{\text{Predicted Field Energy} * \text{Mass of casing}}{\text{Mass of cement} * \text{Pipe ID} * \text{Formation Young's Modulus} * \text{Annular Area}}$$

Sample	Ultimate Compressive Strength (psi)	Young’s Modulus (psi)	Poisson’s Ratio	Tensile Strength (psi)	Anelastic Strain	Predicted Field Energy	Impact Strength (in-lb/in ²)	Density	Water to Cement Ratio	Success Rate
Field 1	1885.00	1.24E+06	0.23	161.00	1.10E-05	2.00E+06	4.20	15.6	0.48	89%
Field 2	1685.00	6.51E+05	0.16	114.60	8.49E-05	2.00E+06	1.96	15.8	0.84	43%

TABLE 5: DATA FOR FIELD TESTED SAMPLES

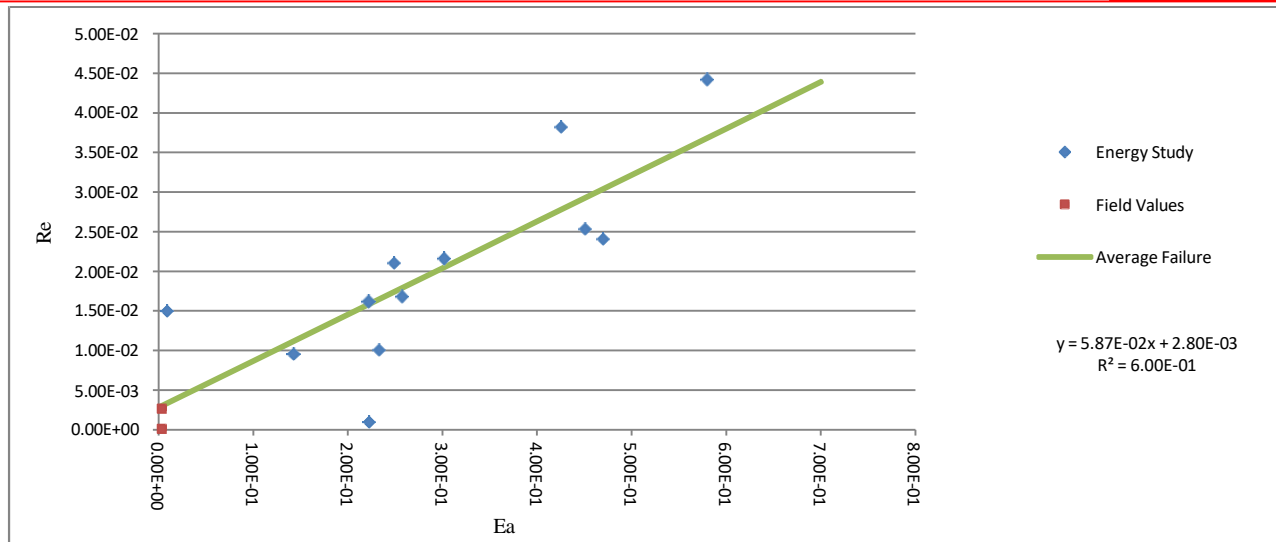


FIGURE 6: INCLUDING FIELD DATA IN EA VS RE PLOT

The field data fit this relationship well. The system labeled Field 1 had nearly a 90% success rate in preventing SCP when applied in the field. This point falls on the Average Failure line, indicating it would survive the predicted energy applied. System Field 2 had around a 40% success rate. As can be seen here, that system falls far below the Average Failure line indicating the mechanical properties of this cement system are not adequate for the estimated applied energy.

Conclusions

The results from this study shed more light on designing cement for the life of the well. This study is a preliminary look at how a dimensionless ratio can be used to analyze a cement in the laboratory and have the ability to scale it up to field size to predict how successful a cement will be. The major conclusions are as follows:

1. Energy analysis on a cement sheath is complicated
2. Magnitude of an individual mechanical property cannot foretell a cement's seal integrity.
 - a. No one mechanical property can be used to successfully tell if a cement system will be adequate or not for the life of the well.
3. Many properties need to be considered when designing a cement system for a particular well

- a. Short term and long term needs for a cement system should be understood and considered when designing
 - b. Properties identified in this study to address long term isolation are: Young's modulus, Poisson's ratio, tensile strength, impact strength, anelastic strain potential, and compressive strength
4. The correlations found in this study need to be refined, however they show a general pattern in energy resistance of cements and how that can be predicted on a lab scale and then applied to field data.
- a. This model, with further refinement, may be used to predict the properties needed from a cement to withstand predicted stress for the life of the well.
5. Future efforts will focus on further developing this model. To achieve this:
- a. A reliable and accurate prediction of the stress imparted on a cement sheath over the life of the well is needed.
 - b. Additional data points to strengthen the current model will be included.
 - c. Other cement properties such as flexural strength will be considered in future calculations.

Acknowledgements

Funding for this project is provided by RPSEA through the "Ultra-Deepwater and Unconventional Natural Gas and Other Petroleum Resources" program authorized by the U.S. Energy Policy Act of 2005. RPSEA (www.rpsea.org) is a nonprofit corporation whose mission is to provide a stewardship role in ensuring the focused research, development and deployment of safe and environmentally responsible technology that can effectively deliver hydrocarbons from domestic resources to the citizens of the United States. RPSEA, operating as a consortium of premier U.S. energy research universities, industry, and independent research organizations, manages the program under a contract with the U.S. Department of Energy's National Energy Technology Laboratory.

Works Cited

- Bassett, J., Watters, J., & Sabins, F. (2012). Focus on Cement Design and Job Execution Increase Success for Shale Cementing Operations. *Americas Unconventional Resources Conference* (p. SPE 155757). Pittsburgh, PA: Society of Petroleum Engineers.
- Bassett, J., Watters, J., Combs, K., & Nikolaou, M. (2013). Lowering Drilling Cost, Improving Operational Safety, and Reducing Environmental Impact through Zonal Isolation Improvements for Horizontal Wells Drilled into the Marcellus Shale. *Unconventional Resources and Technology Conference* (p. SPE 168847). Denver, CO: Society of Petroleum Engineers.
- Goodwin, K. J. (1990). Cement Sheath Stress Failure. *Annular Technical Conference and Exhibition* (p. SPE 20453). New Orleans, LA: Society of Petroleum Engineers.

Jones, P., & Berdine, D. (1940). Oil-Well Cementing. *Drilling and Production Practice*.

McDaniel, J., Shadravan, A., & Watters, L. (2014). Cement Sheath Durability: Increasing Cement Sheath Integrity to Reduce Gas Migration in the Marcellus Shale Play. *SPE Hydraulic Fracturing Technology Conference* (p. SPE 168650). The Woodlands, Texas: Society of Petroleum Engineers.

Sabins, F. (2004). *MMS Project 426 long Term Integrity of Deepwater Cement Systems Under Stress/Compaction Conditions*. Summary Report for MMS.

Schmelzl, E., & Daniel Schlosser, D. A. (2014). CTU Deployed Frac Sleeves Benchmark Horizontal Multi Stage Frac Isolation Performance. *SPE Western North America and Rocky Mountain Joint Regional Meeting* (p. SPE169574). Denver, Colorado: The Society of Petroleum Engineers.

Wilkins, R. P. (1989). A new Approach to the Prediction of Gas Flow After Cementing. *SPE/IADC Drilling Conference*. Society of Petroleum Engineers.